

**Cu-BASED METAL-ORGANIC POLYHEDRA FOR
ENCAPSULATION AND CONTROLLED DELIVERY OF
GLYCINE BETAINE TO RICE CROP**

by

Ranjita Saikia

A Thesis Submitted in the Partial Fulfilment of the Requirements for the Degree
of Master of Science in Bio-Nano Material Science and Engineering

Examination Committee: Dr. Raffaele Ricco (Chairperson)

Dr. Suriyan Cha-um (Co-chairperson)

Dr. Tanujjal Bora

Dr. Pranab Dutta (External Expert)

Nationality: Indian

Previous Degree: Bachelor of Science (Honors) in Agriculture

Assam Agricultural University

Jorhat, Assam, India

Scholarship Donor: AIT Scholarships

Asian Institute of Technology

School of Engineering and Technology

Thailand

May 2024

AUTHOR'S DECLARATION

I, Ranjita Saikia, hereby certify that the guidelines set out by the 'Asian Institute of Technology' were followed strictly in the research done for my thesis. The content was meticulously produced on my own after much research and analysis. It is all original. I have made sure to properly credit and mention any external resources that I used for the research. This thesis is completely original and has never been submitted for credit toward a different degree or certification at any other institution. This paper is a true copy of the original thesis, complete with any final revisions.

Dated: 7th May, 2024

Name: Ranjita Saikia

Signature: *Ranjita Saikia*

ACKNOWLEDGMENTS

I would like to express my sincere gratitude to all who played a part in making my thesis a success.

First, I would like to extend my heartfelt thanks to my supervisor, Dr. Raffaele Ricco, Assistant Professor, 'Bio-Nano Materials Science and Engineering', for his direction, constant support, and invaluable insights throughout the study process. His skills and support assisted a lot in developing this work I want to sincerely thank every person on my thesis committee, Dr. Tanujjal Bora, Associate Professor and Director, 'Bio-Nano Materials Science and Engineering' and 'Center of Excellence in Nanotechnology', Dr. Suriyan Cha-um, Scientist, Researcher, 'NSTDA', and Pranab Dutta, Associate Professor, 'Central Agricultural University', Meghalaya, India, for their immense help, constructive feedback, and valuable suggestions. Additionally, I would like to thank Dr. Rujira Tisarum, Scientist, 'NSTDA', Dr. Chamath Yahampith, post-doctoral researcher, Anan Saenkhamai, Ph.D. student, Apichaya Pakkard, Ph.D. student and Md. Abdul Kaiyum, an Alumnus of AIT, who gave every bit of useful information and was there for me anytime I needed assistance. Special thanks are owed to the 'National Center for Genetic Engineering and Biotechnology', 'NSTDA', whose financial and instrumental assistance enabled me to devote the required time and resources to this research.

I would also like to deeply appreciate my family and friends for their tremendous encouragement and support during my career. I also like to thank my colleagues and fellow researchers for their collaborative mindset.

Additionally, I would want to express my gratitude to 'Asian Institute of Technology' and 'Bio-Nano Materials Science and Engineering' for granting me access to their cutting-edge facilities, and resources that were essential for carrying out our research and guaranteeing the veracity of our findings.

ABSTRACT

Agriculture plays a crucial role in providing sufficient food supply, but it faces enormous challenges in maximizing the supply of agrochemicals to increase crop yields while minimizing the adverse environmental impacts of these chemicals. The repeated and unchecked use of these agricultural chemicals might be dangerous to the economy, the environment, and human health. Nanotechnology offers enormous promise in agriculture by synthesizing agrochemical delivery systems with controlled release properties, improving application efficacy and environmental safety while minimizing the negative impacts on non-target species. In recent times, there has been an increase in the use of nano-porous materials in agriculture as hosts for encapsulation of species, such as agrochemicals, allowing precise and regulated release of them. Particularly, the discovery of an entirely novel group of compounds known as Metal-Organic Frameworks (MOFs) and Metal-Organic Polyhedra (MOPs) has proven to have remarkable promise for aiding targeted delivery of agrochemicals. They are particularly important as a carrier because of their extensive surface area and adaptable pores that can take in certain guest molecules. It is important to remember that MOPs are a very new and active research area. The present study explored copper-based Metal-Organic Polyhedra (Cu-MOPs) as novel carriers for encapsulation and targeted delivery of the plant osmolyte Glycine betaine (GB), therefore alleviating salt stress. The Cu-MOPs were synthesized via a one-step procedure at room temperature by utilizing Basic Copper Carbonate (BCC) as the metal source and Isophthalic acid, and 5-amino isophthalic acid as the organic ligands for Cu-MOP-1 and Cu-MOP-2, respectively. The Cu-MOPs were also synthesized in the presence of the chemical Glycine betaine (GB), which was taken as a guest. The encapsulation efficiency, loading percentage, and release kinetics of the Cu-MOPs were determined to check the better one. Characterization methods of MOPs include FTIR, UV-analysis, XRD, etc. The MOP giving the better encapsulation and release profile was selected and used for controlled delivery of GB to the salt-sensitive rice variety Pathumthani-1 (PTT1), grown under different concentration of salt solution (0 mM and 150 mM NaCl) under greenhouse condition to alleviate salt stress. The effectiveness in mitigating the salt stress was determined by comparing the performance of the GB@MOP with pure GB.

CONTENTS

	Page
AUTHOR'S DECLARATION	ii
ACKNOWLEDGMENTS	iii
ABSTRACT	iv
CONTENTS	v
LIST OF TABLES	vii
LIST OF FIGURES	viii
LIST OF ABBREVIATIONS	x
CHAPTER 1 INTRODUCTION	1
1.1 Background of the Study	1
1.2 Statement of the Problem	6
1.3 Objectives of the Study	8
1.4 Scope of the Study	8
1.5 Limitations of the Study	9
1.6 Organization of the Study	9
CHAPTER 2 REVIEW OF LITERATURE	10
2.1 Porous Materials in Agriculture	11
2.2 Metal-Organic Frameworks (MOFs) in Agriculture	13
2.3 Copper-based Metal-Organic Frameworks (Cu-MOFs)	16
2.4 Metal-Organic Polyhedra (MOPs)	18
2.5 Copper-based Metal-Organic Polyhedra (Cu-MOP):	21
2.6 Abiotic Stressors Affecting Plants	23
2.7 Role of GB in Salinity Stress Tolerance	26
2.8 MOPs for Targeted Delivery of GB	28
2.9 Summary	28
CHAPTER 3 METHODOLOGY	31
3.1 Flowchart of the Research	31
3.2 Materials	32
3.3 Procedure	32
3.3.1 Solvothermal Synthesis of Copper Isophthalate, Cu-MOP-1	32

3.3.2 Synthesis of Copper Isophthalates, Cu-MOPs from BCC	33
3.4 Characterization	34
3.5 Glycine Betaine (GB); the Guest	34
3.6 Calibration Curve of the GB	35
3.7 Encapsulation of the Guest	35
3.8 Determination of Glycine Betaine in Supernatant	37
3.9 Release Profile of the Guest from the Cu-MOPs	37
3.10 Application to Rice Plants	38
3.11 Plant Assessment Parameters	39
3.12 Statistical Analysis	42
CHAPTER 4 RESULTS AND DISCUSSIONS	43
4.1 Characterization Results of the Compounds	43
4.2 Encapsulation of the Guest	51
4.2.1. Glycine Betaine Calibration Curve	52
4.2.2. Theoretical Weight and Obtained Weight of MOPs	53
4.2.3. Encapsulation Efficiency and Loading Capacity of MOPs	54
4.3 Release Study of GB from Cu-MOPs	56
4.4 Plant Analysis	59
4.4.1 Plant Morphological Analysis	59
4.4.2 Plant Physiological Assay	63
4.4.3 Plant Biochemical Assay	71
CHAPTER 5 CONCLUSIONS AND FUTURE RECOMMENDATIONS	80
5.1 Conclusion	80
5.2 Future Recommendations	81
REFERENCES	82

LIST OF TABLES

Tables	Page
Table 2.1 Different Pesticides Nanocarriers	13
Table 2.2 List of Some Metal-Organic Polyhedra (MOPs) in Literature	19
Table 3.1 Table Representing Different Ratios of GB/MOP (varies Vertically) and Ligand/BCC (varies Horizontally) to be taken for the Synthesis of MOPs and Encapsulation of the Guest to Happen Simultaneously	36
Table 3.2 Treatments with GB@MOP, MOP, GB, and Control (water) with Different Concentrations	39
Table 4.1 Table Showing the Comparison between Theoretical Weight, Obtained Weight, and % Weight of Cu-MOPs	53
Table 4.2 Loading Capacity (LC; mg/g) of GB@MOP-1 and GB@MOP-2 with Different Concentrations of GB and with Different Molar Ratios of Ligand and BCC	54
Table 4.3 Korsmeyer Peppas Fitted Data Values	58
Table 4.4 Significance Levels in Both the Independent and Combined impacts of various Morphological, Physiological, and Biochemical Factors	74
Table 4.5 Values of the Morphological Analysis of the Plants Along with the Mean Difference Level	75
Table 4.6 Values of the Physiological (Chlorophyll) Analysis of the Plants Along with the Mean Difference Level	76
Table 4.7 Values of the Physiological (Photosynthetic parameters) Analysis of the Plants Along with the Mean Difference Level	77
Table 4.8 Values of the Physiological and Biochemical Analysis of the Plants Along with the Mean Difference Level	78

LIST OF FIGURES

Figures	Page
Figure 1.1 The Diagrammatic Representation of Metal-organic Frameworks for the Controlled Delivery of Pesticides to the Plants, Minimizing Losses to the Environment	2
Figure 1.2 Schematic Diagram of a) OPA-MOF, b) HKUST-1, and c) Cu-MOP-1	8
Figure 2.1 Flowchart Representing different Porous Materials used for Agrochemical Delivery in Agriculture	12
Figure 2.2 A Conceptual Diagram on how OPA-MOF is Produced, how Bacteria break down the Structurally Integrated Oxalate, and how this Mineralization occurs when Applied to Soil	15
Figure 2.3 Structure of HKUST-1 (A Copper-based MOF)	18
Figure 2.4 Schematic Representation of the Conversion of Cu-MOP-1 as a Porous Monomer to Cu-MOF-Bipy Framework by using Bipyridine as a Rigid N-based Ditopic Linker	21
Figure 2.5 Schematic Diagram of a) Cu-MOP-1, b) Benzene-3,5-Dicarboxylic Acid linker, and c) 5-Aminobenzene-1,3-Dicarboxylic Acid Linker	23
Figure 2.6 Adverse Effects of Salt Stress on Rice Plants	25
Figure 2.7 Biosynthesis of Glycine Betaine in Higher Plants	27
Figure 3.1 Research Flow Chart	31
Figure 3.2 Schematic Representation of Preparation of MOP	34
Figure 3.3 Chemical Structure of Glycine Betaine	35
Figure 3.4 Schematic Representation of Preparation of GB@MOP	37
Figure 3.5 Schematic Diagram of Release Study of GB from MOPs	38
Figure 4.1 FTIR Analysis of Cu-MOP-1, GB, GB@MOP-1, and Standard MOP	43
Figure 4.2 FTIR Analysis of Cu-MOP-2, GB@MOP-2, and GB	45
Figure 4.3 XRD Analysis of Cu-MOP-1, GB@MOP-1, GB@MOP-1 Released and Basic Copper Carbonate (BCC)	46
Figure 4.4 XRD Analysis of Cu-MOP-2, GB@MOP-2, GB@MOP-2 Released and Basic Copper Carbonate (BCC)	48
Figure 4.5 ICP-OES Analysis of Cu-ions Release Profile from Cu-MOP-1	49

Figure 4.6 Picture of the Synthesized Materials	51
Figure 4.7 Calibration Curve of GB: a) Absorbance of GB, b) Linear fitting GB	52
Figure 4.8 Bar Graph Representing the Encapsulation Efficiency (EE; %) of Cu-MOP-1 and Cu-MOP-2 with Different Concentration of GB and with Different Molar Ratios of Ligand and BCC	54
Figure 4.9 Release Kinetics of GB from: a) Cu-MOP-1, and b) Cu-MOP-2	57
Figure 4.10 Bar Graph Showing a) Root Length, and b) Shoot Height at Different Treatments under NaCl 0 mM and 150 mM	59
Figure 4.11 Pictures of the Morphology of Rice Plants under a) NaCl 0 mM, and b) NaCl 150 mM	61
Figure 4.12 Bar Graph Showing a) Root Biomass, and b) Shoot Biomass of Rice Plants at Different Treatments under NaCl 0 mM and 150 mM	62
Figure 4.13 Bar Graph Showing a) NDVI, and b) SPAD value for Plants at Different Treatments under NaCl 0 mM and 150 mM	63
Figure 4.14 Bar Graph Showing values of a)Chlorophyll a, b)Chlorophyll b, c)Total Chlorophyll, and d)Carotenoid levels in Plants with Different Treatments under NaCl 0 mM and 150 mM	65
Figure 4.15 Bar Graph Showing ‘a)Net photosynthetic rate (Pn), b)Stomatal conductance (gs), and c)Transpiration rate (E)’ of Rice Plants with Different Treatments under NaCl 0 mM and 150 mM	67
Figure 4.16 Bar Graph Showing ‘Maximum Quantum yield of PSII (Fv/Fm)’ of Rice Plants a) under Different Treatments and b) under NaCl 0 mM and 150 mM	68
Figure 4.17 Bar Graph Showing ‘Photon yield of PSII (Φ PSII)’ of Rice Plants a)under Different Treatments and b)under NaCl 0 mM and 150 mM	69
Figure 4.18 Bar Graph Showing Osmotic Potential (MPa) of Rice Plants with Different Treatments under NaCl 0 mM and 150 mM	70
Figure 4.19 Bar Graph Showing Proline Content of Rice Plants with Different Treatments under NaCl 0 mM and 150 mM	72

LIST OF ABBREVIATIONS

1,3-BDC	= Benzene-1,3-Dicarboxylic Acid (Isophthalic acid)
FW	= Fresh Weight
Gm	= Gram
Ha	= Hectare
HKUST-1	= 'Hong Kong University of Science and Technology'
µg	= Microgram
mg	= Milligram
µM	= Micro molar
mM	= Milli molar
MOF	= 'Metal-Organic Framework'
MOP	= 'Metal-Organic Polyhedra'
NDVI	= 'Normalized Difference Vegetation Index'
NH ₂ -bdc	= 5-Amino-Isophthalate
NO ₂ -bdc	= 5-Nitro-Isophthalate
NSTDA	= 'National Science and Technology Development Agency'
OH-bdc	= 5-Hydroxy-Isophthalate
OPA-MOF	= Oxalate-Phosphate-Amine-MOF
SPAD	= 'Soil Plant Analysis Development'
t Bu-bdc	= 5-Tert-Butyl-Isophthalate

CHAPTER 1

INTRODUCTION

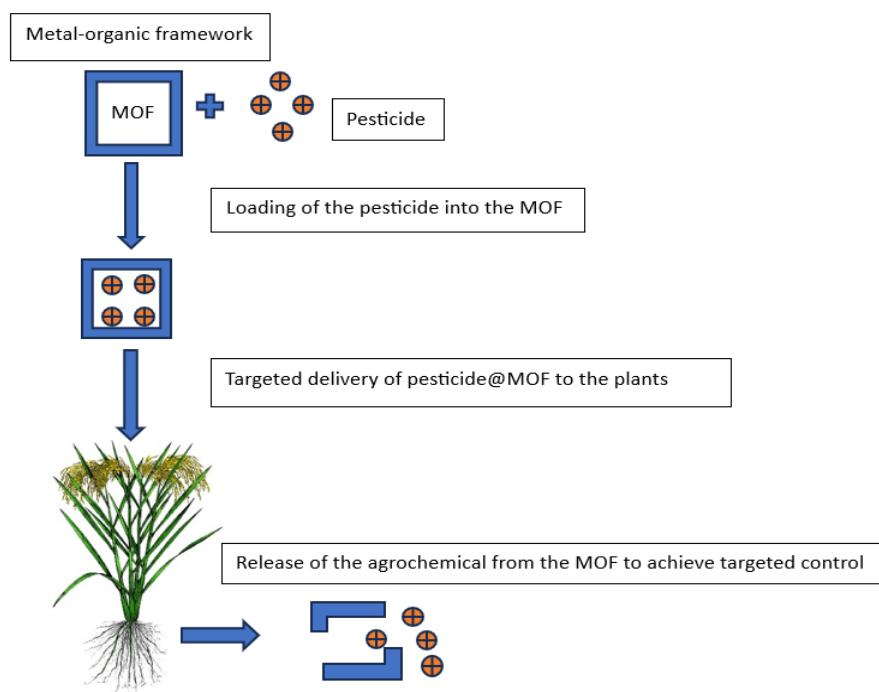
1.1 Background of the Study

The world's population is increasing rapidly and is projected to exceed 9 billion people by 2050. Currently, there are over 800 million undernourished people in the globe. By 2050, the number of undernourished individuals will rise to more than 2 billion depending on current food production and agricultural growth rates (Usman et al., 2020). The increase in agricultural productivity has therefore become the need of the hour. To enhance agricultural output and fulfill the global food demand, agrochemical production and consumption, such as the use of pesticides, fertilizers, and plant growth regulators have been rapidly expanding (Grillo et al., 2021). Pesticides worth more than \$3 billion tons, or \$55 billion, are being used to manage diseases in crop annually (Slattery et al., 2019; Pandey et al., 2018). By the year 2050, it is anticipated that the use of pesticides will increase by 2.7-fold to address the rising demand for food (Ecobichon, 2001; Kenawy et al., 1992).

Controlled agrochemical release as a reaction to environmental stimuli is essential to lower agricultural input, increase nutrient release efficiency, and reduce the harmful effects of pesticides on the environment as well as human health (Shan et al., 2020). To create controlled-release formulations (CRFs) of agrochemicals, a variety of inorganic and organic nanoporous materials, including clay minerals, activated carbon, siliceous compounds, organic and inorganic polymers, biochar, metal/metal oxide nanoparticles, etc., have been employed extensively (Yusoff et al., 2016). 'Metal-Organic Frameworks' (MOFs) represent complex porous crystalline substances consisting of metal nodes (such as Cu, Fe, Zn, Cr, Ti, Zr, Al, etc.) and organic linkers (such as O-donor linkers or N-donor linkers or both N and O-donor linkers) (Vasseghian et al., 2022), that can be used for this purpose (figure 1.1).

Figure 1.1

The Diagrammatic Representation of Use of Metal-organic Frameworks for the Controlled Delivery of Pesticides to the Plants, Minimizing Losses to the Environment.



MOFs offer infinite possible uses in sustainable agriculture because of their incredible features, especially as flexible agrochemical delivery systems. These properties include i) small cavities that are readily functionalized; ii) greater surface area and volume of the pores; iii) can be synthesized in large amounts; iv) more stable than other similar nano-porous materials; and v) prevents toxic effects in plants and animals as a result of their accumulation after degradation (Rojas et al., 2022). For example, a copper-based MOF (CuBTC) was reported by Liu and coworkers in 2022 as a non-toxic carrier of the insecticide Avermectin, transferring it efficiently and without any losses to the target (insect). The MOF was loaded with the insecticide Avermectin (AM@CuBTC) for controlling the Pine wilt disease in trees (Liu et al., 2022).

Similar to MOFs, there is a different group of porous material known as ‘Metal-Organic Polyhedra’ (MOPs), they are discrete, naturally porous geometries that are put together via coordination bonds between metal and a metal linker. MOPs are therefore viewed

as a subclass of coordination cages distinguished by their strong coordination connections, which are often ‘metal-carboxylates’, and ‘persistent porosity in the solid state’. Similar to their MOF counterparts, MOPs have a rich and complex structural chemistry. MOPs are similar to MOFs in terms of architecture and porosity (Albalad et al., 2022). MOP, being a porous monomer, can be polymerized by relying on the coordination interactions between labile metals and ligands (Carné-Sánchez et al., 2018).

Agrochemicals comprise chemical compounds used in agriculture such as fertilizers, chemicals for plant protection (insecticides, fungicides, herbicides, rodenticides, nematicides, etc.), and plant growth regulators and osmolytes (gibberellins, cytokinin, proline, glycine betaine, etc.). To reduce the gap between food production and consumption and fulfill the growing demand for food, agrochemicals are frequently used in agriculture. Traditional formulations of agrochemicals often evaporate, experience an early breakdown, or drift in the spraying before reaching the desired target. Because of this, farmers routinely add a great deal of agrochemicals to the plants and soil. This leads to an overuse of agrochemicals, which harms the environment (plants, soil, and water), and human health, and reduces agrochemical release efficiency (An et al., 2022).

Plants require fertilizers that contain primary elements such as nitrogen, phosphorus, and potassium to meet their nutritional demands. Urea, which meets 80% of plant requirements for nitrogenous fertilizers is extremely soluble in water and prone to loss (Q. Zhu et al., 2020). When nitrogenous compounds are sprayed to a rice field, denitrification, volatilization, runoff, and liquidation all lead to leaching. Leaching contributes between 30 and 50 % of the total nitrogen lost, predominantly as nitrate, denitrification, 10 to 30 % as N₂ volatilization, and 20 to 30 percent as ammonia. Oxides of nitrogen such as nitrogen dioxide (NO₂) and nitric oxide can pollute the air and water systems, causing eutrophication (An et al., 2022).

Only 0.1% of the pesticides used on agricultural fields reached the intended pests; 99.9% of them leaked into the environment due to the unregulated discharge of the pesticide formulations. It has also been demonstrated that pesticides containing organochlorines, such as DDT, are harmful to a wide range of animals, both terrestrial

and aquatic. The effects might be androgenic and estrogenic. Along with organochlorines, other major contributors to chronic toxicity in animals include organophosphates, pyrethroids, carbamates, thiocarbamates, triazoles, and triazines (Vasseghian et al., 2022).

A total of 3.5 million metric tons of agrochemicals were used worldwide in 2020. According to statistics provided by the UN FAO, out of 4.2 million tonnes of pesticides used annually in 2019, just over half (53%) were herbicides, followed by bactericides and fungicides (23%), and insecticides (17%). According to studies, exposure to pesticides can cause several health problems, which include neurological disorders, cancer, and birth defects. Pesticides can have both short-term and long-term detrimental effects on people (Laohaudomchok et al., 2021).

In Thailand, rice is an extremely significant crop economically. The total area under rice cultivation is roughly 10,407,272 hectares, and in 2018, 32 million tons of rice were produced for both international and domestic markets (Kongcharoen et al., 2020). Rice exported from various nations provide a significant source of income. Paddy crops are grown in a variety of locations with varying temperatures, climate, and soil-water parameters. Therefore, the productivity of paddy is greatly affected by a lot of biotic as well as abiotic stressors. Insect pests, fungi, bacteria, viruses, and herbicide toxicity are a few examples of biotic stressors that cause major damage to the crop. Due to damage from pests, diseases, and drought, the major rice-producing regions in Asia only reach 40% of the overall production efficiency (Anami et al., 2020).

Also, the yield of different food crops including rice are negatively impacted by different types of abiotic stressors, such as salt, drought, cold, and heat (El-Ramady et al., 2018). Cultivation of crops is significantly hampered by salt stress, which also harms plant health, seed germination, and total crop output. High-saline soils have adversely affected about 45 million hectares of irrigated land worldwide, causing an annual loss of 1.5 million hectares of agricultural land (Munns & Tester, 2008). High salinity has a variety of negative effects on plants, including water stress, malnutrition, ion toxicity, change of metabolic functions, membrane disorganization, reduced division of cells and growth, and genotoxicity (Abogadallah, 2010). When combined, these impacts slow down the growth, development, and yield of plants.

Plants have evolved various strategies for dealing with diverse abiotic stressors as a normal reaction to prevailing environmental challenges and to secure their survival. One of the most common methods used by plants to modify their osmotic potential in response to salt stress is the accumulation of appropriate noncytotoxic solutes at high cell concentrations. These suitable solutes vary amongst plant species and are distinguished by their low molecular weight and remarkable solubility (Hannachi & Van Labeke, 2018). ‘Osmolytes’ are quaternary amines, such as ‘betaines, sugars (mannitol, trehalose, and sorbitol), and amino acids (proline)’ (McNeil et al., 1999; Rhodes & Hanson, 1993). A quaternary ammonium molecule called ‘glycine betaine (GB)’ is one of the most important endogenous osmoregulators that helps to alleviate the negative effects of several abiotic stimuli on plant development, including salt, drought, heat, and light (Malekzadeh, 2015).

Abiotic stress frequently causes plants to start the biosynthesis of GB. Extreme drought conditions, together with frequently occurring heat and salt problems, might encourage the GB synthesis in higher plant chloroplasts, which protects the photosynthetic system from dehydration effects (Ashraf & Foolad, 2007a). Only a few species of plants, mostly those belonging to the Poaceae family and other halophytes, can biosynthesize and store GB in their tissues. This serves as a defense mechanism against abiotic challenges like salt (Annunziata et al., 2019). Additionally, it requires a lot of energy for GB to be biosynthesized in plant tissues (Mäkelä et al., 1996). To increase the plant's resistance to abiotic conditions like salt, GB hence be applied exogenously. Exogenous GB enhances abiotic stress-induced expression of genes in plant cells, which in turn limits ROS production and accumulation (Annunziata et al., 2019).

The exogenous application of GB is however subjected to losses from environmental factors viz. light, temperature, humidity, wind, microbes, pH, etc., which reduces its effectiveness and reduces farmer's profit. The production of formulations that are efficient, affordable, less toxic, and ecologically beneficial is therefore very crucial. In this context, MOFs and MOPs are particularly effective nanocarriers thanks to their advanced porous nature that enhances the effectiveness as well as efficiency of conventional agrochemical formulations.

1.2 Statement of the Problem

Crop diseases are the biggest threat to crop growth and production. Globally, it is known that 9,000 insects and mite species, 8,000 weed species, 50,000 species of fungi, bacteria, and viruses, and more than 50,000 species of plant pathogens cause crop damage. According to calculations, the farming sector might lose ‘78%, 54%, and 32%, respectively’, of its fruits, vegetables, and grain output if pesticides aren't utilized to control these pests (Singh et al., 2022). Therefore, it is imperative to use synthetic pesticides, such as fungicides, insecticides, herbicides, acaricides, nematicides, etc., to provide protection to crops against pests and fertilizers (mainly containing the major elements like N, P, and K) to boost total crop yields and attain global food security.

According to several studies (Kumar et al., 2019; Usman et al., 2020; Guha et al., 2020; Pourzahedi et al., 2018; Iavicoli et al., 2017; Miller, 2004), traditional agrochemical formulations like solutions, suspension, emulsifiable concentrate (EC), dust, granules, emulsions, etc., often exhibit very low use efficiency, and a large portion of the applied chemicals (98% of applied insecticides and 95% of herbicides) fail to reach their intended targets. This is a result of excessive run-off, inconsistent application rates, or poor rates of absorption or adsorption. Before reaching the intended area, traditional fertilizers lose between ‘50 and 70 % of the nitrogen, 80 % of the phosphorus, and 60 % of the potassium’ they contain in the environment. Over 50 percent of these nutrients are lost through leaching and runoff and they end up in groundwaters and surface waters (Guha et al., 2020; Pourzahedi et al., 2018).

Because of this, traditional agrochemicals frequently need to be applied more than once and in higher concentrations to control pests and give necessary nutrients (Usman et al., 2020, Kumar et al., 2019; Guha et al., 2020; Pourzahedi et al., 2018; Iavicoli et al., 2017). The extensive use of traditional fertilizers, pesticides, and other chemicals has negative impacts on non-target species, pollutes soil and water, exposes more people to pesticides through the food chain, and increases pathogen resistance to pesticides, in addition to raising input prices.

Apart from the pests and diseases, the productivity of crops can be seriously threatened by some abiotic stressors like drought, salinity, heat, UV radiations, and extreme temperatures (Mahmood-ur-Rahman et al., 2019a). Among all, drought and salinity

stress are the ones that can cause major losses in the yield of the crop. A diverse range of substances, including ‘compatible solutes’ such as GB, trehalose, and proline, as well as ‘plant growth regulators’ such as gibberellic acid, cytokinins, paclobutrazol, and salicylic acid, are currently being studied for their potential to alleviate the effects of ‘drought and salinity stress’ (Tisarum et al., 2019).

GB serves as a pivotal component in cell ‘osmotic adjustment, organelle maintenance (chloroplasts, mitochondria), and water-use efficiency in plants’ during water stress. It is an osmolyte accumulated in plants against drought and salinity stresses (Ashraf & Foolad, 2007; Kurepin et al., 2015). According to reports, rice crops are GB non-accumulating plants with very little amount of GB [$1 \mu\text{mol g}^{-1}$ dry weight (DW)]. However, it can be exogenously applied to the rice crop just like the other agrochemicals to protect the crops from stress conditions. Externally administered GB may assist in mitigating the effects of environmental stressors such as salinity and drought, as well as promote stress recovery (Ashraf & Foolad, 2007).

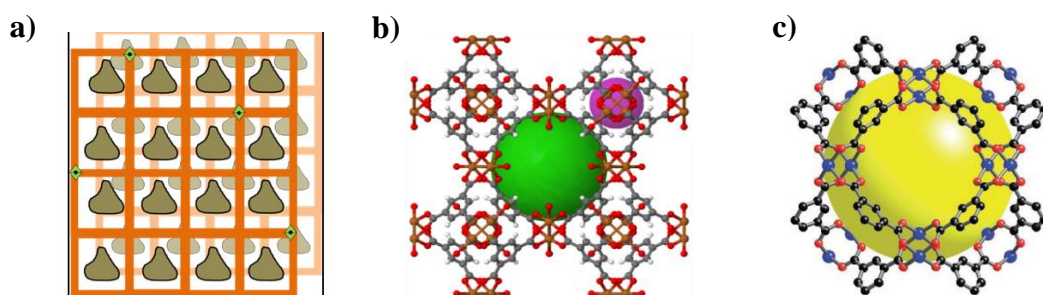
To enhance the stability and efficacy of agrochemicals while being used, to reduce the abuse of agrochemicals, and to solve the problems caused by application of the agrochemicals on plants, soil, water, and human health, they must now be delivered to plants in a regulated and targeted manner, necessitating the adoption of novel techniques. Many different methods have been developed by researchers to encapsulate agrochemicals within an appropriate host material to ensure their controlled release. A few inorganic/organic nanocarriers have been devised to carry agrochemicals, including metal or metal oxide nanoparticles, dendrimers, nanomaterials based on carbon, silica, and polymeric micelles (J. Yang et al., 2021). However, they have major limitations that significantly restrict their use in agriculture, including poor biodegradability, limited cargo loading capacity, and uncontrolled drug release (J. Yang et al., 2021).

Therefore, researchers have developed a variety of methods to enclose these agrochemicals inside porous solid materials having both organic and inorganic traits given all the capabilities. MOFs are a class of incredible and newly developed organic-inorganic hybrids that have been used in agriculture because of their exceptional physical and chemical characteristics, such as their ease of synthesis and

functionalization, adjustable pore sizes, flexible arrangement, high surface area, high biocompatibility, high cargo load capacity, and fine biodegradability (J. Yang et al., 2021). Moreover, little study has been done on the application of ‘Metal-Organic Polyhedra’ (MOPs) in agriculture.

Figure 1.2

Schematic Diagram of a) OPA-MOF, b) HKUST-1, and c) Cu-MOP-1



1.3 Objectives of the Study

Following are the objectives of the present study:

1. To create Copper-based MOPs (Cu-MOPs) from Basic copper carbonate and Isophthalic acid, and 5-Amino isophthalic acid.
2. To evaluate the capacity of the MOPs to encapsulate and release Glycine Betaine (GB), an osmolyte, at various pHs compatible with specified plant and soil conditions respectively.
3. To use the MOP that provides improved encapsulation and release for controlled delivery of GB for the treatment of salinity stress in rice plants.

1.4 Scope of the Study

The current work intends to create porous copper-based Metal-Organic Polyhedra (Cu-MOPs) that can encapsulate Glycine betaine (GB), evaluating the encapsulation capability, loading percentage, and stability of the product. Additionally, this research attempts to accomplish a regulated release of GB from MOPs over time under pH values suitable to specified plant and soil conditions. Finally, the encapsulated MOPs will be employed to deliver GB to rice plants for salinity stress management.

1.5 Limitations of the Study

Following are the limitations of the current study:

1. Since the MOPs are made of copper, excessive amounts of copper can lead to toxicity in soil and the environment.
2. The study involves the assessment of MOPs made of only one element (Cu).
3. The size of the MOP cages is well-defined, they can't be changed (less flexible).
4. The study involves the assessment of only one type of guest chemical (Glycine Betaine) and one crop (rice).
5. Due to the experiment's short duration, impacts at the key fruiting stage could not be seen. The effects of GB were only evaluated up to the seedling stage.

1.6 Organization of the Study

The thesis is organized into the following parts:

- Chapter 1. Introduction
- Chapter 2. Review of Literature
- Chapter 3. Methodology
- Chapter 4. Results and Discussions
- Chapter 5. Conclusions and Future Recommendations

CHAPTER 2

REVIEW OF LITERATURE

Crops are attacked by many different biotic and abiotic stressors. Biotic stressors comprise fungi, bacteria, viruses, viroid, nematodes, weeds, and insects (Natalini & Palma, 2023). Numerous different chemical classes are utilized as pesticides, and a wide range of pesticides are made to kill certain pests. Although pesticides provide many benefits for protecting crops, inappropriate pesticide application can have a variety of unfavorable effects (such as toxic residues that pose possible health risks and contaminate the environment) (S. Kumar et al., 2019b). Traditional pesticide formulations have several issues, including ‘poor solubility in water, non-selective action, and uncontrolled release in the environment’, which leads to overuse of pesticides by farmers (Beggel et al., 2010; Birnbaum, 2013; Grant et al., 2011).

In addition to biotic stressors, abiotic stressors like ‘drought, soil salinity, extreme heat and cold, and heavy metals’ are significant limiting variables impacting crop output both qualitatively and quantitatively. However, exogenous treatments utilizing small biomolecules can reduce the harmful consequences of stress caused by non-living factors. For instance, the foliar application of biomolecules such as ‘melatonin’, ‘glutathione’, ‘proline’, and ‘glycine betaine’ reduce the negative impacts of abiotic stresses on plants and offers an alternative to the use of transgenic plants, therefore these compounds are required to counteract abiotic stresses (Khalid et al., 2022). However, their broad usage is constrained by technical issues with field application, potential side effects, and challenges in figuring out the right dose. Attention has been drawn to nano-encapsulated systems because they provide regulated distribution of active ingredients and shield them with biomaterials from the environment (Sampedro-Guerrero et al., 2023).

Plants need fertilizers to fulfill their nutritional demands (nitrogen, phosphorus, potassium, and other elements) which is necessary for their growth and development. They are crucial to agricultural productivity, yet conventional delivery methods are inefficient, which causes environmental deterioration and other issues. Around 50–55 % of the increase in crop productivity in emerging countries was due to chemical

fertilizers (Babu et al., 2022). However, use efficiency of the applied nutrients is very low, such as ‘nitrogen (30–40%), phosphorus (15–20%), potassium (50–55%), and micronutrients (2–5%)’ (Babu et al., 2022). This caused an excessive amount of soil nutrient mining, which resulted in a net negative soil nutrient balance of about 10 million tonnes and negatively impacted the health of the soil (Chugh et al., 2021). Unchecked use of agrochemicals raises agricultural costs and lowers farmer profits (Diatta et al., 2020). For example, using nitrogenous fertilizers excessively harms the groundwater and results in eutrophication in aquatic habitats (Chhipa, 2017; Ye et al., 2020).

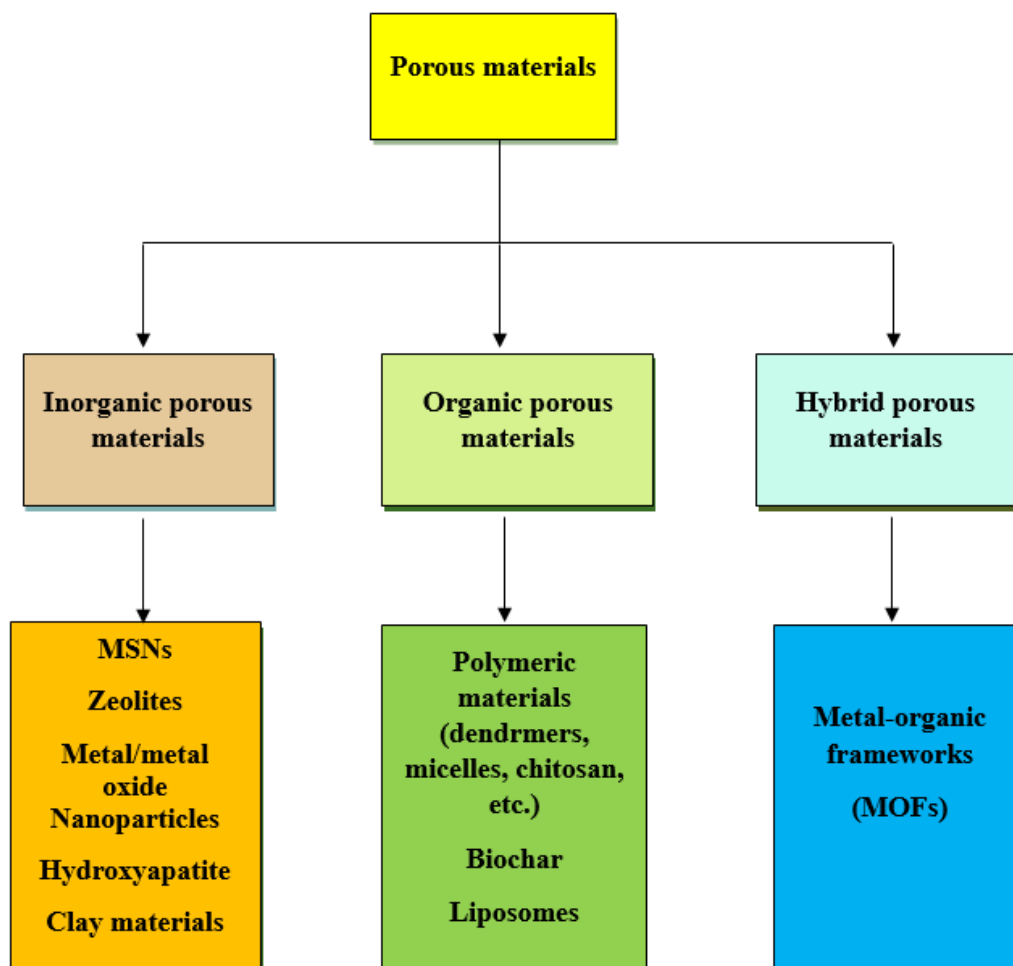
Controlled delivery systems for pesticides, fertilizers, and other chemicals that are used to mitigate the abiotic stressors in plants could increase their effectiveness and decrease runoff into the environment, helping to reduce environmental pollution brought on by the overuse of agricultural inputs. Agriculture may become sustainable by depending on new approaches that might boost agricultural output while protecting environmental quality.

2.1 Porous Materials in Agriculture

Due to essential features including vast surface area, adjustable pore size, simple access to active regions, and their inherent property to control diffusion, porous materials were discovered as the best-suited carrier to address the aforementioned drawbacks in agrochemicals. The use efficiency of agrochemicals has been found to increase as a result of using porous materials, to reduce the agrochemical load (Sharma et al., 2021). These characteristics not only allow a slow and regulated release but also enable these substances to hold onto a significant quantity of fertilizers and pesticides inside their structure (Singh et al., 2022). Porous materials consist of inorganic, organic, and hybrid types and include materials like hydroxyapatite, zeolite, nano-clay, mesoporous silica NPs (MSNs), charcoal, polymers, carbon-based materials, and metal-organic frameworks (MOFs) (Figure 2.1). They have been extensively researched for fertilizer, herbicide, pesticide, and sensing uses (Sharma et al., 2021).

Figure 2.1

Flowchart Representing Different Porous Materials used for Agrochemical Delivery in Agriculture.



Porous materials are categorized as macroporous (pore size greater than 50 nm), mesoporous (2-50 nm), or microporous (less than 2nm) (L. Wu et al., 2020). Some of the nano-porous materials used more often to distribute agricultural pesticides and fertilizers are listed in Table 2.1.

Table 2.1*Different Pesticides Nanocarriers (Singh et al., 2022)*

Materials	Insecticides loaded	Formulation release
Silica nanoparticles grafted with alginate	Lambda-cyhalothrin	Emulsion
Biogenic silica grafted with Neem bark extract	Azadirachtin	Immersion
Mesoporous silica	Thiamethoxam	Methanol solution
Tetrabutylammonium bromide	Avermectin	Dialysis
Carbon nanoparticles	Emamectin	Physical adsorption
Cellulose-based microcapsule	Chlorpyrifos	Acetone solution
Polydopamine@poly (N-isopropyl acrylamide)	Imidacloprid	Solution in water
Mesoporous Silica Nanoparticles	Iron	Stimuli-responsive
OPA-MOF (Oxalate-Phosphate-Amine-based MOF'S)	Iron and Phosphate	Cation Exchange
Surfactant Modified Zeolite A (SMZ)	Phosphate	---
Sodium Alginate	Nitrogen	Light triggered

2.2 Metal-Organic Frameworks (MOFs) in Agriculture

Classical porous materials including zeolites, MSNs, and activated carbon, despite their reduced cost and better stability, have certain drawbacks such as irregular pores, non-uniform structure, and a lack of clear structure-property connections. As a result, much scientific research is still being conducted to develop higher-performing superior porous materials for diverse applications (Jiao et al., 2019).

MOFs are relatively a new family of substances that combine both the organic and inorganic features of porous materials, they are created using strong connections to link inorganic and organic components (reticular synthesis). Organic components are typically ditopic or polytopic carboxylates (as well as other similarly negatively charged compounds) that, when connected to metal-containing components, produce

structurally rigid crystalline structures with typical porosity of more than 50% of the MOF crystal volume. Surface area values for such MOFs generally vary from 1000 to 10,000 m²/g, surpassing classic porous materials like carbons and zeolites (H. Furukawa et al., 2013).

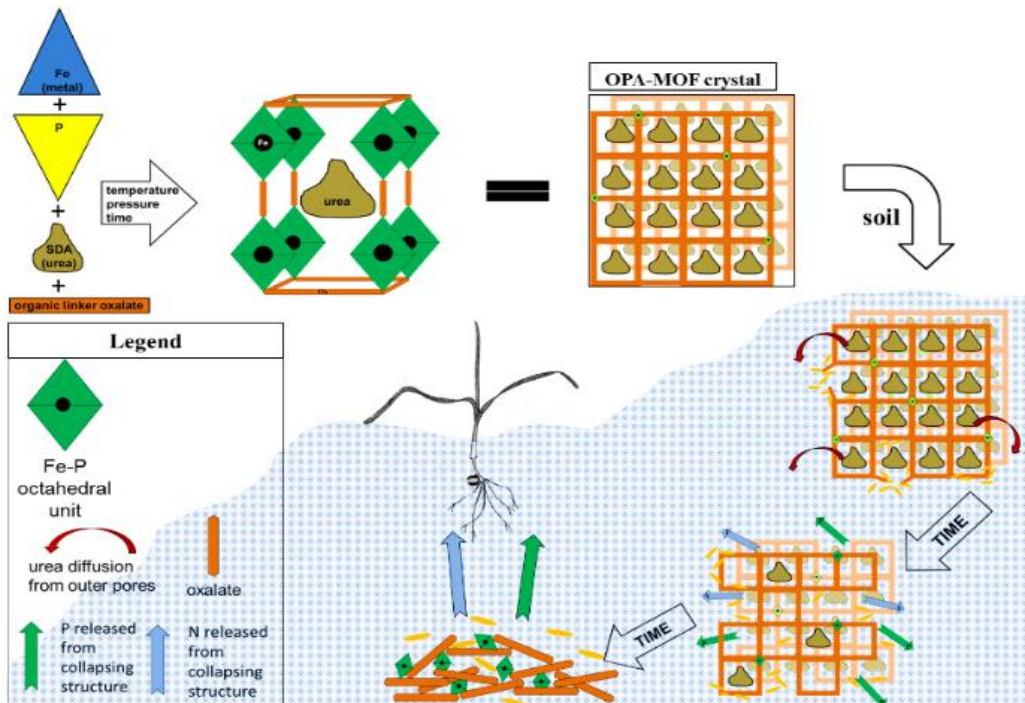
In general, the inorganic nodes of MOFs that are made up of metal cations can be monovalent such as Ag⁺, Cu⁺, etc., divalent such as Mg²⁺, Fe²⁺, Mn²⁺, Cu²⁺, Ni²⁺, Co²⁺, Cd²⁺, Zn²⁺, etc., trivalent such as Sc³⁺, V³⁺, Al³⁺, Fe³⁺, Cr³⁺, Ga³⁺, In³⁺, etc., or tetravalent such as Ti⁴⁺, Zr⁴⁺, Hf⁴⁺, Ce⁴⁺, etc. (Yuan et al., 2018). The researchers have extensively investigated the use of MOF in the storage of gas, drug storage and delivery, size, shape, and enantio-selective catalysis, gas or vapor separation, and fluorescent, and luminescent materials (Kuppler et al., 2009), however, their use in agrochemical delivery is a new sector.

MOFs are excellent porous materials for transport, encapsulation, and controlled release of fertilizers, pesticides, and growth regulators with minimal loss. In addition, to serve as a nanocarrier for the fertilizer's delivery, MOFs can serve as a self-nutrient supplier. Because of their porous nature, MOFs can easily interact with plants both through their interior and exterior surfaces (Chauhan et al., 2022).

The usage of an iron-based MOF ('OPA-MOF', OPA: oxalate–phosphate–amine) for possible agrochemical delivery was first reported and shown in 2015 by Anstoetz et al. OPA-MOFs, which are composed of an 'iron-phosphate' center connected by oxalate, showed the 'slow release of N (urea) and P (phosphate) fertilizers' through microbial oxalate breakdown. The release of N was demonstrated to be quick; however, the bioavailability of P was substantially lower than that of traditional phosphate fertilizers, which might be ascribed to soil acidity caused by MOF breakdown. Nevertheless, it was a good example of the potential of MOFs for slow and controlled-release farming operations (Figure 2.2) (Anstoetz et al., 2015).

Figure 2.2

A Conceptual Diagram on how OPA-MOF is Produced, how Bacteria break down the Structurally Integrated Oxalate, and how this Mineralization occurs when Applied to Soil (Anstoetz et al., 2015).



An example of the use of ‘MOFs’ for encapsulating fungicide was reported by Zhao et al. in 2022. An ‘iron-based MOF’ was loaded with tebuconazole fungicide. The amount of loading was around 30% by weight, and controlled release trials indicated that the release was gradual and persistent, reaching around 91% in 30 hours. Tebuconazole's phytotoxic effects on wheat seedlings decreased when the loaded MOFs were used in comparison to tebuconazole which was treated traditionally. The plants displayed improved growth regarding the ‘weight, length, and chlorophyll content’ as a result of the MOFs' supply of the iron nutrient, in addition to their antifungal effects (Zhao et al., 2022).

The insecticide Avermectin was loaded onto the ‘MOF CuBTC’ to combat the bug *Bursaphelenchus*. With a total release of 92% in 12 hours, it was discovered that the regulated release was pH-dependent. The insecticide was targeted directly to the insect larvae' intestines by injecting dead wood with the loaded MOF. Avermectin was also

shielded against photodegradation by the MOFs, with a retention of 69% after 120 hours at a pH of 9.0 (Liu et al., 2022).

Atrazine (herbicide) was loaded onto MOF-5, which was based on zinc terephthalate, in research reported by Lee et al. Following that, they created a composite using poly (vinyl alcohol)/starch (PVA/ST) by electrospinning the loaded MOF-5. According to research on herbicide release, putting the herbicide into MOFs and then creating composites resulted in lower herbicide release rates than combining atrazine with the polymer matrix (Lee et al., 2022).

Zhang et al. created MOFs based on copper with the specific purpose of encapsulating the plant hormone ethylene. The ripening of climacteric fruits, such as avocados and bananas, was managed with the use of these MOFs (Shan et al., 2020).

2.3 Copper-based Metal-Organic Frameworks (Cu-MOFs)

Generally, copper (Cu II) is the most employed metal in MOFs. The distinguished features of copper-metal organic frameworks (MOFs) include distinctive pore sizes, redox activity, varied proportions, biocompatibility, flexible design, high loading capacity, and increased biocompatibility (Liu et al., 2020). Copper-based MOFs can be employed as a nanocarrier for agrochemicals and as a nutrient supplier by releasing copper ions owing to MOF breakdown under various environmental conditions.

Copper (Cu) is one of the eight essential plant micronutrients, others include iron (Fe), boron (B), zinc (Zn), molybdenum (Mo), nickel (Ni), chlorine (Cl), and manganese (Mn) (Welch & Shuman, 1995). Copper is crucial for CO₂ assimilation and ATP production. It is the primary component of proteins like cytochrome oxidase and plastocyanin, which are both involved in the photosynthetic process. Generally, 5–30 mg kg⁻¹ Cu is considered to be safe in plant tissues. The suggested amount of copper for food crops is 30 mg kg⁻¹. ‘Normal soil Cu concentrations vary from 2.0 to 100 mg kg⁻¹’ (Kumar et al., 2021). Both monovalent (+1) and divalent (+2) forms of copper can be found in biological systems (Mir et al., 2021).

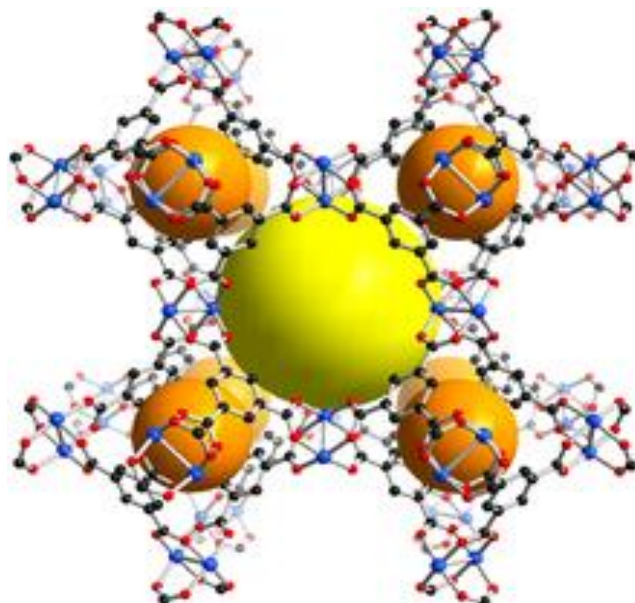
Cu²⁺ is known for its antifouling, antifungal, and antibacterial qualities, which makes it useful in agriculture not merely as fertilizer but also for managing plant diseases

(Sierra-Serrano et al., 2022). Copper was classified as a pesticide by the USEPA in 2008, and copper-based substances are widely utilized in different agricultural situations. Every year, millions of tonnes of copper are used, mainly for crop protection. Cupric ions, the active ingredient in copper pesticides, may be found in a wide range of formulations, including different salts and complex forms (Husak, 2015). Furthermore, copper (Cu), as a traditional transition metal, is regarded as one of the most appealing catalysts for usage in the oxidation of alcohols due to its abundant supply, low price, non-toxic qualities, and high catalytic effectiveness (Taher et al., 2017).

The initial report on Cu-MOF 1, also known as HKUST-1, was published in the year 1999 (Chui et al., 1999). The structure comprises a 1,3,5-benzene tricarboxylate (BTC) ligand that interacts with copper ions within a cubic lattice arrangement, specifically adopting the Fm-3m space group. It has a 3-dimensional system of intersecting big, 9 x 9 Å square-shaped pores. Cu (II) ions form dimers within the HKUST-1 structure, with each copper atom forming a connection with four atoms of oxygen from the water molecules and the BTC linkers. The initial coordination sphere of the Cu (II) ion contains water molecules, indicating that these species may eventually acquire a coordinative void (Lin et al., 2012). HKUST-1, because of its high porosity is an excellent option for the regulated release and encapsulation of agrochemicals.

Figure 2.3

Structure of HKUST-1 (A Copper-based MOF)



2.4 Metal-Organic Polyhedra (MOPs)

‘Metal-Organic Polyhedra’ (MOPs) are analogues of MOFs and a distinct class of coordination cages, that may host and adsorb species in solutions and have permanent pores in the solid state (Carné-Sánchez et al., 2019). MOPs use directed metal-ligand coordination interactions that may be used to create discrete molecular structures with interior cavities. The molecular composition and hybrid metal-organic surface of the MOPs offer a strong orthogonal surface reactivity which may be accessed in both the solution and solid states (Khobotov-Bakishev et al., 2022).

On the MOP’s surface, the various functional groups may be precisely counted and located and as a result, their chemical reactivity, stability, and processability may be carefully controlled while retaining their porosity (Legrand et al., 2019). However, the persistent porosity of MOPs in the solid state stems from the fact that, unlike other coordination cages, their cavities remain intact as they activate or dissolve (Gosselin et al., 2020, Lee et al., 2021). Spherical MOPs, often referred to as nanocages or nanospheres, are single-cage structures as opposed to the infinite metal-organic coordination networks made by MOFs.

MOP's polyhedral structure offers structural features like (i) two established surfaces (internal and external), (ii) a single internal cavity, which can be accessed through the cage's windows, (iii) orthogonal, directional, and finite reactive sites on both surfaces (i.e., axial metal sites and organic functionalities), and (iv) versatile solubility, which are not present in MOFs (Albalad et al., 2022). A variety of organic linkers and metal ions were used to create metal-organic polyhedra (MOPs), with two kinds of MOPs, pyridine- and carboxylate-based MOPs, being the most common (Samanta S., 2023). Some of the important MOPs present in the literature are stated in Table 2.2.

Table 1.2

List of Some Metal-Organic Polyhedra (MOPs) in Literature

MOPs	Ligands used	Reference
$\text{Cu}_{24}(\text{1,3-bdc})_{24}$	Isophthalic acid	(T.-H. Chen et al., 2016)
$\text{Mo}_{24}(\text{t Bu-bdc})_{24}$	5-tert-butyl-isophthalate	(Lorzing et al., 2019)
$\text{Cu}_{24}(\text{NH}_2\text{-bdc})_{24}$	5-amino-isophthalate	(Xie et al., 2019)
$[\text{Rh}_2(\text{bdc})_2]_{12}$	Isophthalic acid	(S. Furukawa et al., 2016)
$\text{Cr}_{24}(\text{OH-bdc})_{24}$	5-hydroxy-isophthalate	(Lorzing et al., 2017)
$\text{Cu}_{24}(\text{NO}_2\text{-bdc})_{24}$	5-nitro-isophthalate	(T.-H. Chen et al., 2016)

Three types of ligands were found to be coordinated with the metal ions: those comprising N donors, those containing O donors, and those having mixed donor atoms. However, N donor-based ligands are more stable than O donor-based ligands (Samanta S., 2023). Typically, MOPs are created by a 'coordination-driven self-assembly process' by bringing together the 12-metal ion paddle wheel and 24 carboxylate ligands. But MOPs made of labile metal-carboxylate bonds easily break down when guest molecules especially solvent molecules are removed from the cavities (Zhao & Yan, 2020).

MOPs behave as porous monomers in the construction of long porous networks due to their unique surface reactivity and intrinsic porosity, however, the lack of stability, solubility in required solvents, and limited reactivity of MOPs have long prevented them from being used as monomers for subsequent self-assembly reactions (Mollick et al., 2019). Solubility of MOPs can however be increased by modifying the surface of the MOPs with bulky groups to prevent them from interacting with each other or by using hydrophobic or hydrophilic moieties to increase their solubility in the organic solvents or water respectively (Khubotov-Bakishev et al., 2022).

Methods to improve the stability and robustness of MOPs in the solution include one of the following: protecting the metallic node, using metal ions that can form strong intermetallic connections, boosting the strength of the metal-ligand interaction, or utilizing chelating groups (Khubotov-Bakishev et al., 2022). Metals ions having higher valence with high coordination numbers form strong intermetallic bonds and can form MOPs of high stability, for example, Rhodium (Rh) metal forms MOPs having unique, sturdy structures, simple processabilities, and various functionalities due to the strong Rh-Rh bonds in the paddle-wheel units and the diverse chemistry of unsaturated Rh sites (Zhao & Yan, 2020).

Zhang, as well as Furukawa and Kitagawa, used the di-rhodium paddle-wheel motifs, which have strong rhodium-rhodium and rhodium-carboxylate bonds, independently to create reliable Rh (II)-based MOPs. However, being one of the earth metals, rhodium is toxic to plants and the environment. Also, Rhodium-based MOPs are not as biocompatible to the plants as copper is, they are robust and stable; as a result, they do not break easily and accumulate in the soil, which might be hazardous to the soil if used in high quantities.

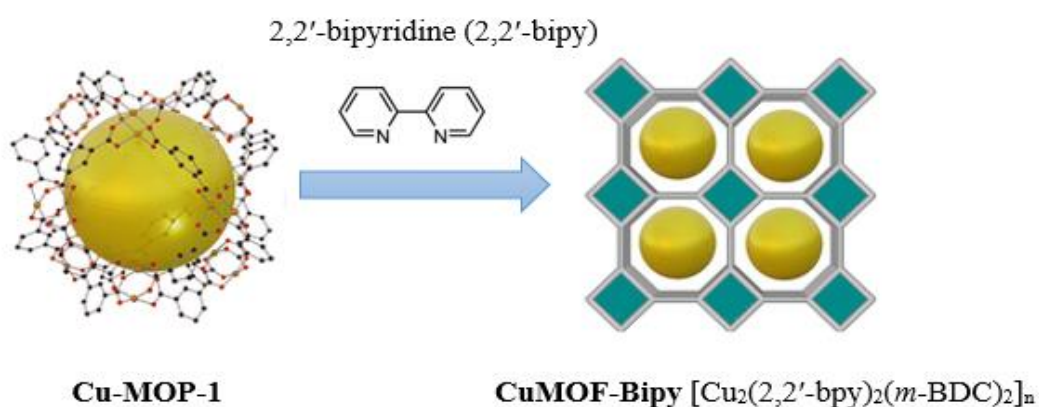
MOPs may self-assemble into porous networks that are both crystalline and amorphous via Coordination-driven Self-assembly. Open metal sites in MOPs that are exposed have been used to drive this process. Three distinct forms of coordination reactions may be used to accomplish it. One of them involves self-assembly of the MOP after being surface-functionalized with coordinating moieties (McManus et al., 2004), linkage of MOP monomers through N-based ditopic ligands (Chun et al., 2009; J.-R. Li et al., 2009), this technique has been utilized effectively to convert MOPs into

crystalline MOFs using rigid ligands, to create soft amorphous materials using flexible ligands, and to assemble MOPs by coordinating them with additional metal ions (Grancha et al., 2021).

MOPs can also be assembled via Supramolecular Non-coordinative bonds that involve non-covalent interactions including ‘ π - π stacking’, ‘H-bonding’, and ‘hydrophobic/hydrophilic’ or ‘electrostatic interactions’ (Gosselin et al., 2020). Another process to assemble MOPs is Covalent Polymerization which utilizes strong covalent bonds (Nam et al., 2017).

Figure 2.4

Schematic Representation of the Conversion of Cu-MOP-1 as a Porous Monomer to Cu-MOF-Bipy Framework by using Bipyridine as a Rigid N-based Ditopic Linker (Abbas et al., 2023).



2.5 Copper-based Metal-Organic Polyhedra (Cu-MOP):

The most extensively studied MOPs are known as Cu-MOPs, which are primarily made of 1,3-benzendicarboxylate (BDC) derivatives and Cu (II) paddle-wheel clusters. They are easily fabricated in the presence of an organic base by the spontaneous production of Cu (II)-carboxylate linkages. In contrast, since the coordination interaction between Rhodium metal and lateral carboxylate groups of the paddle-wheel structures are inert, the ligand replacement process using Rh (II) acetate dimers must take place at nearly extreme conditions. So, microwave and solvothermal heating methods were used to create the Rh (II)-based MOPs (Zhao & Yan, 2020).

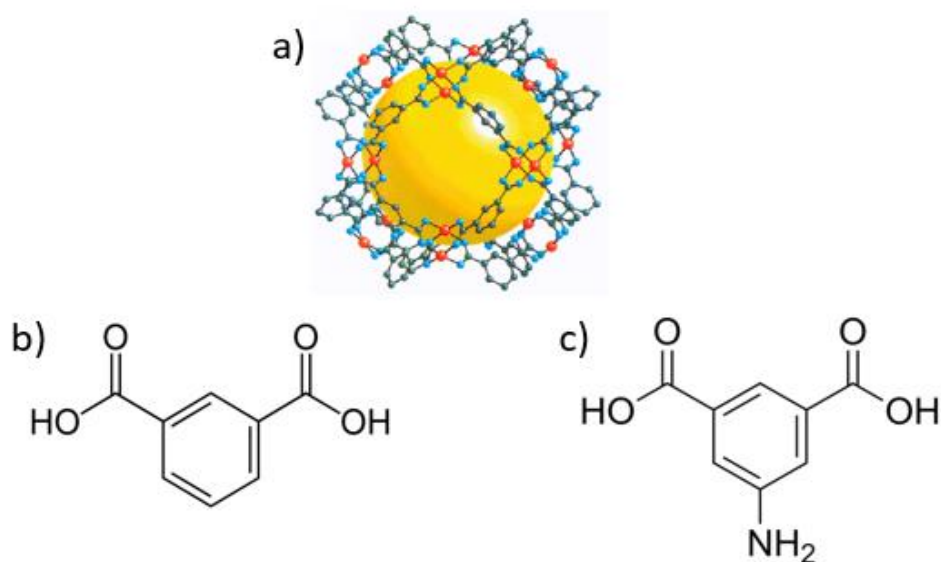
Cu-MOPs, however, have less hydrolytic and chemical stability as a result of the lability of the Cu-carboxylate bond. The ability of Cu-MOPs to undergo covalent polymerization and coordination processes may be restricted. The high surface density of functional groups found on MOP can be used by external agents to communicate with the labile nodes and increase the stability of Cu-MOPs by shielding the weak metal-carboxylate bonds from ligand exchange or hydrolysis (Li & Zhou, 2010).

To accomplish this, the MOP's organic backbone is connected to an organic shell around it. The type of shielding utilized might be either hydrophobic or hydrophilic depending on the shell. Zhou et al. described a method to stabilize the Cu-MOPs by covalently attaching polyethylene glycol chains to a cuboctahedral Cu-MOP (named *pi-CuMOP*; also known as 'Cu(pi)') formulated as $[\text{Cu}_2(\text{pi})_2]_{12}$ (in which *pi* refers to the ligand '5-(prop-2-ynoxybenzene)-1,3-dicarboxylic acid'), via a 'copper(I)-catalyzed, azide-alkyne cycloaddition'. The resulting structure showed greater stability and prevented interactions between the water molecules and the Cu (II) paddlewheel (Zhao et al., 2011).

Yaghi et al. reported the formation of a robust metal-organic cuboctahedron by Cu (II) ion bonding with carboxylate groups on a benzene ring. This structure was successfully produced by heating a 1:1 combination of copper nitrate and the ligand benzene-1,3-dicarboxylic acid to 85°C. Dimethylformamide (DMF) was used as the main solvent in the process, while ethanol was used as a co-solvent (Eddaoudi et al., 2001).

Figure 2.5

Schematic Diagram of a) Cu-MOP-1, b) Benzene-3,5-Dicarboxylic Acid linker, and c) 5-Aminobenzene-1,3-Dicarboxylic Acid Linker



2.6 Abiotic Stressors Affecting Plants

A multitude of both living organism-related (biotic) and non-living environmental (abiotic) stresses detrimentally affect the crops. Among the abiotic stressors such as salinity, drought, heat, extreme temperatures, UV radiation, etc., drought and salinity stress can cause the highest loss in yield (Mahmood-ur-Rahman et al., 2019). The salinity of the soil is an unfavorable environmental variable that significantly affects crop growth, yield, and seed germination (Y. Yang & Guo, 2018). Plants exposed to salt stress can experience ionic and osmotic effects, such as disruption of membrane structure, metabolic toxicity, and the production of reactive oxygen species (ROS) like hydrogen peroxide (H₂O₂), which can lead to oxidative damage. ROS can interact with various sorts of biomolecules, including DNA, proteins, and lipids, resulting in radical chain reactions, peroxidation, and membrane leakage (Abdus Sobahan et al., 2016).

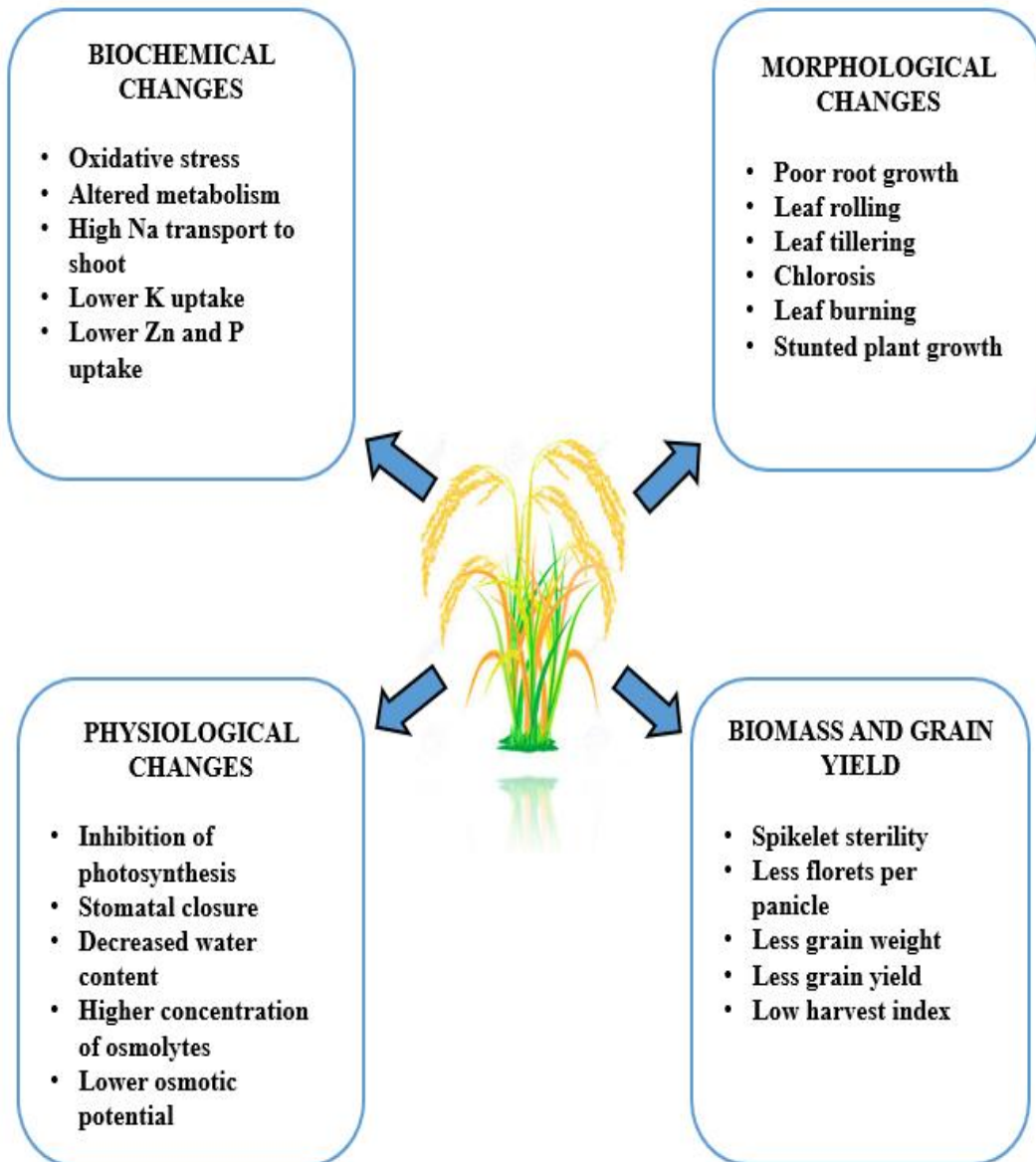
Known by its Scientific name, *Oryza sativa*, and a member of the Gramineae family, rice is the staple diet of more than 50% of the global population (Brar et al., 2017). Rice crops are very sensitive to salt stress which causes decreased growth, grain output, and development (S. Ahmed et al., 2021). Under high salt conditions, plants experience

morphological changes such as impaired root system, chlorosis, reduced tillers per plant, decreased biomass, fewer spikelets per panicle, shorter plant height, reduced grain weight, and a greater number of sterile florets, which ultimately lower harvest indices and grain yield (Hakim et al., 2014; Machado & Serralheiro, 2017; Razzaq et al., 2020; van Zelm et al., 2020). Beyond morphological changes, salinity stress in rice plants also causes modifications in physiological processes such as water control and photosynthesis, as well as changes in biochemical pathways and yield indices including grain quality and quantity (Figure 2.6) (Razzaq et al., 2020).

Pathum Thani-1 (PTT1), a widely favored aromatic rice cultivar in Thailand, is highly sought after for cultivation in irrigated lowland areas owing to its exceptional yield and excellent cooking characteristics. Its popularity stems from its ability to be grown throughout the year, attributed to its insensitivity to changes in photoperiod, allowing for up to three crop harvests annually. However, according to reports, both the 'seedling and reproductive stages' of PTT1 are sensitive to salt stress, which limits its growth and yield (Cha-Um & Kirdmanee, 2007). In comparison to salt-tolerant cultivars that express genes linked to starch metabolism during salt stress, it has been discovered that the sensitive cultivar (PTT1) showed decreased starch breakdown and lower sugar accumulation in plants under salt stress (Rahman et al., 2017).

Figure 2.6

Adverse Effects of Salt Stress on Rice Plants



2.7 Role of GB in Salinity Stress Tolerance

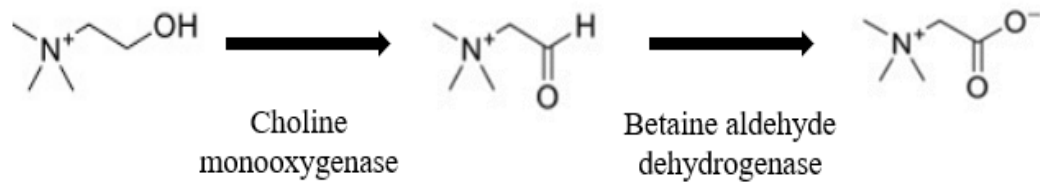
Glycine betaine (GB) is a quaternary amine with a zwitterionic character, it is naturally accumulated in a variety of species and is linked to abiotic stress tolerance. These "compatible solutes" or "osmolytes" are low-molecular-weight water-soluble substances. GB is prevalent primarily in chloroplasts, where it is essential for thylakoid membrane modification and protection, preserving photosynthetic efficiency. Glycine betaine plays an important role in increasing the salt tolerance of plants by osmotic adjustments. The osmotic balance in the roots and leaves helps to maintain water absorption and turgidity of the cell, enabling physiological activities such as photosynthesis and cell expansion to occur (Abdus Sobahan et al., 2016).

Studies have shown that plants that collect GB naturally, thrive in salty and drought-prone environments. Additionally, many plants that would not ordinarily be able to accumulate GB are made salt-tolerant by an exogenous supply of GB (Sidhu Murmu & Purnendu Sekhar Bera, 2017). Proline content in salt-tolerant cultivars increases as a result of exogenous GB application, however, exogenous GB application leads to a decrease in proline levels in salt-sensitive cultivars (Demiral & Türkan, 2006).

The primary function of GB in mitigating salt stress is to modify the uptake of nutrients, as it substantially lowers the concentration of Na^+ in plant tissues while simultaneously increasing the concentration of K, N, and P. This improves osmosis, and the growth and development of plants stressed by NaCl, and to a lesser degree, strengthens the defense system of antioxidants (Sofy et al., 2020). GB naturally accumulates at high concentrations (4–40 $\mu\text{mol g}^{-1}$ FW) in plants such as sugar beet and spinach and functions as an osmoregulator under abiotic stress conditions (Chen & Murata, 2011). Plants that naturally collect GB have been shown to thrive in salty and drought-prone environments (Chen & Murata, 2008). In plants, two enzymatic processes convert choline into an intermediate aldehyde and subsequently to GB (Figure 2.7).

Figure 2.7

Biosynthesis of Glycine Betaine in Higher Plants



Major grains like maize, wheat, and barley don't usually collect GB a lot (Niu et al., 2007). This could be primarily a result of these grains producing decreased transcripts for the GB synthesizing enzyme. Rice crops are GB non-accumulator plants with very little GB present in tissues ($1 \mu\text{mol g}^{-1}$ dry weight (DW)) (Rathinasabapathi et al., 1993). However, the overexpression of GB biosynthesis-related genes, such as 'BADH' ('betaine aldehyde dehydrogenase'), and 'CMO' ('choline monoxygenase') has increased abiotic stress tolerance in the plant (Kishitani et al., 2000).

Alternatively, exogenously applied GB on rice plants has proved successful in minimizing the adverse impacts of salt stress on rice plants by decreasing H_2O_2 and membrane lipid oxidation and boosting the transpiration rate under salt stress (Abdus Sobahan et al., 2016). Externally administered GB may quickly penetrate leaves and can be transferred to various other parts, where it can help with stress tolerance. Apart from rice, GB can be exogenously applied to other plants to mitigate abiotic stresses. For example, exogenous GB treatment on tomato plants exposed to either high temperatures or salt stress led to an increase in fruit output of roughly 40% when compared to untreated plants (Ashraf & Foolad, 2007).

Past research reports the role of GB in plant growth and stress management. Studies found that 5 mM GB treatment under salinity conditions dramatically boosted the evolution of the 'photosynthetic rate, transpiration rate, intracellular CO_2 concentration, and stomatal conductance' of cotton seedlings as compared to GB untreated saline treatment (Hamani et al., 2021). The exogenous application of GB greatly increased the activity of antioxidant enzymes under limited irrigation conditions and decreased the buildup of hydrogen peroxide and malondialdehyde in winter wheat. Thus, overall increasing the water use efficiency (Ahmed et al., 2019).

2.8 MOPs for Targeted Delivery of GB

To maintain appropriate glycine betaine concentrations in plants over time, systems for glycine betaine delivery and slow release must be developed. Advanced porous materials like MOPs can be used for this purpose. They are distinct, naturally porous structures with wide surface chemistry because of their peripheral reactive sites and they operate at the molecular level. The minute nanopores within the MOPs' structures facilitate the encapsulation of chemicals, enabling a gradual and regulated release of the substances over an extended period. These controlled delivery mechanisms play a vital role in optimizing chemical utilization, thereby mitigating issues such as excessive use, environmental contamination, input costs, and adverse impacts on non-target organisms.

Research was carried out to find out if applying nano-sized chitosan-glycine betaine to two types of wheat (*Triticum aestivum* L.) will improve their resistance to heat and drought. According to the research, applying nano-sized chitosan-glycine betaine to wheat plants improved their resistance to heat and drought by promoting osmotic adjustment, preserving tissue water, triggering antioxidant defense mechanisms, improving carbon uptake, and boosting the activity of enzymes responsible for grain filling. These outcomes supported plant development and encouraged the formation of yield (Al Masruri et al., 2023).

2.9 Summary

The growing public concern about the possible harm of using agrochemicals in crop production has compelled researchers to look for new, effective, and safer ways to combat diseases, weeds, and undesired plants. In this regard, agriculture has recently paid more attention to nanotechnology research with the overall objective of creating agrochemical delivery systems. Controlled delivery systems based on metal-organic frameworks or metal-organic polyhedral can provide several advantages for the environment, including less agrochemical runoff, less soil and water contamination, and improved crop protection. These materials have the potential for environmentally friendly and sustainable agriculture methods.

Apart from the guest encapsulation for controlled delivery and release in agriculture, MOPs, and MOFs have other applications such as in gas storage, drug delivery, sensing, catalysis, water purification, molecular sieves, the capture of greenhouse

gases, nanoparticle synthesis, and environmental remediation. Research and development activities in this area are anticipated to continue to grow in the upcoming years, producing significant discoveries and breakthroughs. The potential of MOPs and MOFs to solve urgent problems in industries including energy, the environment, and healthcare continues to attract researchers' interest. Although these networks have a lot of potential, they suffer from certain drawbacks such as scalability, expense, and long-term stability that must be overcome when using these materials in agricultural applications, according to the assessment.

Many MOPs and MOFs are susceptible to changes in temperature, humidity, and moisture, which can cause both the structure of the MOF and MOP and the encapsulated crop chemicals to degrade. The slow-release kinetics of the MOFs and MOPs even though essential for controlled delivery and advantageous for long-lasting effects, might not be appropriate in all situations when quick and immediate results are required. Also, the release kinetics of the guest from MOPs or MOFs may not always be exactly in line with the plant's nutrient requirements, resulting in possible fluctuations in nutrient availability and absorption. This uncertainty may significantly affect plant development and production. The synthesis of MOPs and MOFs may be difficult and time-consuming, frequently needing certain conditions and precursors. For agricultural uses, scaling up output may be difficult and expensive.

Also, the production process can be costly because specialized ions of metal and organic ligands are required for the production of various MOPs and MOFs. Widespread adoption may be hampered by this expense in the agricultural sector, where cost-effectiveness is essential. Also, agrochemicals of particular kinds could be less compatible with MOPs and MOFs. MOP materials are discharged into the environment during the research, manufacture, delivery, and application processes. As a result, the harmful effects and risks associated with MOP materials need to be thoroughly examined before large-scale manufacture and use to ascertain their environmental safety.

The toxicity from MOP may come from the metal ions released into the environment or from the organic linkers. Most MOPs and MOFs are made up of toxic heavy metals (transition elements) and crude oil derivatives. For example, the Cu-MOPs can release copper into the soil which is an essential element but can become phytotoxic at higher concentrations and can also disrupt the soil ecosystem. To evaluate the MOP materials' environmental safety, it is critical to ascertain their toxicity and risks. Also, Cu-MOPs need to be optimized properly for certain crops and agrochemicals.

CHAPTER 3

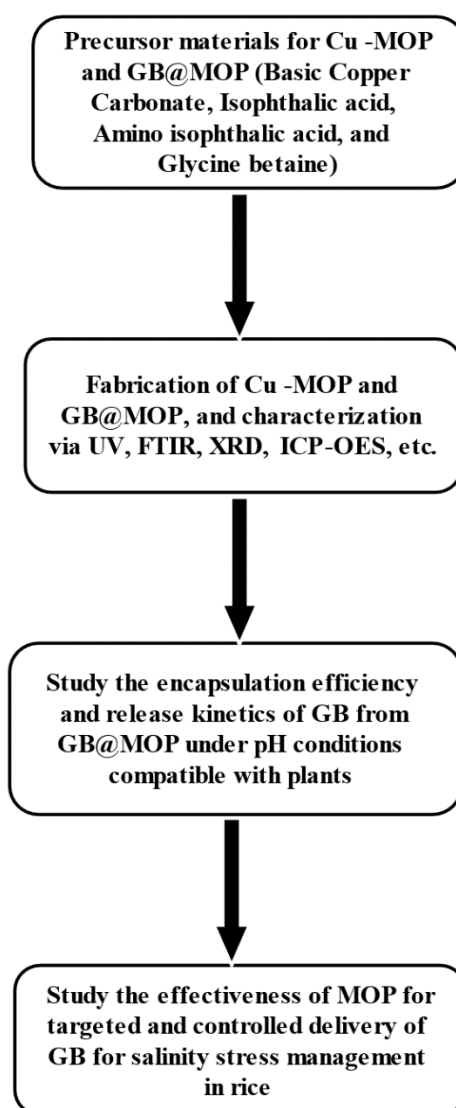
METHODOLOGY

3.1 Flowchart of the Research

The outline of the Research is presented in Figure 3.1

Figure 3.1

Research Flow Chart



3.2 Materials

Cu-MOPs were fabricated from Basic Copper Carbonate (BCC; $\text{Cu}_2\text{CO}_3(\text{OH})_2\text{H}_2\text{O}$) (MW:221.11 g/mol), which is the metal source and isophthalic acid (Benzene-1,3-dicarboxylic acid; MW: 166.14 g/mol) and 5-amino isophthalic acid (5-aminobenzene-1,3-dicarboxylic acid; MW:181.15 g/mol), which are the organic ligands for Cu-MOP-1 and Cu-MOP-2 respectively. The MOPs can be synthesized in either ethanol or methanol solutions; unlike the original recipe (Eddaoudi et al., 2001), however, water has not been used because the ligands are not water-soluble. Although, ethanol is a better option because it is environment-friendly and safe for humans, ultimately, methanol was considered due to higher solubility. The guest GB (Glycine betaine) ($\text{C}_5\text{H}_{11}\text{NO}_2$, MW: 117.148 g/mol) and the seeds of rice have been procured from ‘National Center for Genetic Engineering and Biotechnology’, ‘NSTDA’, which is an agency of the government of Thailand. The rice plants used is Pathum Thani-1 (PTT1), a photoperiod-insensitive aromatic variety popularly grown in Thailand. The variety is salt-sensitive and can be grown all around the year.

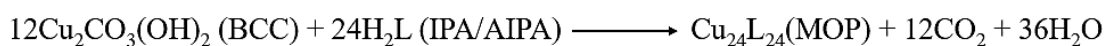
3.3 Procedure

3.3.1 Solvothermal Synthesis of Copper Isophthalate, Cu-MOP-1

According to the literature (Eddaoudi et al., 2001), equimolar amounts of Cu (NO_3)₂·2.5H₂O (0.019 g, 0.082 mmol) and m-BDC acid (0.014 g, 0.084 mmol) was taken in a glass tube with the solvent combination of DMF/C₂H₅OH (1.5/0.5 mL). The tube was heated to 80 °C for 24 hours at a constant pace of 1 °C per minute within a vacuum-sealed chamber. After that, it was progressively cooled down to room temperature (65 degrees for 10 hours and 50 degrees for 4 hours) at a constant rate of 0.1 degrees Celsius per minute. DMF and ethanol solutions were used twice to wash the blue-colored MOP crystals, yielding 0.015 g (65% yield). The process was then repeated to scale up the yield to 1 gram.

3.3.2 Synthesis of Copper Isophthalates, Cu-MOPs from BCC

Similar to the procedure in the literature for the synthesis of HKUST-1 (Ricco et al., 2018), a one-pot synthesis method was used to create Cu-MOPs by changing the metal source and the organic ligands and by taking methanol (according to the standard recipe) as the solvent according to the reaction:

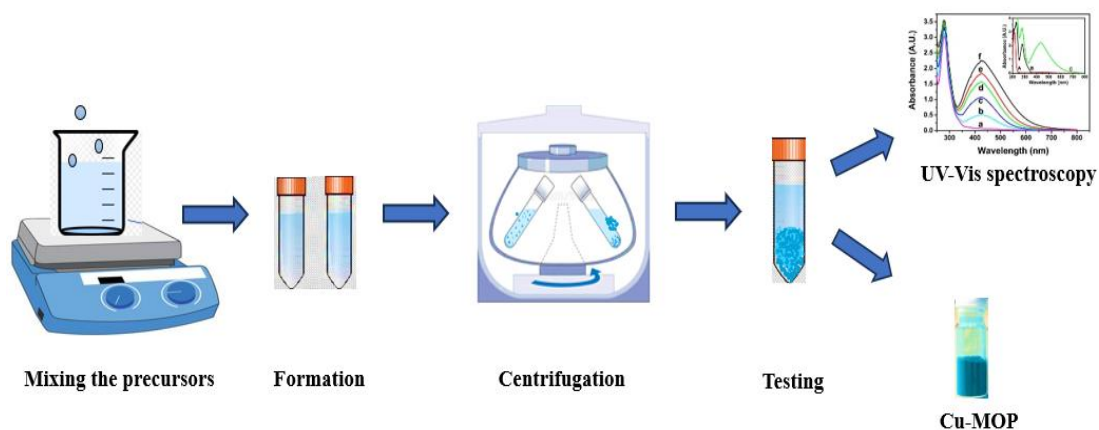


Where L is the isophthalate or the 5-aminoisophthalate ion. The reaction was taken place at room temperature and under mild conditions. The MOPs were first synthesized by taking small amounts of chemicals. The MOPs were synthesized by taking different ligand and BCC ratios i.e. 2:1, 4:1, and 8:1 to study the reaction variables and for optimization of the process. For Cu-MOP-1, in 25 ml of methanol, 90.2 mg (0.54 mmols) of isophthalic acid and 60 mg (0.27 mmols) of BCC were added and mixed altogether. This process maintained a ligand to BCC molar ratio of 2:1 (as per reaction, where 12 BCC and 24 ligand produces 1 MOP cage, $\text{Cu}_{24}(\text{IP})_{24}$). Similarly, the MOP was again synthesized by adding 180.3 mg (1.08 mmols) of isophthalic acid with 60 mg (0.27 mmols) of BCC, and 360.6 mg (2.17 mmols) of isophthalic acid with 60 mg (0.27 mmols) of BCC in 25 mL of solvent maintaining ligand-to-BCC ratios of 4:1 and 8:1 respectively.

The mixture was then stirred for 16 to 24 hours for the reaction to reach completion. Following that, the samples were centrifuged, washed with ethanol three times, and then dried in a hot air oven. Cu-MOP-2 was synthesized using the same procedure, 98.3 mg (0.54 mmols) of 5-amino isophthalic acid and 60 mg (0.27) of BCC were taken in 25 mL of methanol maintaining a 2:1 ligand-to-BCC ratio. The MOP was then synthesized again by adding the same amount of BCC and altering the quantities of 5-amino isophthalic acid, i.e. 196.6 mg (1.08 mmols) and 393.2 mg (2.17 mmols) to maintain ligand-to-BCC ratios of 4:1 and 8:1 respectively (Figure 3.2).

Figure 3.2

Schematic Representation of Preparation of MOP



3.4 Characterization

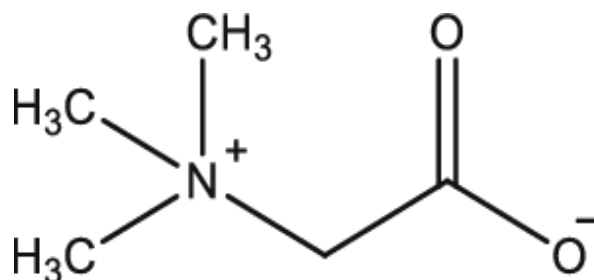
Characterization methods such as UV-Visible analysis (UV Visible spectrometer), Fourier Transform Infrared Spectroscopy (FTIR), Inductively coupled plasma optical emission spectroscopy (ICP-OES), and X-ray diffraction (XRD) methods have been used to determine concentration of chemicals, bonding characteristics, Cu ions release profile, and structural parameters respectively.

3.5 Glycine Betaine (GB); the Guest

The study involves the use of Glycine betaine (Trimethylglycine, GB) ($C_5H_{11}NO_2$, MW: 117.148 g/mol), a quaternary amine with zwitterionic character as the guest which is encapsulated inside the Cu-MOPs. It is a white solid hygroscopic chemical compound. It is a derivative of amino acid that is endogenously produced in plants. It has very high solubility in water and methanol, but it is less soluble in ethanol and insoluble in ether. The structure of glycine betaine is shown in Figure 3.3.

Figure 3.3

Chemical Structure of Glycine Betaine



3.6 Calibration Curve of the GB

GB has a very low maximum of absorbance which can be difficult to estimate directly, therefore a convenient colorimetric test is performed to detect its presence, via UV-Vis spectrophotometry. For this research, the ‘periodide method for the detection of glycine betaine’ was used (Grieve & Grattan, 1983). A calibration curve was constructed by preparing reference standards ranging from 25 $\mu\text{g/mL}$ to 200 $\mu\text{g/mL}$ (specifically, ‘25 $\mu\text{g/mL}$, 50 $\mu\text{g/mL}$, 75 $\mu\text{g/mL}$, 100 $\mu\text{g/mL}$, 125 $\mu\text{g/mL}$, 150 $\mu\text{g/mL}$, 175 $\mu\text{g/mL}$, and 200 $\mu\text{g/mL}$ ’) of glycine betaine. These standard solutions were then diluted with 2 N H₂SO₄ (1:1) and placed in a cold-water bath for temperature control. Subsequently, each solution was treated with 0.02 mL of cold KI-I₂ solution, which was prepared by combining 15.7 g of iodine and 20 g of KI in 100 mL of deionized water. After thorough mixing and vigorous agitation, the solutions were refrigerated at 4 °C for 16 hours. Following this incubation period, the solutions were once again mixed thoroughly and dissolved in 2 mL of dichloromethane. The absorbance of each solution was measured at a wavelength of 365 nm using a spectrophotometer after a 2-hour interval.

3.7 Encapsulation of the Guest

For the encapsulation of GB during synthesis, both MOP-1 and MOP-2 with various ligand-to-BCC ratios (2:1, 4:1, and 8:1) were prepared in the presence of GB, with a molar ratio concerning the MOP of 1:1, 2:1, and 4:1 according to Table 3.1.

Table 2.1

Table Representing Different Ratios of GB/MOP (varies Vertically) and Ligand/BCC (varies Horizontally) to be taken for the Synthesis of MOPs and Encapsulation of the Guest to Happen Simultaneously

RATIOS	LIGAND/BCC	2:1	4:1	8:1
GB/MOP	MOP (Without GB)	-	-	-
	GB@MOP	1:1	1:1	1:1
	GB@MOP	2:1	2:1	2:1
	GB@MOP	4:1	4:1	4:1

After the reaction (overnight), the mixture underwent centrifugation, resulting in the separation of the supernatant for UV-Visible analysis to determine the amount of encapsulation. The MOPs giving the better encapsulation was then fabricated by taking larger volumes of solvent and the precursors (BCC, ligand, and guest) (Figure 3.4). The encapsulation efficiency and loading percentage of those MOPs was calculated as follows:

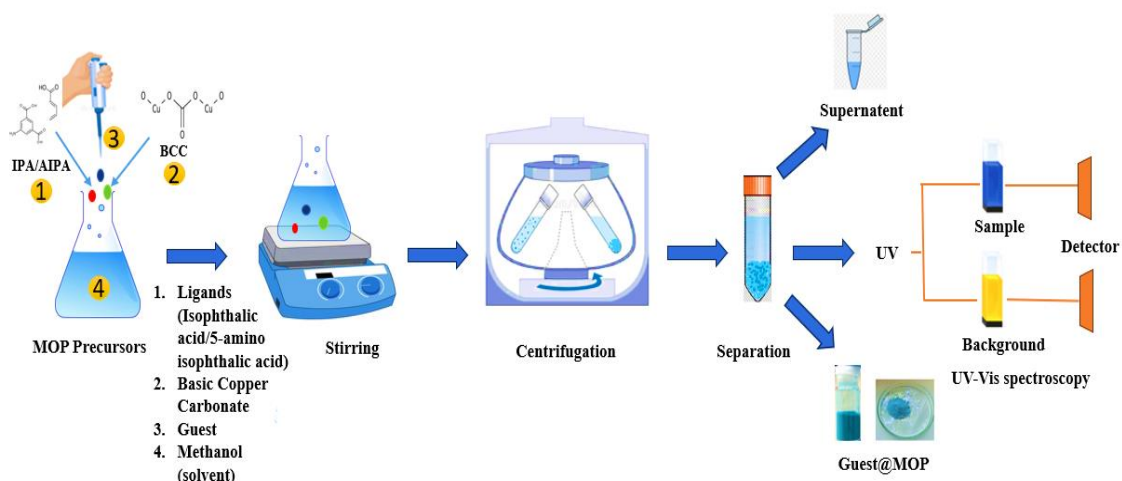
- Encapsulation efficiency (EE%) = $\left(\frac{C_i - C_f}{C_i}\right) \times 100$ (3.1)

‘Where, C_i is the initial concentration, and C_f is the final concentration of GB in the supernatant’

- Loading capacity (mg/g) = $\left(\frac{\text{Mass of the guest in guest@MOP}}{\text{Total mass of guest@MOP}}\right)$ (3.2)

Figure 3.4

Schematic Representation of Preparation of GB@MOP



3.8 Determination of Glycine Betaine in Supernatant

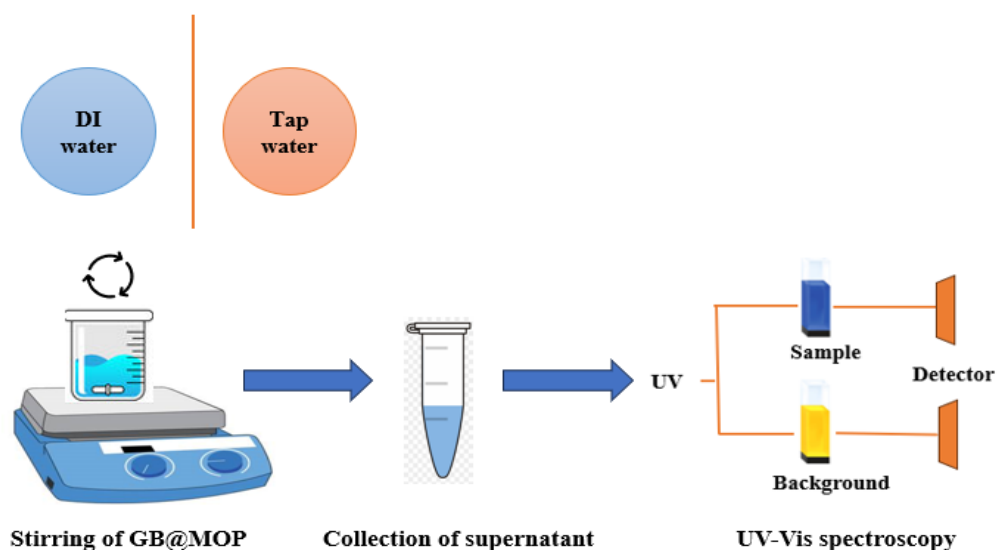
As per the method described in the literature (Grieve & Grattan in 1983), the obtained supernatants were diluted (1:1) in 2 N H₂SO₄ before use. The mixture was divided into aliquots (2 mL) and placed in centrifuge tubes to cool for one hour in cold water. After adding 0.02 mL of cold KI-I₂ solution (prepared by mixing 15.7 g of iodine and 20 g of KI in 100 mL of DI water), the liquid was gently mixed. After being kept at 4 °C for 16 hours, the periodide crystals formed was thoroughly mixed and dissolved in 2 mL of dichloromethane. The absorbance was measured at wavelength 365 nm using a spectrophotometer after two hours. The MOPs giving the highest encapsulation was then be selected for further release and application.

3.9 Release Profile of the Guest from the Cu-MOPs

To study the release profile of the GB@MOPs, the material was dispersed in DI water as well as tap water in a ratio of 1:1. To carry out this process with various GB concentrations within, the MOPs with the highest encapsulation efficiencies were chosen. The release profile was determined by collecting aliquots up to 7 days, and monitoring the concentration of glycine betaine ion solution via UV-visible spectrophotometry using the colorimetric assay. The data was fitted with the appropriate function (Figure 3.5).

Figure 3.5

Schematic Diagram of Release Study of GB from MOPs



3.10 Application to Rice Plants

The MOP giving better encapsulation efficiency and release was used for controlled delivery of GB, an osmolyte to the rice crop. The efficacy of the GB@MOP, MOP, and GB was evaluated against salinity stress in rice seedlings of 14 days. The rice variety PTT1 was used for the experiment because it is susceptible to salt stress.

Application steps are as follows:

A. Priming of rice seeds: At first, the rice seeds have been soaked overnight in Chlorox (10%) solution, to prevent any bacteria or fungi attack on the seeds. Following that, the seeds were planted in a large container containing soil enriched with microbes, with the intention of promoting germination within a greenhouse setting.

B. Transplanting to small pots: The plants at two leaf-stage were then transplanted to small pots with potting soil mixture (compost:soil:sand- 4:2:1). The pots were placed in perforated trays for the water to pass. The trays were nested inside larger trays and filled with water.

C. Application of NPK fertilizer: After 1 week of transplanting, soil application of NPK fertilizer (grade 16-16-16) was done to all the plants at a rate of 2-3 pellets per pot.

D. Application of materials: GB@MOP, MOP, and GB have applied to the plants via foliar spray. A total of 14 treatments have been applied; 7 individual treatments for salt concentrations of 0 mM and 150 mM with 5 replications in a completely randomized block design was studied (Table 3.2). The treatments have been applied after the plants have reached 3-leaf stage.

E. Incubation of plants in salt solution: 7 days after the application of treatments, the plants have been separated, half of the treated plants have been incubated in salt solution of concentration 150 mM and half of them have in incubated in water only (0 mM NaCl).

Table 3.2

Treatments with GB@MOP, MOP, GB, and Control (water) with Different Concentrations

NaCl 0 mM	NaCl 150 mM
T1: Control = 0 mM	T1: Control = 0 mM
T2: GB = 12.5 mM	T2: GB = 12.5 mM
T3: GB = 25 mM	T3: GB = 25 mM
T4: GB@MOP = 12.5 mM	T4: GB@MOP = 12.5 mM
T5: GB@MOP = 25 mM	T5: GB@MOP = 25 mM
T6: MOP = 12.5 mM	T6: MOP = 12.5 mM
T7: MOP = 25 mM	T7: MOP = 25 mM

3.11 Plant Assessment Parameters:

A. Plant Morphological Assays

This includes measurement of root length, shoot height, leaf numbers, and plant biomass. A ruler was employed to gauge the root and shoot lengths, along with counting the leaf number on the main culm. The height of the plants was measured from the base to the apex of the tallest leaf, and the root lengths were measured from the base to the farthest tip of the roots. To ensure representative data collection, a total of five plants

were carefully selected for each treatment group for these measurements. Both root and leaf biomass have been measured. For every treatment, five healthy rice plants were chosen to represent the average biomass for that treatment. The fresh weight of the samples subjected to the treatments was taken and then dried at 85 °C, and the dry matter of the samples was weighed after 2 days for measuring the biomass.

B. Plant Physiological Assays

i) Chlorophyll Content: Chl_a, Chl_b, Total chlorophyll content, and Total Carotenoid (C_{x+c}) concentrations have been determined for the rice leaves (Shabala et al., 1998). For the process, 100 milligrams of leaf tissues were combined and homogenized using a homogenizer in a glass vial containing 5 mL of acetone. The extracted solution was incubated at 4 °C in the refrigerator for 48 hours. Using acetone as a blank and an UV–VIS spectrophotometer (DR6000TM UV-VIS Spectrophotometer, HACH®, Loveland, CO, USA), the concentrations of ‘Chl_a, Chl_b, and total carotenoid (C_{x+c})’ were determined at 662, 645 and 470 nm, respectively.

Final concentrations of the pigments were calculated according to the following formula:

$$[\text{Chl}_a] = 9.784D_{662} - 0.99D_{645}$$

$$[\text{Chl}_b] = 21.42D_{645} - 4.65D_{662}$$

$$\text{Total chlorophyll} = \text{Chl}_a + \text{Chl}_b$$

$$[\text{C}_{x+c}] = 1000D_{470} - 1.90[\text{Chl}_a] - 63.14[\text{Chl}_b]/214$$

ii) Fluorescence Measurements: The chlorophyll a fluorescence was measured. The maximal quantum yield (F_v/F_m) and photon yield (Φ_{PSII}) of PSII were collected from the upper surface (adaxial surface) of fully matured leaves. This data was gathered using a ‘Fluorescence Monitoring System’ (FMS 2, manufactured by ‘Hansatech Instruments Ltd.’ based in ‘Norfolk, UK’) that operates in pulse amplitude modulation mode. The methodology employed adhered to the guidelines outlined by (Maxwell & Johnson, 2000). A leaf was subjected to the modulated measurement beam of far-red light (LED light exhibiting a typical peak at wavelength 735 nm) after being accustomed to dark conditions for 30 minutes using leaf clips. Then, utilizing 1.6-second bursts of saturating light ($>6.8 \mu\text{mol m}^{-2} \text{s}^{-1}$ PAR) under weakly modulated red light ($<0.5 \mu\text{mol}$

$\text{m}^{-2} \text{s}^{-1}$), the initial (F_0) and maximal (F_m) fluorescence yields were monitored and automatically computed using FMS software. By deducting the F_0 from the F_m , one may compute the variable fluorescence yield (F_v), which is a measure of the maximal quantum yield of PSII photochemistry. Furthermore, after 45 seconds of lighting, a steady state was attained, and the photon output of PSII (Φ_{PSII}) was calculated as $\Phi_{\text{PSII}} = (F_m' - F) / F_m'$.

iii) Photosynthesis Parameters: A portable photosynthesis system (Model 'LI 6400, LI-COR® Inc., Lincoln, NE, USA') with an infrared gas analyzer was used to quantify the 'net photosynthetic rate (P_n ; $\mu\text{molm}^{-2}\text{s}^{-1}$), stomatal conductance (g_s ; $\text{mmolm}^{-2}\text{s}^{-1}$), and transpiration rate (E ; $\text{mmolm}^{-2}\text{s}^{-1}$)'. The exact and reliable evaluation of these crucial plant physiology-related characteristics was made possible by this apparatus.

iv) SPAD and NDVI Measurements: The leaf chlorophyll in fully expanded leaf was measured by using a handheld chlorophyll meter ('SPAD-520 Plus, Konica Minolta, Osaka, Japan'), according to the method described in the literature (Hussain et al., 2000). SPAD is frequently employed as a gauge of photosynthetic activity and plant health. The basis for how SPAD meters operates is the idea that the chlorophyll content of plant leaves absorbs light.

Another handheld sensor known as Green-seeker (Trimble HCS-250) was used to measure the plant health and vigor in terms of NDVI readings. NDVI gave important information on the general health and vigor of the plants that were being studied. The NDVI is based on the idea that healthy vegetation absorbs more visible light and reflects more near-infrared light. The near-infrared reflectance, or NIR, and the red reflectance, or Red, are the two terms that make up the NDVI formula. Higher NDVI values often correlate with denser and healthier vegetation, whereas lower values may be indicative of bare soil or stressed vegetation (Cabrera-Bosquet et al., 2011).

v) Osmolarity Analysis: To determine the osmolarity of leaves of the rice seedlings (Lanfermeijer et al., 1991), Fresh leaf tissues weighing 100 mg were finely chopped into minute fragments before being placed into a 1.7 mL micro tube. Using a rod, the tissues were thoroughly crushed while being stirred. After that, a 10 μL aliquot of the

resulting extract was carefully deposited onto a disc-shaped filter paper within an osmometer chamber ('5520 Vapro[®], Wescor, Utah, USA'). The osmolarity was then measured. Next, by applying the conversion factor for osmotic potential, the osmolarity value (c , mmol kg^{-1}) was converted into its corresponding osmotic potential measurement (ψ_s , MPa) (Fu et al., 2010).

Osmotic potential: $\psi_s = -2.58 \times c \times 10^{-3}$

where, c is the osmolarity in mmol/kg .

C. Plant Biochemical Assay

i) Proline assay: The leaf section of the rice plant was tested for proline content (Bates et al., 1973). Following pulverization in a mortar using liquid nitrogen, 100 mg of freshly crushed leaf tissues were transferred into a 1.7 mL microcentrifuge tube. Subsequently, 1 mL of 3% sulfosalicylic acid was added, and the mixture was thoroughly vortexed. After a centrifugation period of 10 minutes at 12,000 rpm, 200 μL of the resulting supernatant was carefully extracted from the samples. This was mixed with 200 μL of 'acid-ninhydrin and glacial acetic acid' each by vortexing. The reaction was then stopped by cooling the solution in an ice bath after it had been incubated for an hour at 100 °C in a water bath. Subsequently, 400 μL of toluene was added, mixed using a vortex, and allowed to come to room temperature. A mixture of 900 μL toluene and 100 μL chromophore was prepared. The chromophore's absorbance was measured at '520 nm' using a spectrophotometer after it was extracted with toluene, with toluene serving as the blank. A plot of the proline standard was created with concentrations ranging from 0 to 250 ppm.

3.12 Statistical Analysis

The experimental setup followed a 'Randomized Completely Block Design' (RCBD), incorporating five biological replicates ($n = 5$) for each treatment condition. A 'two-way analysis of variance' (ANOVA) was conducted utilizing the statistical program Statistix 10 for windows.

CHAPTER 4

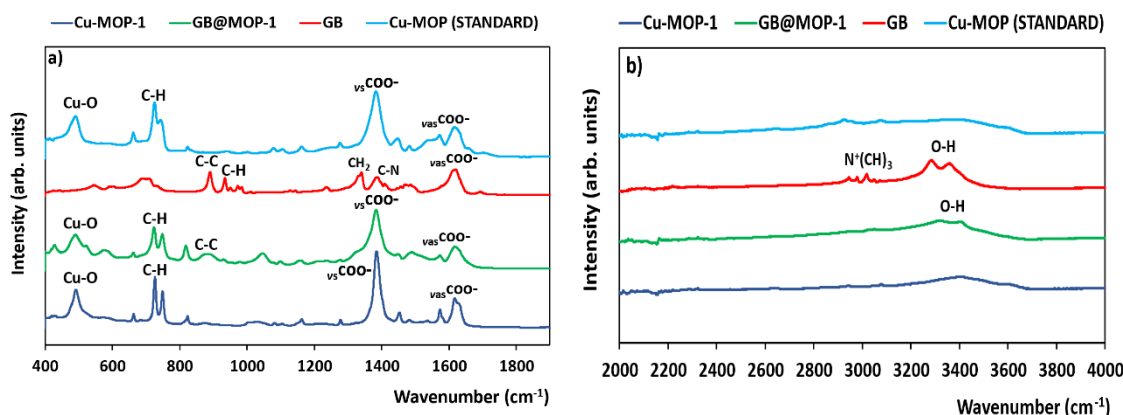
RESULTS AND DISCUSSIONS

This section provides a thorough examination of the findings from methodical studies on the synthesis, characterization, and performance analysis of Cu-MOPs as glycine betaine (GB) encapsulation matrix. The encapsulation and loading efficiency, release kinetics, and structural integrity of Cu-MOP-encapsulated GB formulations are all explained by the experimental results, which are supported by a number of analytical methods. The results not only advance our knowledge of Cu-MOPs as bioactive component carriers but also pave the way to the creation of specialized solutions with improved efficacy and broad application. The aim is to contribute to the development of sustainable agriculture practices by offering accurate insights into the feasibility of Cu-MOPs as an effective vehicle for controlled-release delivery. This chapter has been divided into four sections:

4.1 Characterization Results of the Compounds:

Figure 4.1

FTIR Analysis of Cu-MOP-1, GB, GB@MOP-1, and Standard MOP



Standard MOP is the one which was synthesized by solvothermal synthesis method, described in the literature (Eddaoudi et al., 2001). In case of Standard MOP, Cu-MOP-1, and GB@MOP-1 (Figure 4.1), the observed peaks at 1570 and 1393 cm⁻¹ could be associated to asymmetric and symmetric stretching modes of coordinated carboxylic

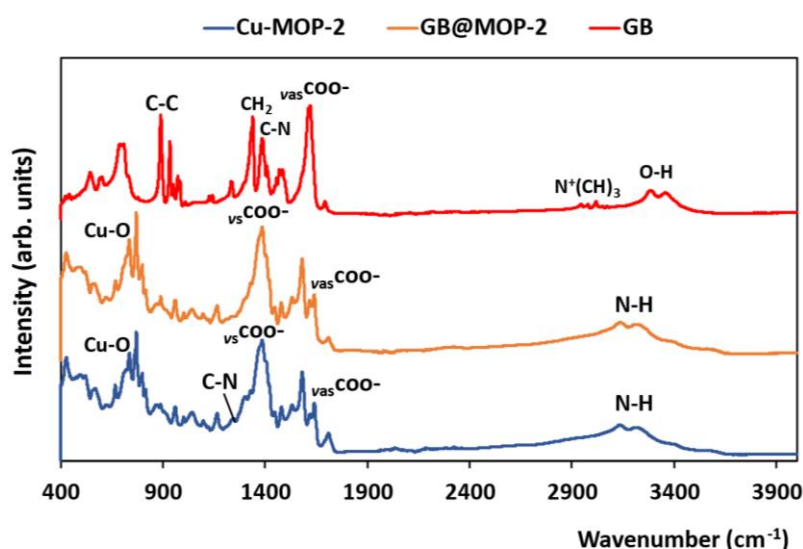
acid respectively, this is in line with earlier studies that used isophthalic as the organic ligand (Salama et al., 2018). Additionally, the peak observed at 1624 cm^{-1} could be due to the considerable shifting of stretching vibration of the carbonyl group (C=O) within the carboxylic acid of the ligand (m-BDC), the stretching of C=O group in the ligand generally appears between $1690\text{-}1750\text{ cm}^{-1}$ (Laboudy et al., 2011), the shifting might happen due to deprotonation and coordination of the C=O group of the ligand with Cu^{2+} to form the MOP (Lestari et al., 2016). All the compounds under analysis exhibit this distinctive peak at 1624 cm^{-1} because of the presence of C=O group in the molecular structure due to the ligand. The presence of this peak in GB was due to the presence of C=O group in its structure.

The peak observed at 720 cm^{-1} is likely attributed to the $\gamma(\text{C-H})$ vibration of the aromatic rings, the presence of such aromatic rings shows that the organic ligand (linker) is present in the final product (Salama et al., 2018). The peak at 488 cm^{-1} could be related to Cu-O bending modes (Bagheri & Ghaedi, 2020). The peaks of the standard MOP were similar to the synthesized Cu-MOP-1, hence it can be said that the Cu-MOP-1 can be successfully synthesized under ambient temperature conditions, without involving the solvothermal process.

For GB, the peak at 1393 cm^{-1} could be attributed to the stretching vibration mode of C-N group (Viertorinne et al., 1999) and the 1624 cm^{-1} peak is assigned to asymmetric stretch of betaine COO^- group (Li et al., 2015). The peak at 938 cm^{-1} is due to the bending vibration of C-H group, and the peak at 3025 cm^{-1} could be because of $\text{N}^+(\text{CH}_3)_3$ stretching vibrations according to the literature (Viertorinne et al., 1999). The peaks 3292 and 3375 cm^{-1} in GB-MOP-1 and GB can be attributed to the OH- stretching of the carboxylic group of GB. The peak for 890 cm^{-1} in GB is due to the C-C stretching vibrations (Latha et al., 2017). The presence of this peak in GB@MOP-1 indicates the presence of GB in the compound GB@MOP-1. The peak at 1323 cm^{-1} corresponds to CH_2 wagging vibrations (Latha et al., 2017).

Figure 4.2

FTIR Analysis of Cu-MOP-2, GB@MOP-2, and GB

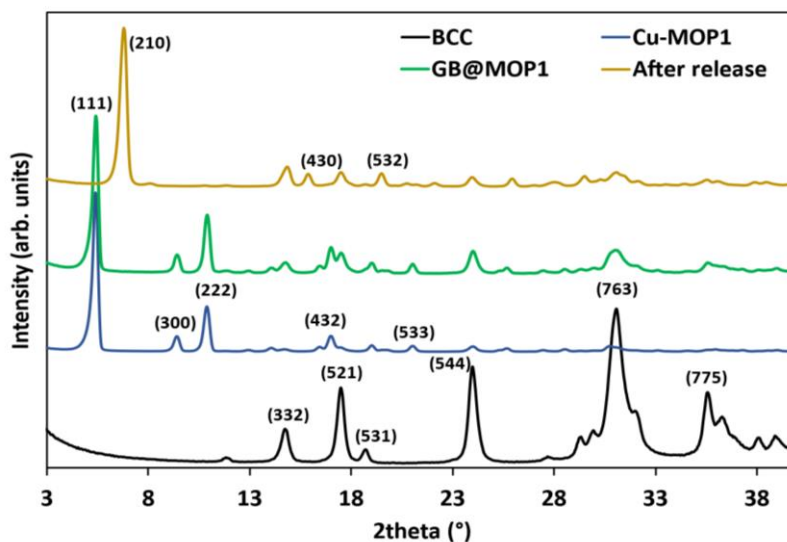


The FTIR spectrum of Cu-MOP-2 and GB@MOP-2 reveals distinct peaks at 1389 and 1645 cm⁻¹, which correspond to the symmetric and antisymmetric stretching modes of the coordinated -COO group from the ligand, indicating their presence in the compound (Fatima et al., 2022). The N-H stretching was assigned to weaker peaks at 3170 and 3250 cm⁻¹, which is consistent with the value reported in the literature. Furthermore, the vibration of C-N stretching attributed to the amino group was identified within the spectral range of 1350 to 1280 cm⁻¹, consistent with findings reported in existing literature references (Karabacak et al., 2009). In this study, a minor peak was observed at 1285 cm⁻¹ in Cu-MOP-2, which is less distinct in GB@MOP-2 due to complex formation, this peak can be used to indicate the presence of aromatic amino group in the structure, which is contributed by the ligand. The peak of 731 cm⁻¹ at both the spectrum could be attributed to the Cu-O bending (Bagheri & Ghaedi, 2020).

Moreover, there was a remarkable resemblance in the spectra that were obtained from both substances. Thus, it can be concluded that GB@MOP-2 does not allow for the reliable detection of the guest molecule (GB) (no peaks of GB). This constraint may be explained by the metal-organic framework's (MOP) cage-like structure, which can completely enclose the guest molecule. The whole of the GB molecule was therefore trapped inside the MOP cages and could not be identified by spectroscopic analysis.

Figure 4.3

XRD Analysis of Cu-MOP-1, GB@MOP-1, GB@MOP-1 Released and Basic Copper Carbonate (BCC)



An analysis using X-ray diffraction techniques was conducted on the samples Basic Copper Carbonate (BCC), Cu-MOP-1, Cu-MOP-2, GB@MOP-1, GB@MOP-1 after release GB@MOP-2, and GB@MOP-2 after release to confirm that the MOP's crystalline phases were extremely pure. The crystallite size of Cu-MOP-1 was determined by the Scherer equation (equation 4.1),

$$D = \frac{k\lambda}{\beta \cos\theta} \quad (4.1)$$

Where, D = The size of the crystallite (nm), λ = X-ray wavelength, k = Shape factor (0.9), β = Breadth at FWHM in radian, θ = Diffraction angle in radian.

In Figure 4.3, the intense peaks at smaller 2θ angles are indicative of the microporous nature of the materials according to the published literature (Panella et al., 2006). Numerous microscopic holes or cavities are known to be present in the structure of these materials. The XRD patterns of both Cu-MOP-1 and GB@MOP-1 exhibit a pronounced peak at $2\theta = 5.45$. Additionally, these compounds showed similar peak locations at $2\theta = 9.65, 11, 17.15,$ and 20.9 . Although BCC peaks were present in the XRD pattern of the MOP and GB@MOP, their intensity is not particularly high,

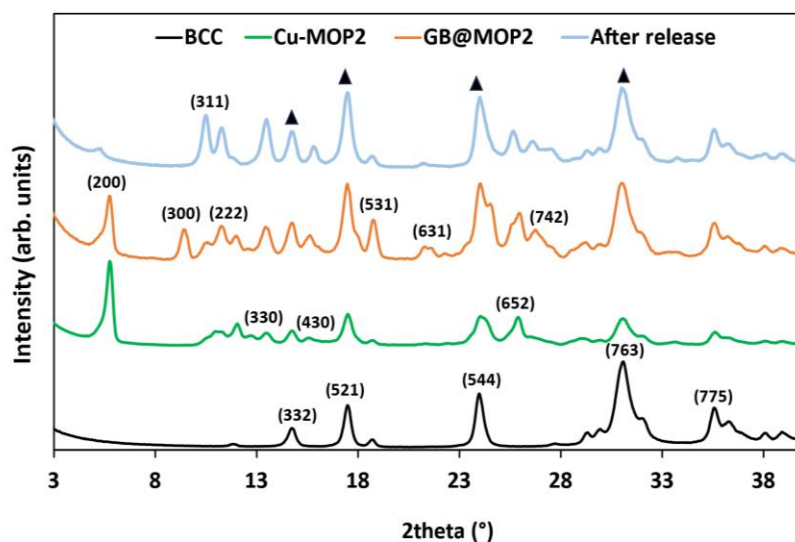
indicating a successful conversion process. The XRD patterns of both Cu-MOP-1 and GB@MOP-1 when compared, indicate that the host material's crystallinity was maintained after loading of the guest.

The appearance of additional peaks and alterations in peak locations in the XRD pattern of the released MOP may indicate changes in the material's crystalline structure. The newly observed peak at $2\theta = 6.75$ indicates the possibility of an unfamiliar phase or structural alterations in the material, perhaps resulting from changes in the unit cell or an entirely distinct crystal structure. This might be of particular significance since it implies a change in the properties of the MOP. Furthermore, the peaks at $2\theta = 16.1$ and 19.65 provides more credence to the idea that the material undergoes phase transitions or structural alterations. These peaks may represent particular lattice arrangements or crystallographic planes inside the material, revealing insights about its atomic-scale structure.

The existence of free BCC particles inside all the compounds is suggested by the presence of peaks at $2\theta = 24.4$ and 31.4 , which are normally associated with BCC crystal structure, in all compounds. The comprehension of the composition and structure of the material is further improved by this observation. The hkl values of the planes have been indicated on the figure.

Figure 4.4

XRD Analysis of Cu-MOP-2, GB@MOP-2, GB@MOP-2 Released and Basic Copper Carbonate (BCC)



The XRD pattern of Cu-MOP-2 and its subsequent products clearly shows that Cu-MOP-2 has less crystallinity than Cu-MOP-1 (Figure 4.4). The patterns of Cu-MOP-2 and GB@MOP-2 showed similar peaks at $2\theta = 13.65, 15.8, \text{ and } 25.8$. However, GB@MOP-2 showed additional peaks at $2\theta = 9.6, 11.5, 18.9, 21.5, \text{ and } 26.95$, perhaps suggesting the formation of a new phase due to loading of GB or the existence of GB crystals on the surface of the MOP. The XRD patterns of Cu-MOP-2 and GB@MOP-2 showed the presence of several BCC peaks (Figure 4.4). This indicates that there was an incomplete reaction during the synthesis process or the reaction didn't reached completion. The presence of BCC peaks suggests that the conversion process was not optimized, or that specific reaction conditions were poor. BCC peaks were present in the released MOP also.

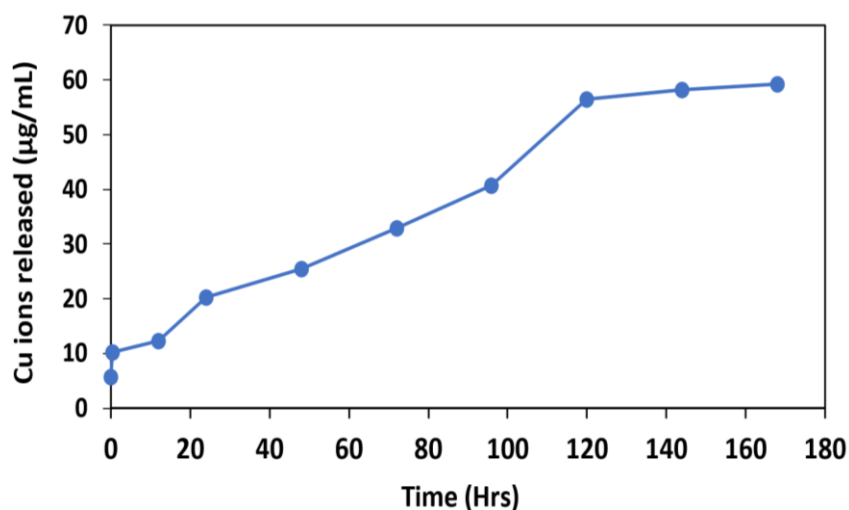
The peak at $2\theta = 11.5$ was also observed in the XRD pattern of the GB@MOP-2 and released MOP, which might be attributed due to the presence of GB particles and indicate the presence of GB in the release pattern. Moreover, the released MOP showed a pattern similar to the GB@MOP-2 molecule, except for a single extra peak that was seen at $2\theta = 10.6$. This resemblance indicates that either the release of GB from the MOP

was not fully completed, or there was no noticeable disintegration of the GB@MOP-2 complex even after the release event.

Research is required to properly understand the ramifications of these discoveries and refine the conversion process for better synthesis and performance of the MOP. Overall, the XRD study offers significant insights into the crystalline structure, phase transitions, and the existence of distinct structural elements in the materials. Additional research and analysis may provide additional information about these structural alterations and their effects.

Figure 4.5

ICP-OES Analysis of Cu-ions Release Profile from Cu-MOP-1



The Cu-MOP-1's copper release behaviour was investigated using the methods outlined by (Ren et al., 2015). As shown in the Figure 4.5, a standard curve was developed from stock solutions containing elemental copper in DI water in a ratio of 1:1 that allowed the measurement of copper concentrations emitted from Cu-MOP-1 across different time intervals. The analysis showed a steady discharge of Cu ions from the Cu-MOP-1 with time throughout the observation period. The released copper ion concentration grew gradually, suggesting a continuous release profile. By the end of the 5th day (120 hrs), the Cu-ions stabilized, indicating that nearly all of the Cu ions had been released by then. The release study was conducted for seven days at pH 6.5 (DI water), which is

consistent with the pH of the rice leaves. Generally, '5–30 ppm of Cu is considered satisfactory in plant tissues and the maximum limit of copper for food crops is 30 ppm' (V. Kumar et al., 2021).

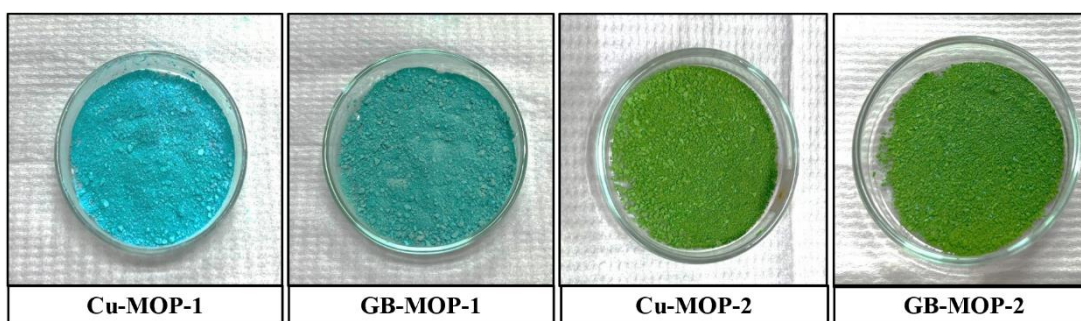
Concentrations higher than that can cause toxicity in plants. The present study found that the levels of Cu ions in solution had reached about 30 ppm after 3 days. The copper release study was conducted for up to 7 days since the plants were analyzed 7 days after the treatments were applied. In this study, 50 mg of MOP were mixed with 50 mL of DI water (1:1), resulting in a concentration of 1000 ppm of MOP in the water. After 7 days, the release of copper ions was measured at 60 ppm, exceeding the recommended maximum limit of 30 ppm for plants. This finding indicates that to achieve a safer level of 30 ppm of copper ions, only a 500 ppm concentration of MOP would be needed to be applied to plants, significantly (20-60 times) lower than the concentrations used in the present study.

Surprisingly, despite this higher concentration of copper ions, the treated plants did not exhibit any major morphological changes in the plants due to copper toxicity. This could be due to several reasons, the environmental conditions, such as soil composition, pH, organic matter content, and microbial activity, can influence copper bioavailability and plant response. These factors can modify the way copper interacts with plant roots and tissues. Also, the plants might have shown symptoms later than 7 days, but the analysis was done at the 7th day. Therefore, the plants might not have enough time to manifest the visible symptoms.

The considerable amount of copper ions, however, raises the possibility of physiological and biochemical alterations in the treated plants. However, it is important to remember that the analysis of the 'physiological and biochemical effects of salt stress' in plants was the exclusive focus of this study. Studies may aim to further explore and get a thorough comprehension of the effects of Cu ions on the physiology and biochemistry of plants.

Figure 4.6

Picture of the Synthesized Materials



4.2 Encapsulation of the Guest

The GB is incorporated inside the MOPs by in-situ synthesis, i.e. by synthesizing the MOPs in the presence of GB. The GB calibration curve was made (Figure 4.7) first to determine the amount of GB inside the MOPs by determining the concentration through the absorbance values of GB.

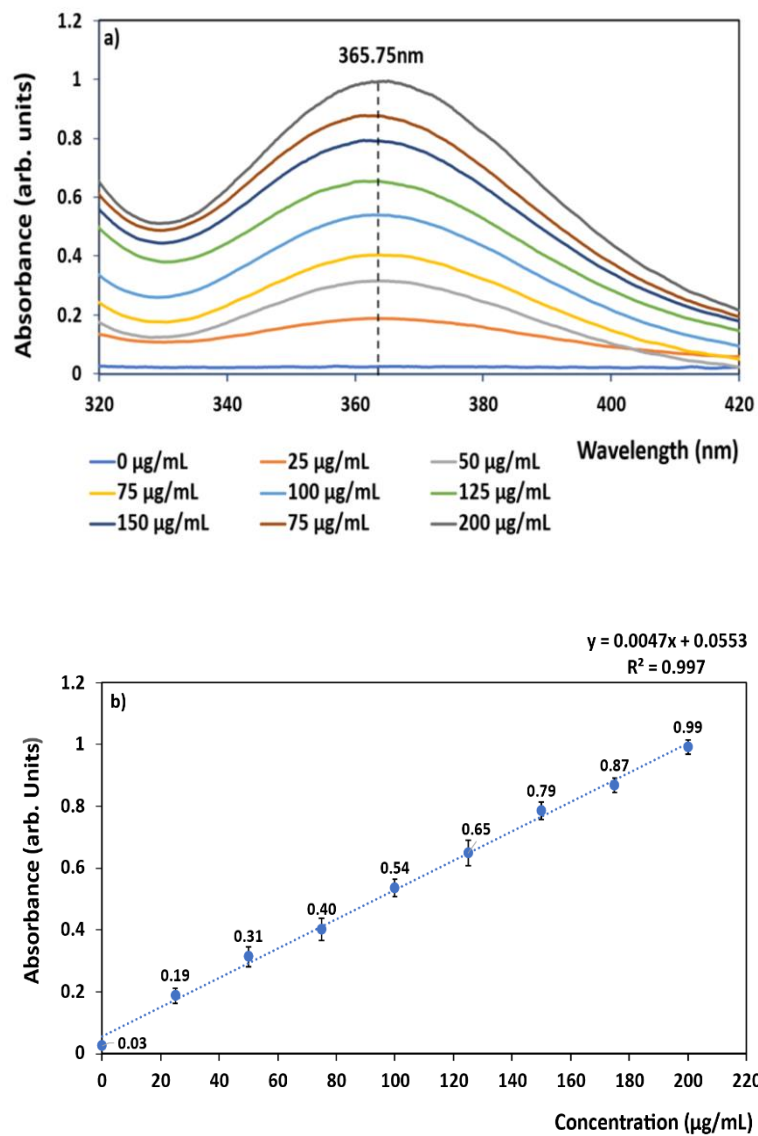
Several processes that promote guest loading may be involved in interactions between the guest molecules and MOP structures. Dipole forces, electrostatic attractions, hydrogen bonds, coordination bonds and other interactions are a few examples of frequent interactions (Wittmann et al., 2019).

Glycine betaine was used in the present study as the guest to load into Cu-based MOP containing carboxylate ligand. Given that the glycine betaine has both carboxylate and quaternary ammonium groups, which are positively and negatively charged, respectively. These charged groups can form hydrogen bonds with either the functional groups found in the isophthalic acid ligand or the nearby water molecules. The complex's solubility and stability may be enhanced via hydrogen bonding. Therefore, in the current investigation, H-bonding is the primary mechanism for glycine betaine loading. Despite being a weak intermolecular force, H-bonding is more powerful than dipole and dispersion forces (Wittmann et al., 2019).

4.2.1. Glycine Betaine Calibration Curve

Figure 4.7

Calibration Curve of GB: a) Absorbance of GB, b) Linear fitting of GB



4.2.2. Theoretical Weight and Obtained Weight of Cu-MOPs

Table 4.1

Table showing the Comparison between Theoretical Weight, Obtained Weight, and % Weight of Cu-MOPs

Ratio of Ligand to BCC	Obtained weight	Theoretical weight	Weight %
Cu-MOP-1(IPA:BCC=2:1)	69.6	123.5	56.3%
Cu-MOP-1(IPA:BCC=4:1)	73.55	123.5	60%
Cu-MOP-1(IPA:BCC=8:1)	77.53	123.5	63%
Cu-MOP-2 (AIPA:BCC=2:1)	71.64	131.7	54.4%
Cu-MOP-2 (AIPA:BCC=4:1)	75.6	131.7	57.4%
Cu-MOP-2 (AIPA:BCC=8:1)	79.56	131.7	60.4%

$$\text{Where, weight \%} = \left(\frac{\text{Obtained weight of MOP}}{\text{Theoretical weight of MOP}} \right) \times 100 \quad (4.2)$$

The theoretical weight of a MOP is computed using chemical formula and stoichiometry. The obtained weight is the weight of the synthesized MOP acquired throughout the experimental procedure. It can differ from the theoretical weight due to variables like incomplete reactions, contaminants, solvent residues, or wastage during purification and processing.

4.2.3. Encapsulation Efficiency (EE; %) and Loading Capacity (LC; mg/g) of the Cu-MOPs

Figure 4.8

Bar graph representing the Encapsulation Efficiency (EE; %) of Cu-MOP-1 and Cu-MOP-2 with Different Concentration of GB and with Different Molar Ratios of Ligand and BCC

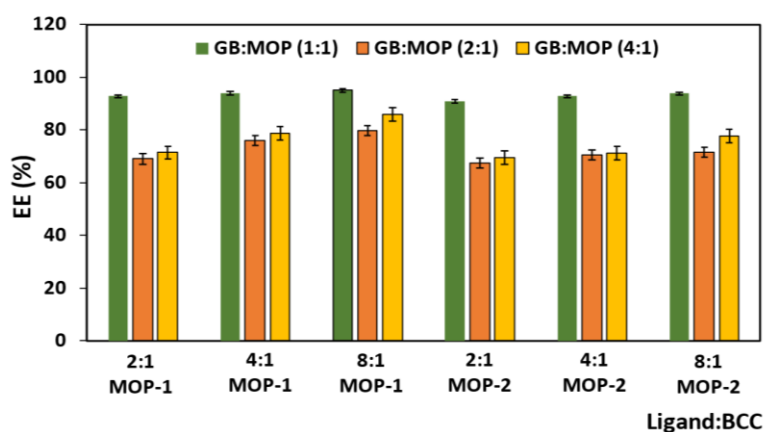


Table 4.2

Loading Capacity (LC; mg/g) of GB@MOP-1 and GB@MOP-2 with Different Concentrations of GB and with Different Molar Ratios of Ligand and BCC

Ligand:BCC	GB:MOP	LC (mg/g)	
		GB@MOP-1	GB@MOP-2
2:1	1:1	33.4 mg/g	32 mg/g
2:1	2:1	50 mg/g	47.4 mg/g
2:1	4:1	98.2 mg/g	93.3 mg/g
4:1	1:1	32.2 mg/g	31 mg/g
4:1	2:1	52 mg/g	47 mg/g
4:1	4:1	101.7 mg/g	90.6 mg/g
8:1	1:1	30.9 mg/g	30 mg/g
8:1	2:1	51.6 mg/g	45.4 mg/g
8:1	4:1	105 mg/g	94 mg/g

It can be inferred from Figure 4.8 and Table 4.2 that the both EE% and LC of Cu-MOP-1 is higher than Cu-MOP-2, which is why Cu-MOP-1 was considered better for targeted delivery of GB in plants.

For GB amounts to be considered, the GB to MOP ratio of 1:1 showed the highest EE%, (almost 100%), this nearly full encapsulation indicates that the guest material has been entirely encapsulated inside the structure. This might imply that there are possible vacancies in the structure, suggesting that there is still an opportunity to optimize the encapsulation procedure for optimal effectiveness. Also, the loading capacity of 1:1 ratio of GB to MOP was the lowest among all. Thus, investigating the 2:1 and 4:1 ratio of GB to MOP is essential to improve the encapsulation process. Since the GB to MOP ratio of 4:1 showed the highest loading capacity, it had been considered the better one.

Although for the same amount of GB, the EE and LC is slightly higher in Cu-MOP-1 with a ligand to BCC molar ratio of 8:1 than 4:1 and 2:1, a large amount of solvent is required for its synthesis due to isophthalic acid's low solubility in methanol, therefore it is not cost-effective to employ that. On the other hand, Cu-MOP-1 with a ligand-to-BCC molar ratio of 2:1 does not require too many precursors; therefore, it is cost-effective and can be considered for further optimization and efficacy tests.

So, Cu-MOP-1 with a ligand to BCC molar ratio of 2:1 has been synthesized in bulk amounts for further encapsulation and release studies, and GB to MOP ratio of 4:1 was considered for synthesis of GB@MOP-1. For synthesis in bulk amounts 1 g (4.52 mmol) of BCC and 1.503 g (9.046 mmol) of isophthalate were added to 100 ml of methanol (considering the low solubility of isophthalate in methanol) and stirred overnight to yield 1.108 g (54 % yield) of MOP. For the synthesis of GB@MOP-1, 176.6 mg of GB was added to the reaction mixture containing BCC and isophthalate of the aforementioned amounts. The process yielded 1.24 g (55.5 % yield) of GB@MOP. The EE % was improved and found to be 77.4 %.

Amount of GB in the GB@MOP (1.24-1.108) g = 0.132 g = 132 mg

Amount of GB left after encapsulation (176.6-132) mg = 44.6 mg

Therefore, Loading Capacity of MOP = (176.6-44.6) mg/1.24g

$$= 132 \text{ mg} / 1.24 \text{ g}$$

$$= 106.5 \text{ mg/g}$$

4.3 Release Study of GB from Cu-MOPs

Given that the release investigation was conducted in water, the release of GB molecules from the MOP was caused by GB's higher solubility in water. In general, molecules of GB exhibit a greater affinity for water (H₂O) in comparison to MOP molecules that include carboxylic acids. The hydrophilic character of GB, which has both positively and negatively charged groups (quaternary ammonium and carboxylate), is responsible for its greater affinity for water. Through hydrogen bonds and electrostatic interactions, these charged groups have a positive interaction with water molecules (Wittmann et al., 2019). Hence when the MOP is dispersed in water, GB molecules come out from it in the solution in a controlled manner.

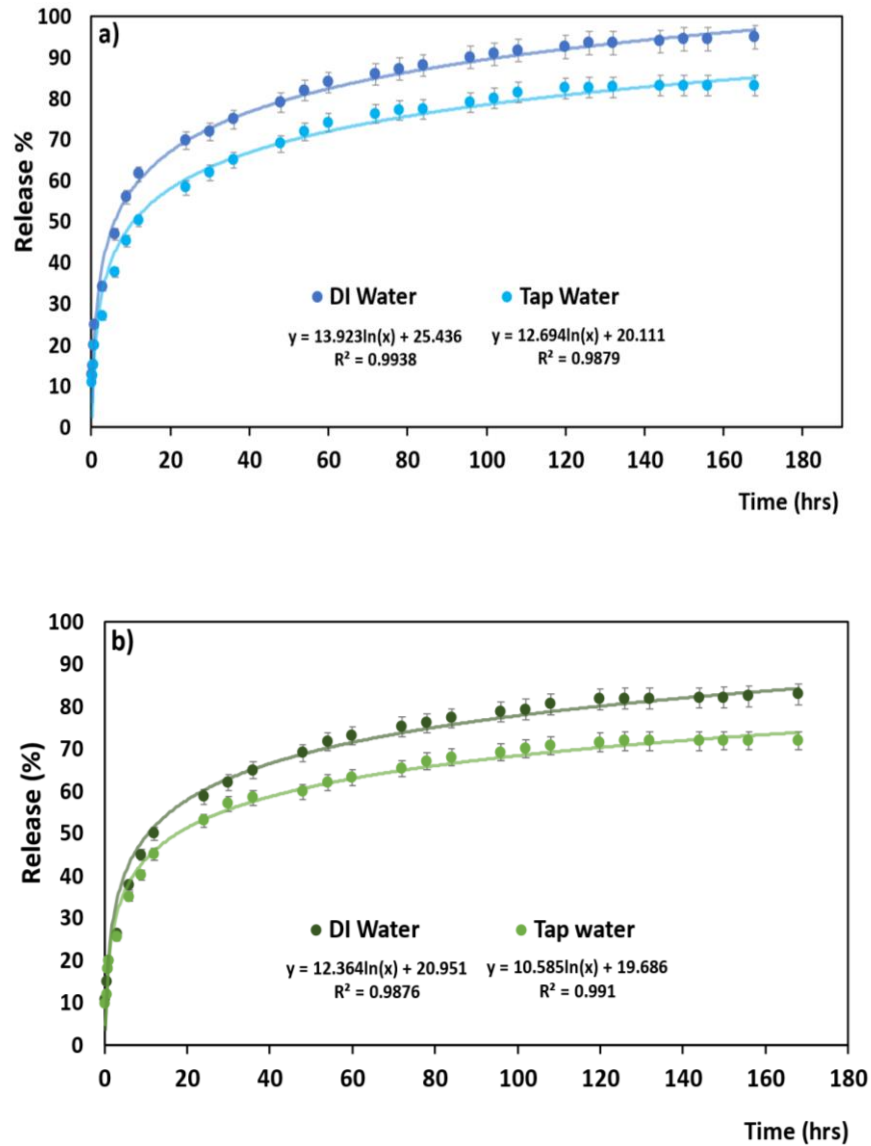
To study the release profile of the GB@MOPs, the material was dispersed in DI (pH 6.5) and Tap water (pH 7.5). The pH of DI water was found same as the pH of the rice leaf, i.e., 6.5. Therefore, for plant application, DI water was used to disperse the material. The experimental data collected in this release study were applied to equation 4.3, commonly referred to as 'Korsmeyer-Peppas (KP) equation'.

$$\frac{M_t}{M_\infty} = Kt^n \quad (4.3)$$

Where, $\frac{M_t}{M_\infty}$ is the fractional permeated drug in time 't', 'K' is the release rate constant, and 'n' is the release exponent. The values of n can be differed for different transport. The value of n is equal to or less than 0.5 for Fickian diffusion process, for non-Fickian diffusion, the n value is between 0.5 and 1, and for super case II transport, the n value is greater than 1. The Korsmeyer Peppas curve fitting model has been previously reported for drug release mechanisms from porous materials (I. Y. Wu et al., 2019).

Figure 4.9

Release Kinetics of GB from: a) Cu-MOP-1, and b) Cu-MOP-2



The study involved using non-linear regression methods to align the data with the Korsmeyer Peppas model. By using this method, the researchers were able to learn more about the release kinetics of drugs from porous networks. The particular parameters obtained from this fitting procedure are listed in Table 4.3.

Table 4.3*Korsmeyer Peppas Fitted Data Values*

Items	Parameter	DI water (pH 6.5)	Tap water (pH 7.5)
GBMOP-1	K	29.75	24
	n	0.24	0.25
	r ²	0.983	0.986
GBMOP-2	K	24.5	22.7
	n	0.25	0.24
	r ²	0.987	0.985

The release rate of GB was faster in DI water as compared to tap water, this could possibly be because of the presence of numerous ions in tap water that can interact with the molecules of the guest. These interactions might make the guest molecules less soluble or prevent it from dispersing throughout the delivery system. On the other hand, DI water is devoid of these ions, creating a more ideal environment for the release. In both DI and tap water, the release of GB commences after 15 min.

In the present study, the Korsmeyer-Peppas (KP) model's n value is smaller than 0.5 (0.2), indicating a Fickian diffusion process (Bayer, 2023). This suggests that the rate of release of guest is exactly proportional to the gradient in guest concentration within the matrix (guest molecules moves from high concentration region to low concentration region). Understanding Fickian release is essential for developing drug delivery systems with consistent and regulated release rates, which can be critical for optimizing effectiveness and reducing adverse effects.

It is clear from the results that the release kinetics of GB from Cu-MOP-1 is higher than Cu-MOP-2 in both DI and tap water (Figure 4.9), amino groups and copper ions from Cu-MOP-2 might form a stable structure with tighter binding sites that make it harder for glycine betaine molecules to detach and be released. This results in a lower release rate. So, Cu-MOP-1 have been selected for further analysis on the rice plants to assess the controlled release and targeted delivery of GB to rice plants.

4.4 Plant Analysis

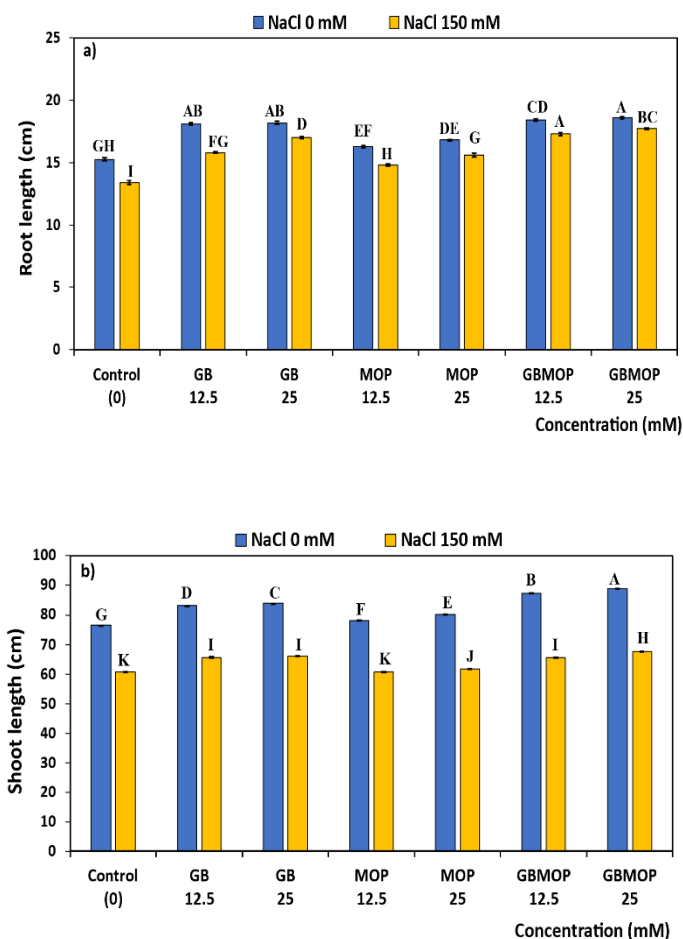
This part of the section contains the results of the analysis done on the rice plants after the application of the materials.

4.4.1 Plant Morphological Analysis

This includes measurements of Root Length, Shoot Height, Leaf Count, Shoot Biomass, and Root Biomass.

Figure 4.10

Bar Graph Showing a) Root Length, and b) Shoot Height at Different Treatments under NaCl 0 mM and 150 mM. “Values are means of Five Replications. Vertical bars represent Standard Error. Bar columns with different Uppercase letters are Statistically Significant based on Tukey’s Honest Significant Difference test at $P < 0.05$ ”.



The study found that plants exposed to salt stress (NaCl 150 mM) had shorter root and shoot lengths as compared to plants cultivated in non-stressful (NaCl 0 mM) conditions (Figure 4.10). However, the plants exposed to salt stress that were given GB@MOP at doses of 12.5 mM and 25 mM showed longer roots and shoots compared to other treatments. The untreated plants under salt stress, on the other hand, showed the slowest rate of growth, with shorter shoot heights and root lengths. Furthermore, plants given GB treatment at a concentration of 12.5 and 25 mM showed growth rates that were quite similar to the plants that were treated with GB@MOP.

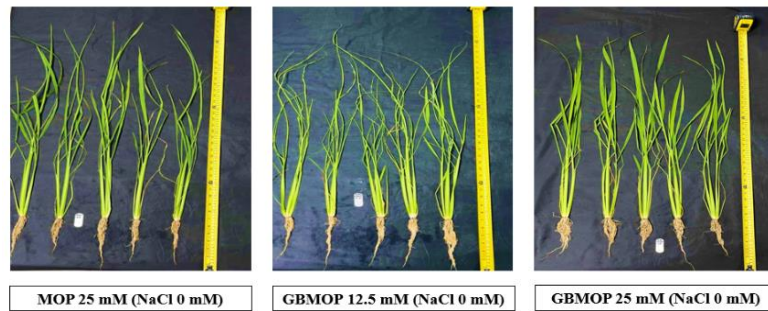
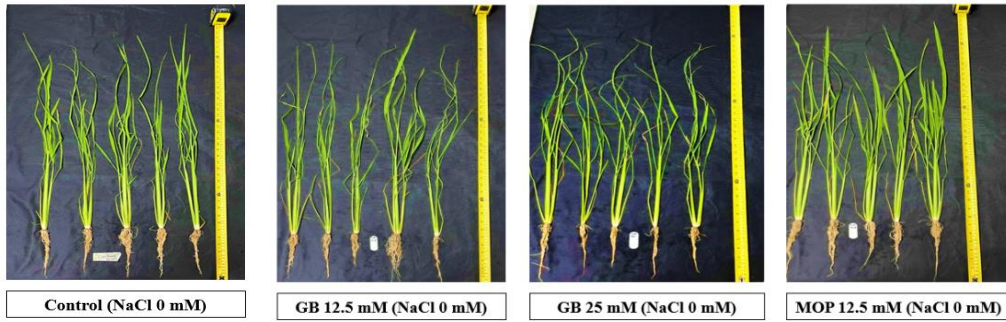
In plants grown under normal conditions, root length, root length, height of shoot, and leaf count were notably higher than in salt-stressed plants. Under normal conditions, every plant had three leaves in the main culm; under salt stress, however, the plants only had two leaves. However, regardless of the treatments, there was no variation in the number of leaves between the treatments, both under normal and stressed conditions. Hence, the analysis of the mean difference cannot be done for the leaf count. The results of this study show that the controlled and targeted delivery of GB using MOP considerably enhanced overall growth performances in salt-stressed rice plants, including root length, height of shoot, and leaf count.

According to the published literature (Khadouri et al., 1970), under abiotic stress conditions like salt and drought which inhibited plant growth, exogenous GB application provides comparative advantage to plants by improving the morphological parameters of plants including root length, height of shoot, and leaf count. Thus, the targeted delivery of GB via MOP for control of salt stress in plants can be of utmost importance and can be researched further for future applications.

Figure 4.11

Pictures of the Morphology of Rice Plants under a) NaCl 0 mM, and b) NaCl 150 mM

a)



b)

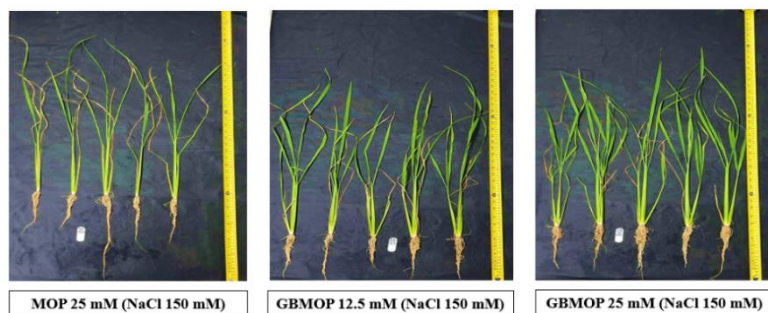
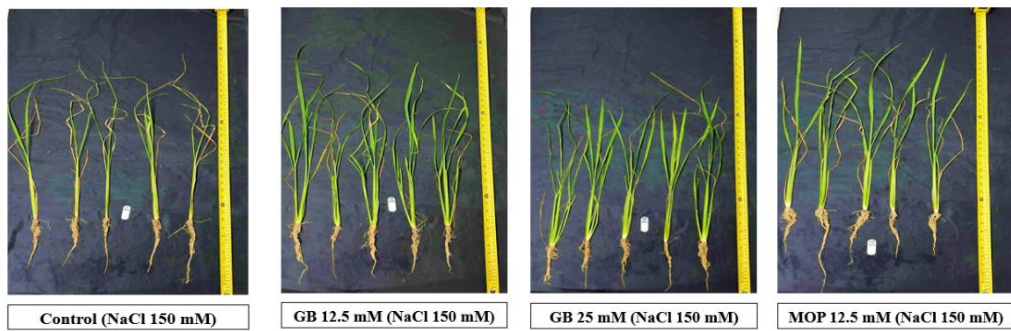
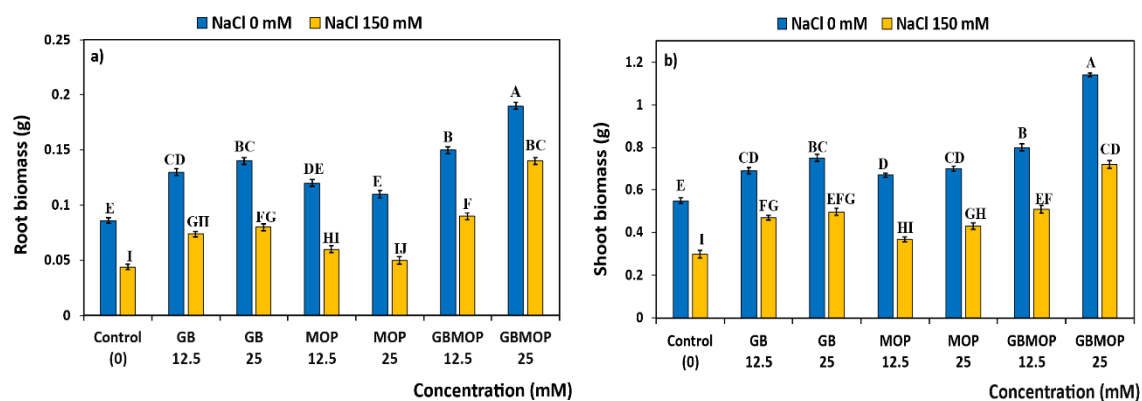


Figure 4.12

Bar Graph Showing a) Root Biomass, and b) Shoot Biomass of Rice Plants at Different Treatments under NaCl 0 mM and 150 mM. “Values are means of Five Replications. Vertical bars represent Standard Error. Bar columns with different Uppercase letters are Statistically Significant based on Tukey’s Honest Significant Difference test at $P < 0.05$ ”.



Both root and shoot biomass demonstrated a similar trend under salt stress conditions. In contrast to plants grown under normal conditions, stressed plants exhibited a significant reduction in the dry weight (biomass) of both the shoot and the root (Figure 4.12). Notably, plants treated with GB@MOP at a dose of 25 mM showed the maximum biomass for both the shoot and the root, irrespective of whether they were subjected to 0 mM or 150 mM NaCl stress. Under circumstances of salt stress, the biomass of the plants treated with MOP and those left untreated (control) was lower than that of the other treatments. As compared to those, the biomass of the plants treated with GB at doses of 12.5 mM and 25 mM was significantly higher, but it was lower than that of the plants treated with GB@MOP at dosages of 12.5 mM and 25 mM.

Literature studies reveals that when GB is applied exogenously to stressed plants, it tends to increase the dry weights of the roots and shoots (Shemi et al., 2021). As a result, when administered GB, both the plant's aboveground (shoots) and belowground (roots) sections tend to develop better, even in harsh conditions. However, the precise effects can differ according to a number of variables, including the kind of plant, the degree of stress, and the time and concentration of glycine betaine administration. The highest biomass was observed in the plants sprayed with GB@MOP at a dose of 25

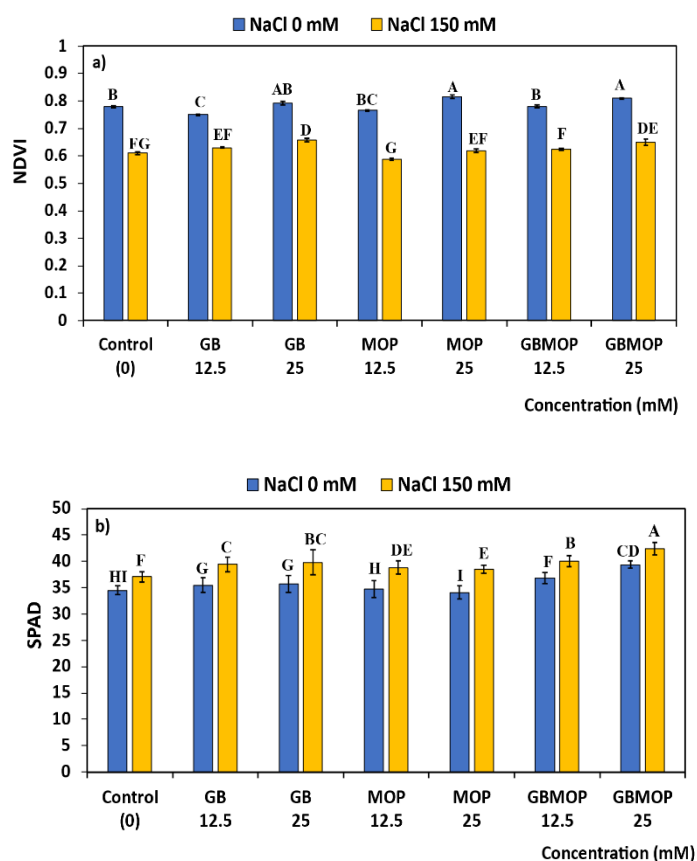
mM, suggesting better growth resistance under salt stress. Hence, this represents the comparative advantage of MOP being used for controlled delivery of GB to the plants.

4.4.2 Plant Physiological Assay

This includes analysis of NSVI, SPAD, Leaf chlorophyll content, Photosynthetic parameters, Chlorophyll fluorescence, and Osmolarity of leaf.

Figure 4.13

Bar Graph Showing a) NDVI, and b) SPAD value for Plants at Different Treatments under NaCl 0 mM and 150 mM. “Values are means of Five Replications. Vertical bars represent Standard Error. Bar columns with different Uppercase letters are Statistically Significant based on Tukey’s Honest Significant Difference test at $P < 0.05$ ”.



NDVI indicates the health and vigor of the vegetation, the results of the present study indicate that the health of the plants under salt stress was inferior to the plants grown under normal conditions (Figure 4.13a). The plants without treatment, and those treated

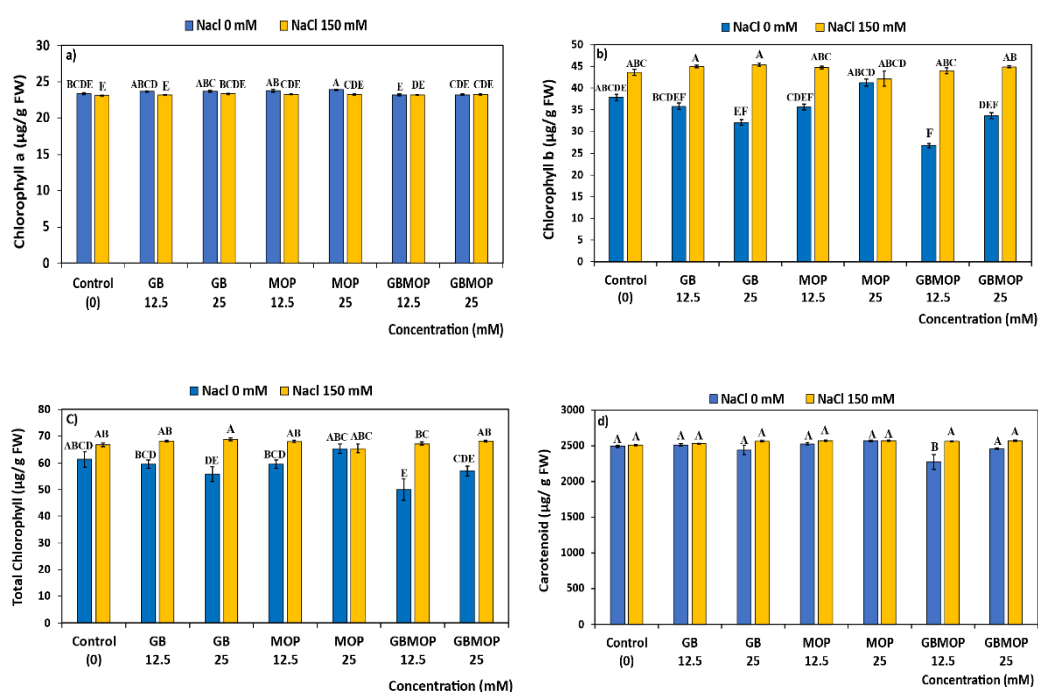
with MOP at 12.5 mM and 25 mM of concentration under salt stress showed lower NDVI values. The plants subjected to salt stress exhibited the most elevated NDVI values when treated with a 12.5 mM and 25 mM dosage of GB and 12.5 mM and 25 mM concentration of GB@MOP. Their NDVI measurements were determined to be nearly equivalent. This is in accordance with published literature (M. Zhu et al., 2022), which states that exogenous application of GB significantly enhances the NDVI readings in plants both under normal and stress conditions. Therefore, according to the study's findings, MOP has been successfully used for the controlled delivery of GB, especially when it comes to improving NDVI readings.

The SPAD value of the plants was found to be increased under salt stress as compared to those grown under normal conditions (Figure 4.13b). The plants treated with GB@MOP at concentrations of 12.5 mM and 25 mM under salt stress had greater SPAD values than those with other treatments. The plants without treatment, and those treated with MOP 12.5 mM and 25 mM under salt stress showed lower SPAD values than GB and GB@MOP treatments. The SPAD values of the plants treated with GB 12.5 mM and 25 mM were intermediate between those of GB@MOP and MOP treatments. A comparable trend was noted for the plants cultivated under normal conditions. The SPAD value typically decreases in plants under stress conditions in accordance with published literature (Islam et al., 2022), however, in contrary to the general trend, the present study found the SPAD value of plants exposed to salt stress exhibited higher SPAD values than those grown under normal conditions.

This discrepancy might be linked to the abnormal growth patterns found in plants under stress conditions since according to some literature, sometimes they can accumulate more amounts of chlorophyll under lower stress levels compared to higher stress levels (Agathokleous et al., 2020). The higher value of SPAD in plants treated with GB@MOP might indicate that those plants experienced lower degree of stress than those with other treatments under salt stress conditions. According to literature (M. Zhu et al., 2022), exogenous GB application under stress conditions protects the chlorophyll from degradation in plants and does not alter the SPAD values, thus protecting the plants from experiencing a high level of stress. Hence, the application of GB@MOP offers an advantage in salt stress conditions over other treatments.

Figure 4.14

Bar Graph Showing values of a) Chlorophyll a, b) Chlorophyll b, c) Total Chlorophyll, and d) Carotenoid levels in Plants with Different Treatments under NaCl 0 mM and 150 mM. “Values are means of Five Replications. Vertical bars represent Standard Error. Bar columns with different Uppercase letters are Statistically Significant based on Tukey’s Honest Significant Difference test at $P < 0.05$ ”.



All treatments showed a minor decrease (1-3%) in the amount of chlorophyll a (Chl_a) in response to salt stress, except for treatments of GB@MOP at doses 12.5 mM and 25 mM. These treatments showed the same content of Chl_a as those grown under normal conditions. Therefore, under salt stress, the concentrations of GB@MOP maintained the Chl_a content at levels similar to plants grown in normal conditions (Figure 4.14a). However, Chl_a content in plants under normal and stress conditions does not show a large difference.

According to the published literature (Bayat et al., 2022), the plant chlorophyll levels normally decrease when they are subjected to any stress conditions. But, in contrast to the normal trend, plants under salt stress displayed a substantial (5-30%) increase in chlorophyll b (Chl_b) under all treatments compared to plants cultivated under normal

conditions except for treatment involving a concentration of MOP 25 mM (Figure 4.14b). At 25 mM concentration of MOP, the plants under stress showed a marginal increase (1-2%) in Chl_b content, which might be attributed to a variety of environmental factors since PTT1 is a rice variety which is sensitive to environmental factors like temperature, pH, cold, etc. The total chlorophyll content (Chl_a + Chl_b) of plants subjected to salt stress exhibited a similar pattern to Chl_b content across all treatments when compared to plants grown under optimal conditions (Figure 4.14c).

Plants under stressed conditions also showed an increase in their carotenoid content (C_{x+c}), however, this rise was much smaller (1-5%) than the significant elevations seen in their total chlorophyll content and chlorophyll b content. However, a significant gain of C_{x+c} (12%) was observed for plants under treatment with GB@MOP at a concentration 12.5 mM under stress compared to normal plants, this gain was also observed for chlorophyll b (40%) and total chlorophyll (26%) content under the same treatment. The increase in chlorophyll and carotenoid levels in plants in all the treatments under a stressful atmosphere may be attributed to the exposure of the plants to a mild level of stress. However, compared to the control group under salt stress, the plants did not show much difference in chlorophyll and carotenoid contents under all treatments.

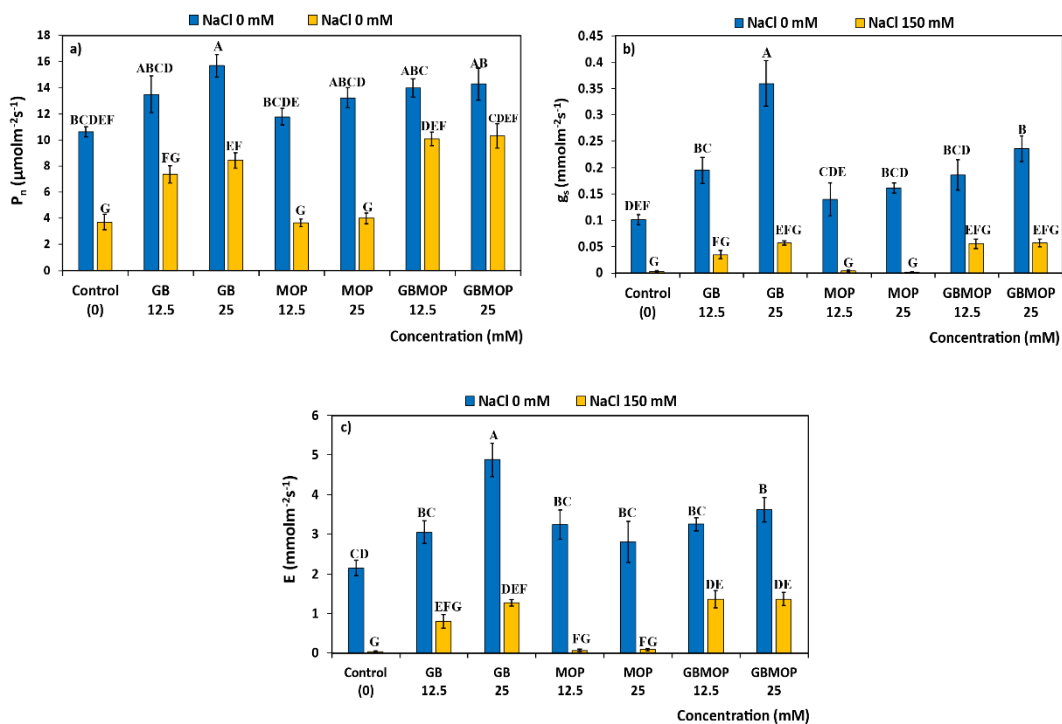
According to existing literature, chlorophyll levels in plants tend to increase under low-level stress and decrease under high-stress conditions (Agathokleous et al., 2020). Hence, the degree of stress experienced by the plants can be estimated by observing the alterations in the chlorophyll content of the plants. Exogenous GB application under stress conditions has been found to increase the chlorophyll pigment concentration in plants according to existing literature (Shafiq et al., 2021) Consequently, plants treated with GB@MOP at a concentration of 12.5 mM exhibited the most significant enhancements in chlorophyll b, overall chlorophyll, and carotenoid levels during stress conditions, likely due to experiencing a lower degree of stress compared to other plants due to the GB application through MOP. These discoveries have broad ramifications for evolution, biotic interactions, and ecophysiology.

Although the plants observed some increase in chlorophyll levels, the increase in chlorophyll and carotenoid levels in plants under stress conditions did not cause any

adverse effects on them. The maximum limit of chlorophyll content in plants is not fixed, it differs among different plant species and environmental conditions (Bayat et al., 2022).

Figure 4.15

Bar Graph Showing 'a) Net photosynthetic rate (P_n), b) Stomatal conductance (g_s), and c) Transpiration rate (E)' of Rice Plants with Different Treatments under NaCl 0 mM and 150 mM. "Values are means of Five Replications. Vertical bars represent Standard Error. Bar columns with different Uppercase letters are Statistically Significant based on Tukey's Honest Significant Difference test at $P < 0.05$ ".



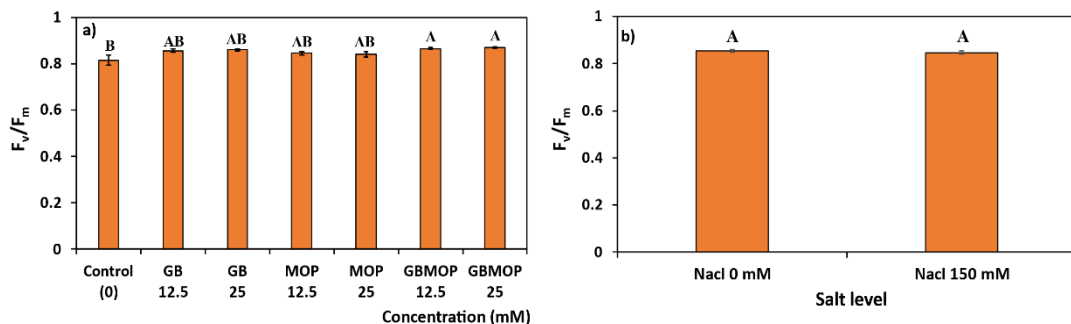
The photosynthetic rate (P_n), rate of stomatal conductance (g_s), and transpiration rate (E) of all treatments were significantly lower under 150 mM salt than when the plants were cultivated under normal circumstances (0 mM) (Figure 4.15). It is noteworthy that the plants treated with GB@MOP at doses of 12.5 mM and 25 mM showed greater P_n , g_s , and E than plants treated with other treatments under salt stress of 150 mM. The values of these parameters in plants treated with GB at doses 12.5 mM and 25 mM were smaller than than GB@MOP treatments but larger than control and treatment with MOP alone under salt stress conditions. Figures 4.15a, b, and c illustrate that while plants

treated with 25 mM GB showed the highest P_n , g_s , and E values under normal conditions (0 mM), the GB@MOP treatments (12.5 mM and 25 mM) showed the highest rates of transpiration, stomatal conductance, and photosynthesis compared to other treatments under salt stress (150 mM).

According to literature, under salt stress conditions, plants experience a reduction in the photosynthetic parameters (Hamani et al., 2020). However, external application of GB has shown to improve these parameters by boosting photosystem activity under stress conditions. Effectivity of GB is increased by delivering it in a targeted manner. Hence, it can be seen from the present study that under stress conditions the treatment of GB@MOP has the comparative advantage over other treatments due to the targeted delivery GB to the plants via MOP.

Figure 4.16

Bar Graph Showing 'Maximum Quantum yield of PSII (F_v/F_m)' of Rice Plants a) under Different Treatments and b) under NaCl 0 mM and 150 mM

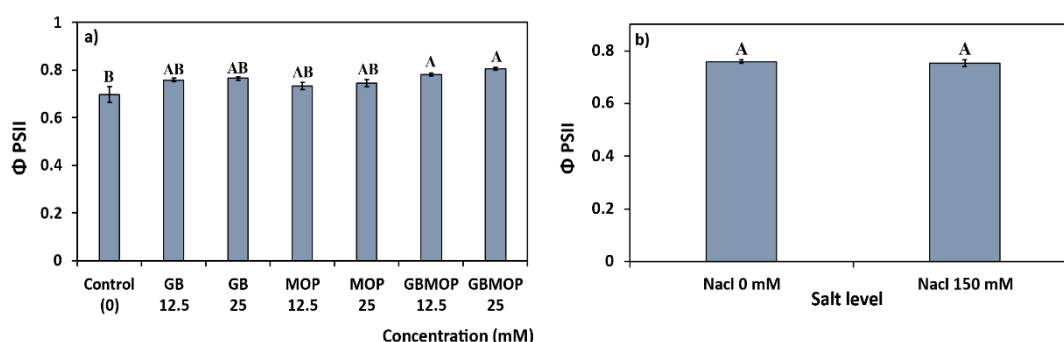


F_v/F_m factor across all the treatments under both factors (normal and salt-stressed conditions) were significantly different (Figure 4.16a). This implies that the treatments under comparison could have a meaningful or substantial influence on one another. The F_v/F_m values of plants treated with GB and GB@MOP at concentrations 12.5 mM and 25 mM were nearly same. These values were notably higher compared to those treated with MOP treatment and control group. However, GB@MOP treatments exhibit the highest F_v/F_m values. The control treatment on the other hand, possessed the lowest values for F_v/F_m .

Similarly, comparing the F_v/F_m values of rice plants under non-stressed conditions and those subjected to salt stress, the graphs did not reveal a significant difference (Figure 4.16b). This suggests that salt stress had no meaningful or detectable effect on the maximum quantum yield of photosystem II (F_v/F_m), indicating a possible resistance of photosynthetic efficiency of plants to salt stress within the limitations of this research.

Figure 4.17

Bar Graph Showing 'Photon yield of PSII (Φ_{PSII})' of Rice Plants a) under Different Treatments and b) under NaCl 0 mM and 150 mM



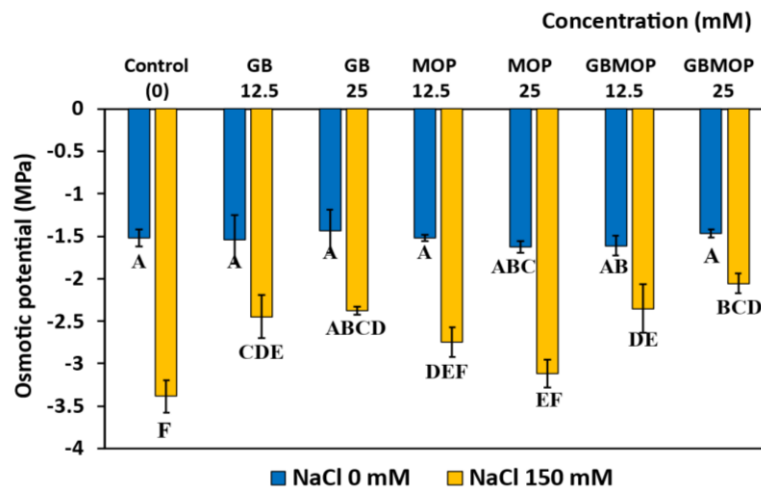
The photon yield of PSII (Φ_{PSII}) exhibited a trend similar to the F_v/F_m across all the treatments. Figure 4.17a indicates significant difference in the photon production of photosystem II (PSII) across all treatments under both factors. Those treated with GB and GB@MOP at doses of 12.5 mM and 25 mM showed virtually similar values for the photon production of PSII. These values were greater than those found in the untreated group and in plants that were just treated with MOP. Notably, out of all the treatments, the control treatment had the lowest and GB@MOP treatments had the highest PSII photon yield. According to this, spraying GB and GB@MOP may have increased PSII photon production, a sign of better photosynthetic efficiency.

Also, there were no discernible variation in the photon yield of plants under normal and salinized conditions (Figure 4.17b). This lack of difference indicates that regardless of the salt stress administered, the PSII activity more especially, the activity associated with electron transport in photosynthesis remained mostly steady. This may be the result of inherited characteristics or plant acclimation responses, but it also shows a degree of resistance or adaptability to salt stress.

According to published literature (Huang et al., 2020), using GB topically in plants can improve water balance, stabilize photosynthetic proteins, scavenge ROS, and maintain membrane integrity, all of which can increase the maximum quantum yield (F_v/F_m) and photon yield (Φ_{PSII}) of the PSII in plants under salt stress conditions. As a result, the controlled and targeted application of GB via MOP as broad scope in the future. This approach reduces loss of GB to the environment, and ensures improved uptake, utilization, and long-term effects of GB, which in turn leads to increased plant productivity and stress tolerance.

Figure 4.18

Bar Graph Showing Osmotic Potential (MPa) of Rice Plants with Different Treatments under NaCl 0 mM and 150 mM. “Values are means of Five Replications. Vertical bars represent Standard Error. Bar columns with different Uppercase letters are Statistically Significant based on Tukey’s Honest Significant Difference test at $P < 0.05$ ”.



The osmotic potential in salt-stressed plants was found to be lower (more negative) than in the plants grown under normal conditions. Compared to plants grown under normal conditions, the salt-stressed plants showed 2-3 times more negative osmotic potential values (Figure 4.18). The salt-stressed plants without treatment exhibited the highest drop in osmotic potential (more negative). In contrast, plants that received GB@MOP treatment at doses 12.5 and 25 mM, and GB at 25 mM have higher values of osmotic potential compared to other treatments and the values of both the treatments were nearly equivalent, however, the values of GB@MOP treatments were still higher than the GB

treatments and also than other treatments. This indicates that GB protects the plants from salt stress and that MOP helps in the targeted delivery of GB to the plants.

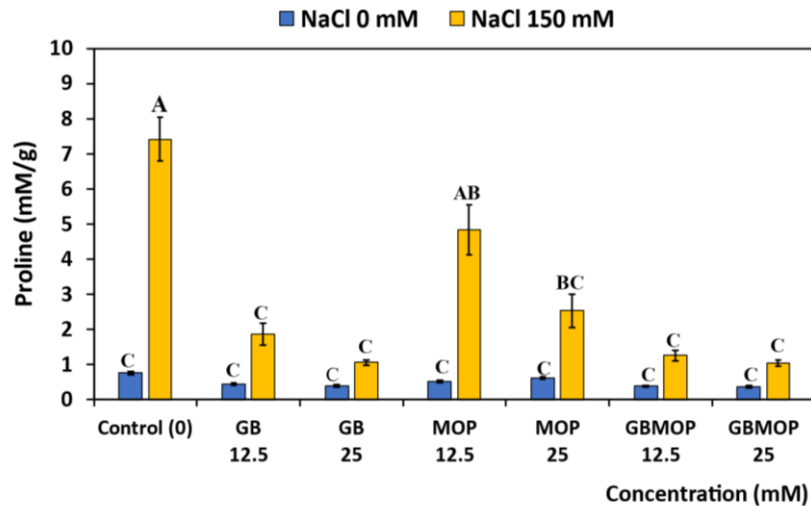
Previous studies have documented the osmolarity levels of plants experiencing salt stress conditions (Cha-Um et al., 2000). Exogenous application of GB leads to enhanced osmotic potential which aids in water absorption, osmotic regulation, and stress tolerance, all of which are essential for plant health and production under stress, and as a result, the osmotic potential is less negative in plants with GB treatments. In present study, the targeted delivery of GB via MOP was found to be effective as the osmotic potential was higher (less negative) compared to other treatments in GB@MOP treatments.

4.4.3 Plant Biochemical Assay

This includes the proline assay. The build-up of proline in plant tissues has been linked to the ability of different plant species to tolerate elevated stress levels. There appears to be a strong relationship between proline concentration and salt tolerance in many plant species since studies have repeatedly shown greater proline concentrations in salt-tolerant plants relative to their salt-sensitive counterparts (Fougère et al., 1991; Madan, 1995). Proline protects the biological membrane and proteins and reduces the ROS levels in plant cells (Ashraf & Foolad, 2007).

Figure 4.19

Bar Graph Showing Proline Content of Rice Plants with Different Treatments under NaCl 0 mM and 150 mM. “Values are means of Five Replications. Vertical bars represent Standard Error. Bar columns with different Uppercase letters are Statistically Significant based on Tukey’s Honest Significant Difference test at $P<0.05$ ”.



Proline content in plants subjected to salt stress of 150 mM was found to be 2-10 times higher than the plants under NaCl 0 mM (Figure 4.19). Moreover, the plants without any treatment (control) exhibited the highest proline accumulation when subjected to 150 mM salt stress, these plants showed about 6 times higher proline accumulation than those grown under normal circumstances without any treatment. On the other hand, under salt stress circumstances, proline accumulation was considerably lower in plants treated with GB@MOP at doses of 12.5 mM and 25 mM, and GB alone at the same concentrations, than in the control group or plants treated with MOP alone (less than half the quantity). This decrease in proline accumulation can be ascribed to the reduced stress encountered by plants treated with GB@MOP and GB as opposed to plants with no treatment and those treated simply with MOP.

Although proline accumulation was higher in plants treated with MOP at doses of 12.5 mM and 25 mM than in plants treated with the same concentration of GB@MOP and GB, it was still lower than in the untreated plants. Control plants accumulated the highest proline under salt stress of 150 mM to combat the stress. Additionally, although,

plants that were treated with the same concentrations of GB@MOP and GB accumulated proline at comparable amounts, the proline accumulation in plants treated with GB@MOP at concentrations 12.5 mM and 25 mM was found to be the lowest of all.

According to the experimental results, plants under salt stress showed higher proline accumulation, where proline buildup is recognized as a stress-related response mechanism in plants, which is consistent with previous research (Fougère et al., 1991; Madan, 1995). Applying GB to stressed plants provided them protection from stress by acting as an osmo-protectant. Hence, plants with treatments containing GB collected less proline because they were under less stress than plants left untreated or treated with MOP alone. Results of the study reveal that the effects of GB@MOP and GB were comparable. GB@MOP treatments were found to be more effective for the majority of the analyses. Therefore, MOP for GB application can be utilized entirely as it adds to targeted delivery without compromising GB and has effects comparable to GB administered alone. This novel approach has great promise for sustainable agriculture as it offers practical ways to control plant stress and enhance crop yield and quality.

Table 4.4

Significance Levels in Both the Independent and Combined impacts of various Morphological, Physiological, and Biochemical Factors

Items	Factors		
	Treatment (T)	Salt (S)	T×S
Root length (cm)	**	**	**
Shoot length (cm)	**	**	**
Biomass root (g)	**	**	*
Biomass shoot (g)	**	**	**
SPAD	**	**	**
NDVI	**	**	**
Chlorophyll a (µg/g FW)	**	**	*
Chlorophyll b (µg/g FW)	*	**	**
Total chlorophyll (µg/g FW)	*	**	**
Carotenoid (µg/g FW)	**	**	**
F _v /F _m	*	NS	NS
PS II	**	NS	NS
P _n (µmolm ⁻² s ⁻¹)	*	**	**
g _s (mmolm ⁻² s ⁻¹)	*	**	**
E (mmolm ⁻² s ⁻¹)	**	**	*
Osmotic potential (MPa)	**	**	**
Proline (mM/g)	**	**	**

*Where, **, *, and NS indicate $P \leq 0.01$, $P \leq 0.05$, and non-significant respectively*

Table 4.5

Values of the Morphological Analysis of the Plants Along with the Mean Difference Level

Factors	Root length	Shoot length	Root biomass	Shoot biomass
Treatment (T)				
T1	14.3 ± 0.3F	68.6 ± 3G	0.06 ± 0F	0.43 ± 0F
T2	16.9 ± 0.4C	74.4 ± 3D	0.10 ± 0C	0.58 ± 0CD
T3	17.6 ± 0.2B	74.9 ± 3C	0.11 ± 0C	0.62 ± 0BC
T4	15.5 ± 0.25E	69.4 ± 3F	0.10 ± 0D	0.52 ± 0E
T5	16.2 ± 0.2D	70.9 ± 3E	0.08 ± 0E	0.56 ± 0DE
T6	17.8 ± 0.2AB	76.5 ± 4B	0.12 ± 0B	0.65 ± 0B
T7	18.2 ± 0.15A	78.2 ± 4A	0.16 ± 0A	0.93 ± 0A
Salt regime (S)				
S _{0mM}	17.4 ± 0.2A	82.5 ± 1.0A	0.13 ± 0A	0.76 ± 0A
S _{150mM}	15.9 ± 0.2B	64.0 ± 0.5B	0.07 ± 0B	0.47 ± 0B
T×S				
T1 × S _{0mM}	15.3 ± 0.1GH	76.44 ± 0.1G	0.086 ± 0E	0.5 ± 0E
T2 × S _{0mM}	18.1 ± 0.1AB	83.1 ± 0.1D	0.13 ± 0CD	0.7 ± 0CD
T3 × S _{0mM}	18.2 ± 0.1AB	83.9 ± 0.1C	0.14 ± 0BC	0.8 ± 0BC
T4 × S _{0mM}	16.3 ± 0.1EF	78 ± 0.1F	0.12 ± 0DE	0.7 ± 0D
T5 × S _{0mM}	16.8 ± 0.1DE	80.1 ± 0E.2	0.11 ± 0E	0.7 ± 0CD
T6 × S _{0mM}	18.4 ± 0.1A	87.38 ± 0.2B	0.15 ± 0B	0.8 ± 0B
T7 × S _{0mM}	18.6 ± 0.1A	88.8 ± 0.1A	1.19 ± 0A	1.1 ± 0A
T1 × S _{150mM}	13.4 ± 0.2I	60.7 ± 0.1K	0.044 ± 0I	0.3 ± 0I
T2 × S _{150mM}	15.8 ± 0.1FG	65.6 ± 0.2I	0.074 ± 0GH	0.5 ± 0FG
T3 × S _{150mM}	17 ± 0.1D	66 ± 0.1I	0.08 ± 0FG	0.5 ± 0EFG
T4 × S _{150mM}	14.8 ± 0.1H	60.7 ± 0.1K	0.06 ± 0HI	0.4 ± 0HI
T5 × S _{150mM}	15.6 ± 0.2G	61.8 ± 0.1J	0.05 ± 0IJ	0.4 ± 0GH
T6 × S _{150mM}	17.3 ± 0.1CD	65.6 ± 0.2I	0.09 ± 0F	0.5 ± 0EF
T7 × S _{150mM}	17.7 ± 0.1BC	67.6 ± 0.2H	0.14 ± 0BC	0.7 ± 0CD

Table 4.6

Values of the Physiological (Chlorophyll) Analysis of the Plants Along with the Mean Difference Level

Factors	Chl_a	Chl_b	Total Chl	C_{x+c}
Treatment				
(T)				
T1	23.2 ± 0C	40.7 ± 2AB	63.9 ± 2AB	2502 ± 9AB
T2	23.4 ± 0.1ABC	40.4 ± 2AB	63.8 ± 2AB	2522 ± 8A
T3	23.5 ± 0.1AB	38.7 ± 3AB	62.3 ± 2.5AB	2503 ± 37AB
T4	23.5 ± 0.1A	40.2 ± 2AB	63.7 ± 2AB	2551 ± 11A
T5	23.6 ± 0.1A	41.7 ± 1A	65.3 ± 1.2A	2569 ± 5.2A
T6	23.2 ± 0.1C	35.4 ± 4B	58.8 ± 3.5B	2416 ± 69B
T7	23.3 ± 0BC	39.2 ± 2AB	62.5 ± 2AB	2513 ± 20AB
Salt regime				
(S)				
S _{0mM}	23.6 ± 0.1A	34.7 ± 1.1B	58.3 ± 1.1B	2467.4 ± 22B
S _{150mM}	23.2 ± 0B	44.3 ± 0.3A	67.5 ± 0.3A	2554.4 ± 5A
T×S				
T1 × S _{0mM}	23.4 ± 0.1BCDE	37.9 ± 3ABCDE	61 ± 3ABCD	2493 ± 16.4A
T2 × S _{0mM}	23.7 ± 0.1ABCD	35.8 ± 2BCDEF	60 ± 1BCD	2513 ± 14A
T3 × S _{0mM}	23.7 ± 0.1ABC	32.12 ± 3EF	56 ± 3DE	2443 ± 65A
T4 × S _{0mM}	23.8 ± 0.2AB	35.7 ± 2CDEF	59.4 ± 1BCD	2527 ± 15A
T5 × S _{0mM}	23.9 ± 0.1A	41.3 ± 2ABCD	65.2 ± 2ABC	2569 ± 8A
T6 × S _{0mM}	23.2 ± 0.1E	26.7 ± 4F	50 ± 4E	2269 ± 103B
T7 × S _{0mM}	23.3 ± 0.1CDE	33.6 ± 2DEF	57 ± 2CDE	2457 ± 9A
T1 × S _{150mM}	23.1 ± 0E	43.6 ± 1ABC	66.7 ± 1AB	2511 ± 9.4A
T2 × S _{150mM}	23.2 ± 0E	45 ± 0.3A	68.2 ± 0.3AB	2530 ± 6A
T3 × S _{150mM}	23.4 ± 0.1BCDE	45.4 ± 0.4A	68.8 ± 0.5A	2564 ± 8A
T4 × S _{150mM}	23.3 ± 0CDE	44.8 ± 0.4ABC	68.1 ± 0.4AB	2574 ± 8A
T5 × S _{150mM}	23.3 ± 0.1CDE	42.1 ± 2ABCD	65.4 ± 2ABC	2569 ± 8A
T6 × S _{150mM}	23.2 ± 0DE	44.02 ± 1ABC	67.2 ± 1BC	2563 ± 4A
T7 × S _{150mM}	23.3 ± 0.1CDE	44.9 ± 0.3AB	68.2 ± 0.3AB	2570 ± 10A

Table 4.7

Values of the Physiological (Photosynthetic parameters) Analysis of the Plants Along with the Mean Difference Level

Factors	F_v/F_m	ΦPSII	P_n	g_s	E
Treatment					
(T)					
T1	0.8 ± 0B	0.6 ± 0B	7.2 ± 1C	0.1 ± 0D	1.1 ± 0.4E
T2	0.8 ± 0AB	0.8 ± 0AB	10.4 ± 1AB	0.1 ± 0BC	2.0 ± 1BCD
T3	0.8 ± 0AB	0.8 ± 0AB	12.1 ± 1A	0.2 ± 0A	3.0 ± 1A
T4	0.8 ± 0AB	0.7 ± 0AB	7.7 ± 1C	0.1 ± 0CD	1.6 ± 1CDE
T5	0.8 ± AB	0.7 ± 0AB	8.6 ± 2BC	0.1 ± 0CD	1.5 ± 1DE
T6	0.9 ± 0A	0.8 ± 0A	12.0 ± 1A	0.1 ± 0BC	2.3 ± 0.3BC
T7	0.9 ± 0A	0.8 ± 0A	12.3 ± 1A	0.2 ± 0B	2.4 ± 0.4AB
Salt regime					
(S)					
S _{0mM}	0.85 ± 0	0.76 ± 0	13.30 ± 0.4A	0.20 ± 0A	3.30 ± 0.2A
S _{150mM}	0.85 ± 0	0.75 ± 0	6.80 ± 0.5B	0.03 ± 0B	0.71 ± 0.1B
T×S					
T1 × S _{0mM}	0.82 ± 0	0.73 ± 0	11 ± 1BCDEF	0.1 ± 0DEF	2 ± 0.2CD
T2 × S _{0mM}	0.85 ± 0	0.75 ± 0	14 ± 1ABCD	0.2 ± 0BC	3 ± 0.3BC
T3 × S _{0mM}	0.86 ± 0	0.76 ± 0	15.7 ± 1A	0.36 ± 0A	4.8 ± 0.4A
T4 × S _{0mM}	0.84 ± 0	0.74 ± 0	12 ± 1BCDE	0.1 ± 0CDE	3 ± 0.4BC
T5 × S _{0mM}	0.85 ± 0	0.74 ± 0	13 ± 1ABCD	0.2 ± 0BCD	3 ± 0.5BC
T6 × S _{0mM}	0.87 ± 0	0.77 ± 0	14 ± 1ABC	0.2 ± 0BCD	3.3±0.2BC
T7 × S _{0mM}	0.87 ± 0	0.8 ± 0	14 ± 1AB	0.24 ± 0B	3.6 ± 0.3B
T1 × S _{150mM}	0.8 ± 0	0.6 ± 0.1	3.7 ± 1G	0.003 ± 0G	0.04 ± 0G
T2 × S _{150mM}	0.86 ± 0	0.76 ± 0	7.4 ± 1FG	0.04 ± 0FG	1 ± 0EFG
T3 × S _{150mM}	0.86 ± 0	0.77 ± 0	8.4 ± 1EF	0.1 ± 0EFG	1 ± 0DEF
T4 × S _{150mM}	0.84 ± 0	0.72 ± 0	3.7 ± 0G	0.004 ± 0G	0.1 ± 0FG
T5 × S _{150mM}	0.83 ± 0	0.75 ± 0	4.0 ± 0G	0.002 ± 0G	0.1 ± 0FG
T6 × S _{150mM}	0.86 ± 0	0.79 ± 0	10.1 ± 1DEF	0.1 ± 0EFG	1.4 ± 0DE
T7 × S _{150mM}	0.87 ± 0A	0.8 ± 0A	10.3 ± 1CDEF	0.1 ± 0EFG	1.4 ± 0DE

Table 4.8

Values of the Physiological and Biochemical Analysis of the Plants Along with the Mean Difference Level

Factors	SPAD	NDVI	Osmotic potential	Proline
Treatment (T)				
T1	35.78 ± 0.4G	0.69 ± 0B	-2.45 ± 0.3C	4.09 ± 1.3A
T2	37.44 ± 0.6D	0.69 ± 0BC	-1.95 ± 0.2AB	1.16 ± 0.3BC
T3	37.79 ± 0.7C	0.73 ± 0A	-1.74 ± 0.1A	0.73 ± 0.1C
T4	36.76 ± 0.7E	0.67 ± 0C	-2.14 ± 0.2ABC	2.68 ± 1AB
T5	36.30 ± 0.74F	0.72 ± 0A	-2.37 ± 0.3BC	1.57 ± 0.4BC
T6	38.47 ± 0.5B	0.69 ± 0B	-2.03 ± 0.2ABC	0.82 ± 0.2C
T7	40.91 ± 0.5A	0.73 ± 0A	-1.91 ± 0.2AB	0.72 ± 0.1C
Salt regime (S)				
S _{0mM}	35.82 ± 0.3B	0.78 ± 0	-1.53 ± 0A	0.50 ± 0B
S _{150mM}	39.45 ± 0.3A	0.63 ± 0	-2.64 ± 0.1B	2.86 ± 0.46A
T×S				
T1 × S _{0mM}	34.50 ± 1HI	0.78 ± 0B	-1.52 ± 0.1A	0.77 ± 0.1C
T2 × S _{0mM}	35.46 ± 1G	0.75 ± 0C	-1.54 ± 0.1A	0.45 ± 0C
T3 × S _{0mM}	35.76 ± 2G	0.79 ± 0AB	-1.43 ± 0.1A	0.40 ± 0C
T4 × S _{0mM}	34.70 ± 2H	0.76 ± 0BC	-1.52 ± 0A	0.52 ± 0.1C
T5 × S _{0mM}	34.08 ± 1I	0.82 ± 0A	-1.62 ± 0.1ABC	0.62 ± 0C
T6 × S _{0mM}	36.88 ± 1F	0.78 ± 0B	-1.61 ± 0.1AB	0.4 ± 0C
T7 × S _{0mM}	39.38 ± 1CD	0.81 ± 0A	-1.47 ± 0.1A	0.37 ± 0.1C
T1 × S _{150mM}	37.08 ± 1F	0.61 ± 0FG	-3.40 ± 0.2F	7.4 ± 1A
T2 × S _{150mM}	39.42 ± 1C	0.63 ± 0EF	-2.44 ± 0.3CDE	1.86 ± 0.3C
T3 × S _{150mM}	39.82 ± 2BC	0.65 ± 0D	-2.38 ± 0ABCD	1.06 ± 0.1C
T4 × S _{150mM}	38.82 ± 1DE	0.59 ± 0G	-2.75 ± 0.2DEF	4.8 ± 1AB
T5 × S _{150mM}	38.52 ± 1E	0.624 ± 0EF	-3.11 ± 0.2EF	2.5 ± 0.5BC
T6 × S _{150mM}	40.06 ± 1B	0.618 ± 0F	-2.35 ± 0.3DE	1.2 ± 0.1C
T7 × S _{150mM}	42.44 ± 1A	0.66 ± 0DE	-2.05 ± 0.1BCD	1.05 ± 0.1C

Note: The standard error values of less than 0.05 are denoted as 0 in the tables above

Where, T1 = Control

T2 = GB 12.5 mM

T3 = GB 25 mM

T4 = MOP 12.5 mM

T5 = MOP 25 mM

T6 = GB@MOP 12.5 mM

T7 = GB@MOP 25 mM

S_{0mM} = Salt at concentration 0 mM (NaCl 0 mM)

S_{150mM} = Salt at concentration 150 mM (NaCl 150 mM)

CHAPTER 5

CONCLUSIONS AND FUTURE RECOMMENDATIONS

5.1 Conclusion

In conclusion, this research investigated the potential use of MOPs as a novel approach for delivering glycine betaine to rice crops in order to provide salinity stress control and management under greenhouse conditions. Experiments and analyses showed that rice plants had continuous uptake of GB due to modified release kinetics with respect to MOPs. Moreover, this regulated delivery system is necessary for optimal plant development, stress tolerance, and ultimately crop growth. Furthermore, the numerous intense peaks observed in XRD patterns indicate that this synthesized MOP is highly micro-porous material which contain many small holes or pores. These pores might serve as a good host for encapsulating glycine betaine and releasing it effectively thus their structural importance in agriculture. In addition to advancing the study of nanotechnology in agriculture, this study offers practical solutions to challenges posed by environmental stresses on rice.

This research also encompasses a range of relationships between plant systems and various MOPs to explain how GB is efficiently delivered. A variety of morphological, physiological, and biochemical experiments have been conducted in order to understand the mechanism of GB, GB@MOP and MOP activities in rice plants. The outcomes are consistent with previous findings which demonstrated that glycine betaine could be used as a remedy for increasing resistance of plants against different environmental stresses like drought and salt. The concentrations of GB@MOP i.e. 12.5 mM and 25 mM were found to be effective under salt stress in most of the parameters. The statistical significance at $p < 0.05$ observed across almost all the parameters reinforces the potential and practical significance of Cu-based MOPs for optimizing GB delivery to rice crops.

5.2 Future Recommendations

The encapsulation and controlled release of Glycine Betaine in rice crops can be revolutionized by harnessing Cu-based Metal-Organic Polyhedra (MOPs) for this purpose, which will enhance crop resilience, production sustainability and thus improve the future generation's food security amidst changing environmental conditions. Presented below are some recommendations for future studies:

Prolonged Field Studies

Long-term effects of MOP-facilitated application of Glycine Betaine on Rice under various environmental circumstances need to be established through extended field trials. There is also a need to conduct multiple seasons of crop testing to identify any weaknesses of MOPs to determine their performance in real agricultural environments.

Synthesis of MOPs Optimization and Stability Analysis

The synthesis procedure of MOPs needs to be improved further for them to become more efficient, scalable, and cost-effective. Also, the stability analysis of MOPs is crucial for understanding their long-term performance and potential applications. It is important to consider alternative methods for making them stable as well as whether they can be produced in large quantities without losing their structural integrity or controlled release properties.

Ecotoxicological Assessments:

To ensure that MOPs remains safe and sustainable options, it's essential to assess the possible build-up of these materials as well as the environmental degradation products that result from their decomposition.

Economic Feasibility of the MOPs:

The economic analysis needs to determine if it would be Cost effective to incorporate MOPs into agronomic practices. The financial impact analysis should assess agricultural returns, resource use and potential savings versus conventional methods.

REFERENCES

- Abbas, M., Maceda, A. M., Xiao, Z., Zhou, H.-C., & Balkus, K. J. (2023). Transformation of a copper-based metal–organic polyhedron into a mixed linker MOF for CO₂ capture. *Dalton Transactions*, 52(14), 4415–4422. <https://doi.org/10.1039/D2DT04162F>
- Abdus Sobahan, M., Akter, N., Murata, Y., & Munemasa, S. (2016). Exogenous Proline and Glycinebetaine Mitigate the Detrimental Effect of Salt Stress on Rice Plants. *Silpakorn U Science & Tech J*, 10(3), 38–43. <https://doi.org/10.14456/sustj.2016.11>
- Abogadallah, G. M. (2010). Insights into the significance of antioxidative defense under salt stress. *Plant Signaling & Behavior*, 5(4), 369–374. <https://doi.org/10.4161/psb.5.4.10873>
- Agathokleous, E., Feng, Z., & Peñuelas, J. (2020). Chlorophyll hormesis: Are chlorophylls major components of stress biology in higher plants? *Science of The Total Environment*, 726, 138637. <https://doi.org/10.1016/j.scitotenv.2020.138637>
- Ahmed, N., Zhang, Y., Li, K., Zhou, Y., Zhang, M., & Li, Z. (2019). Exogenous application of glycine betaine improved water use efficiency in winter wheat (*Triticum aestivum* L.) via modulating photosynthetic efficiency and antioxidative capacity under conventional and limited irrigation conditions. *The Crop Journal*, 7(5), 635–650. <https://doi.org/10.1016/j.cj.2019.03.004>
- Ahmed, S., Heo, T.-Y., Roy Choudhury, A., Walitang, D. I., Choi, J., & Sa, T. (2021). Accumulation of compatible solutes in rice (*Oryza sativa* L.) cultivars by inoculation of endophytic plant growth promoting bacteria to alleviate salt stress. *Applied Biological Chemistry*, 64(1), 68. <https://doi.org/10.1186/s13765-021-00638-x>
- Al Masruri, M. H. K., Ullah, A., & Farooq, M. (2023). Application of Nano Chitosan-glycinebetaine for Improving Bread Wheat Performance under Combined Drought and Heat Stresses. *Journal of Soil Science and Plant Nutrition*, 23(3), 3482–3499. <https://doi.org/10.1007/s42729-023-01265-9>

- Albalad, J., Hernández-López, L., Carné-Sánchez, A., & Maspoch, D. (2022). Surface chemistry of metal–organic polyhedra. *Chemical Communications*, 58(15), 2443–2454. <https://doi.org/10.1039/D1CC07034G>
- An, C., Sun, C., Li, N., Huang, B., Jiang, J., Shen, Y., Wang, C., Zhao, X., Cui, B., Wang, C., Li, X., Zhan, S., Gao, F., Zeng, Z., Cui, H., & Wang, Y. (2022). Nanomaterials and nanotechnology for the delivery of agrochemicals: strategies towards sustainable agriculture. *Journal of Nanobiotechnology*, 20(1), 11. <https://doi.org/10.1186/s12951-021-01214-7>
- Anami, B. S., Malvade, N. N., & Palaiah, S. (2020). Classification of yield affecting biotic and abiotic paddy crop stresses using field images. *Information Processing in Agriculture*, 7(2), 272–285. <https://doi.org/10.1016/j.inpa.2019.08.005>
- Annunziata, M. G., Ciarmiello, L. F., Woodrow, P., Dell’Aversana, E., & Carillo, P. (2019). Spatial and Temporal Profile of Glycine Betaine Accumulation in Plants Under Abiotic Stresses. *Frontiers in Plant Science*, 10. <https://doi.org/10.3389/fpls.2019.00230>
- Anstoetz, M., Rose, T. J., Clark, M. W., Yee, L. H., Raymond, C. A., & Vancov, T. (2015). Novel Applications for Oxalate-Phosphate-Amine Metal-Organic-Frameworks (OPA-MOFs): Can an Iron-Based OPA-MOF Be Used as Slow-Release Fertilizer? *PLOS ONE*, 10(12), e0144169-. <https://doi.org/10.1371/journal.pone.0144169>
- Ashraf, M., & Foolad, M. R. (2007a). Roles of glycine betaine and proline in improving plant abiotic stress resistance. *Environmental and Experimental Botany*, 59(2), 206–216. <https://doi.org/10.1016/j.envexpbot.2005.12.006>
- Ashraf, M., & Foolad, M. R. (2007b). Roles of glycine betaine and proline in improving plant abiotic stress resistance. *Environmental and Experimental Botany*, 59(2), 206–216. <https://doi.org/10.1016/j.envexpbot.2005.12.006>
- Babu, S., Singh, R., Yadav, D., Rathore, S. S., Raj, R., Avasthe, R., Yadav, S. K., Das, A., Yadav, V., Yadav, B., Shekhawat, K., Upadhyay, P. K., Yadav, D. K., & Singh, V. K. (2022). Nanofertilizers for agricultural and environmental sustainability. *Chemosphere*, 292, 133451. <https://doi.org/https://doi.org/10.1016/j.chemosphere.2021.133451>
- Bagheri, A. R., & Ghaedi, M. (2020). Application of Cu-based metal-organic framework (Cu-BDC) as a sorbent for dispersive solid-phase extraction of

- gallic acid from orange juice samples using HPLC-UV method. *Arabian Journal of Chemistry*, 13(5), 5218–5228.
<https://doi.org/10.1016/j.arabjc.2020.02.020>
- Bates, L. S., Waldren, R. P., & Teare, I. D. (1973). Rapid determination of free proline for water-stress studies. *Plant and Soil*, 39(1), 205–207.
<https://doi.org/10.1007/BF00018060>
- Bayat, H., Shafie, F., & Shahraki, B. (2022). Salinity effects on growth, chlorophyll content, total phenols, and antioxidant activity in *Salvia lavandulifolia* Vahl. *Advances in Horticultural Science*, 36(2), 145–153.
<https://doi.org/10.36253/ahsc-12015>
- Bayer, I. S. (2023). Controlled Drug Release from Nanoengineered Polysaccharides. *Pharmaceutics*, 15(5), 1364. <https://doi.org/10.3390/pharmaceutics15051364>
- Beggel, S., Werner, I., Connon, R. E., & Geist, J. P. (2010). Sublethal toxicity of commercial insecticide formulations and their active ingredients to larval fathead minnow (*Pimephales promelas*). *Science of The Total Environment*, 408(16), 3169–3175. <https://doi.org/10.1016/j.scitotenv.2010.04.004>
- Birnbaum, L. S. (2013). When environmental chemicals act like uncontrolled medicine. *Trends in Endocrinology & Metabolism*, 24(7), 321–323.
<https://doi.org/10.1016/j.tem.2012.12.005>
- Brar, D. S., Singh, K., & Khush, G. S. (2017). Frontiers in Rice Breeding. In *The Future Rice Strategy for India* (pp. 137–160). Elsevier. <https://doi.org/10.1016/B978-0-12-805374-4.00006-3>
- Cabrera-Bosquet, L., Molero, G., Stellacci, A., Bort, J., Nogués, S., & Araus, J. (2011). NDVI as a potential tool for predicting biomass, plant nitrogen content and growth in wheat genotypes subjected to different water and nitrogen conditions. *Cereal Research Communications*, 39(1), 147–159.
<https://doi.org/10.1556/CRC.39.2011.1.15>
- Carné-Sánchez, A., Albalad, J., Grancha, T., Imaz, I., Juanhuix, J., Larpent, P., Furukawa, S., & MasPOCH, D. (2019). Postsynthetic Covalent and Coordination Functionalization of Rhodium(II)-Based Metal–Organic Polyhedra. *Journal of the American Chemical Society*, 141(9), 4094–4102.
<https://doi.org/10.1021/jacs.8b13593>
- Chauhan, D., Omar, R. A., Mangalaraja, R. V, Ashfaq, M., & Talreja, N. (2022). Chapter 13 - Metal-organic framework as an emerging material: a novel plant

- growth stimulant. In G. M. Balestra & E. Fortunati (Eds.), *Nanotechnology-Based Sustainable Alternatives for the Management of Plant Diseases* (pp. 323–339). Elsevier. [https://doi.org/https://doi.org/10.1016/B978-0-12-823394-8.00015-9](https://doi.org/10.1016/B978-0-12-823394-8.00015-9)
- Cha-Um, S., & Kirdmanee, C. (2007). An Effective Defensive Response in Thai Aromatic Rice Varieties (*Oryza sativa* L. spp. indica) to Salinity Phanchita Vejchasarn Ministry of Agriculture and Cooperatives. <https://www.researchgate.net/publication/238622705>
- Cha-Um, S., Vejchasarn, P., & Kirdmanee, C. (n.d.). An Effective Defensive Response in Thai Aromatic Rice Varieties (*Oryza sativa* L. spp. indica) to Salinity. In *J. Crop Sci. Biotech* (Vol. 10, Issue 4). www.cropbio.org
- Chen, T. H. H., & Murata, N. (2008). Glycinebetaine: an effective protectant against abiotic stress in plants. *Trends in Plant Science*, *13*(9), 499–505. <https://doi.org/10.1016/j.tplants.2008.06.007>
- Chen, T. H. H., & Murata, N. (2011). Glycinebetaine protects plants against abiotic stress: mechanisms and biotechnological applications. *Plant, Cell & Environment*, *34*(1), 1–20. <https://doi.org/10.1111/j.1365-3040.2010.02232.x>
- Chen, T.-H., Wang, L., Trueblood, J. V., Grassian, V. H., & Cohen, S. M. (2016). Poly(isophthalic acid)(ethylene oxide) as a Macromolecular Modulator for Metal–Organic Polyhedra. *Journal of the American Chemical Society*, *138*(30), 9646–9654. <https://doi.org/10.1021/jacs.6b04971>
- Chhipa, H. (2017). Nanofertilizers and nanopesticides for agriculture. *Environmental Chemistry Letters*, *15*(1), 15–22. <https://doi.org/10.1007/s10311-016-0600-4>
- Chugh, G., Siddique, K. H. M., & Solaiman, Z. M. (2021). Nanobiotechnology for Agriculture: Smart Technology for Combating Nutrient Deficiencies with Nanotoxicity Challenges. *Sustainability*, *13*(4), 1781. <https://doi.org/10.3390/su13041781>
- Chui, S. S.-Y., Lo, S. M.-F., Charmant, J. P. H., Orpen, A. G., & Williams, I. D. (1999). A Chemically Functionalizable Nanoporous Material [Cu₃(TMA)₂(H₂O)₃]_n. *Science*, *283*(5405), 1148–1150. <https://doi.org/10.1126/science.283.5405.1148>
- Chun, H., Jung, H., & Seo, J. (2009). Isorecticular Metal-Organic Polyhedral Networks Based on 5-Connecting Paddlewheel Motifs. *Inorganic Chemistry*, *48*(5), 2043–2047. <https://doi.org/10.1021/ic801784j>

- Demiral, T., & Türkan, I. (2006). Exogenous glycinebetaine affects growth and proline accumulation and retards senescence in two rice cultivars under NaCl stress. *Environmental and Experimental Botany*, *56*(1), 72–79.
<https://doi.org/10.1016/j.envexpbot.2005.01.005>
- Diatta, A. A., Thomason, W. E., Abaye, O., Thompson, T. L., Battaglia, M. L., Vaughan, L. J., Lo, M., & Filho, J. F. D. C. L. (2020). Assessment of Nitrogen Fixation by Mungbean Genotypes in Different Soil Textures Using ¹⁵N Natural Abundance Method. *Journal of Soil Science and Plant Nutrition*, *20*(4), 2230–2240. <https://doi.org/10.1007/s42729-020-00290-2>
- Ecobichon, D. J. (2001). Pesticide use in developing countries. *Toxicology*, *160*(1–3), 27–33. [https://doi.org/10.1016/S0300-483X\(00\)00452-2](https://doi.org/10.1016/S0300-483X(00)00452-2)
- Eddaoudi, M., Kim, J., Wachter, J. B., Chae, H. K., O’Keeffe, M., & Yaghi, O. M. (2001). Porous metal-organic polyhedra: 25 Å cuboctahedron constructed from 12 Cu₂(CO₂)₄ paddle-wheel building blocks [17]. In *Journal of the American Chemical Society* (Vol. 123, Issue 18, pp. 4368–4369). <https://doi.org/10.1021/ja0104352>
- El-Laboudy, H., Shaker, M. A., & Younes, H. M. (2011). Soft Biodegradable Elastomers Based on Poly (Octanediol-Tartarate) for Drug Delivery and Tissue Engineering: Synthesis, Characterization and Biocompatibility Studies. *Soft Materials*, *9*(4), 409–428.
<https://doi.org/10.1080/1539445X.2010.528726>
- El-Ramady, H., Alshaal, T., Elhawat, N., Ghazi, A., Elsakhawy, T., Omara, A. E.-D., El-Nahrawy, S., Elmahrouk, M., Abdalla, N., Domokos-Szabolcsy, É., & Schnug, E. (2018). Plant Nutrients and Their Roles Under Saline Soil Conditions. In *Plant Nutrients and Abiotic Stress Tolerance* (pp. 297–324). Springer Singapore. https://doi.org/10.1007/978-981-10-9044-8_13
- Fatima, A., Ali, A., Shabbir, S., Khan, M., Mehkoom, M., Afzal, S. M., Ahmad, M., Althubeiti, K., Siddiqui, N., Singh, M., & Javed, S. (2022). Synthesis, crystal structure, characterization, Hirshfeld analysis, molecular docking and DFT calculations of 5-Phenylamino-isophthalic acid: A good NLO material. *Journal of Molecular Structure*, *1261*, 132791.
<https://doi.org/10.1016/j.molstruc.2022.132791>
- Fougère, F., Le Rudulier, D., & Streeter, J. G. (1991). Effects of Salt Stress on Amino Acid, Organic Acid, and Carbohydrate Composition of Roots, Bacteroids, and

- Cytosol of Alfalfa (*Medicago sativa* L.). *Plant Physiology*, 96(4), 1228–1236.
<https://doi.org/10.1104/pp.96.4.1228>
- Fu, J., Huang, B., & Fry, J. (2010). Osmotic Potential, Sucrose Level, and Activity of Sucrose Metabolic Enzymes in Tall Fescue in Response to Deficit Irrigation. *Journal of the American Society for Horticultural Science*, 135(6), 506–510.
<https://doi.org/10.21273/JASHS.135.6.506>
- Furukawa, H., Cordova, K. E., O’Keeffe, M., & Yaghi, O. M. (2013). The Chemistry and Applications of Metal–Organic Frameworks. *Science*, 341(6149).
<https://doi.org/10.1126/science.1230444>
- Furukawa, S., Horike, N., Kondo, M., Hijikata, Y., Carné-Sánchez, A., Larpent, P., Louvain, N., Diring, S., Sato, H., Matsuda, R., Kawano, R., & Kitagawa, S. (2016). Rhodium–Organic Cuboctahedra as Porous Solids with Strong Binding Sites. *Inorganic Chemistry*, 55(21), 10843–10846.
<https://doi.org/10.1021/acs.inorgchem.6b02091>
- Gosselin, A. J., Decker, G. E., Antonio, A. M., Lorzing, G. R., Yap, G. P. A., & Bloch, E. D. (2020). A Charged Coordination Cage-Based Porous Salt. *Journal of the American Chemical Society*, 142(21), 9594–9598.
<https://doi.org/10.1021/jacs.0c02806>
- Gosselin, A. J., Rowland, C. A., & Bloch, E. D. (2020). Permanently Microporous Metal–Organic Polyhedra. *Chemical Reviews*, 120(16), 8987–9014.
<https://doi.org/10.1021/acs.chemrev.9b00803>
- Grancha, T., Carné-Sánchez, A., Zarekarizi, F., Hernández-López, L., Albalad, J., Khobotov, A., Guillerm, V., Morsali, A., Juanhuix, J., Gándara, F., Imaz, I., & Maspoch, D. (2021). Synthesis of Polycarboxylate Rhodium(II) Metal–Organic Polyhedra (MOPs) and their use as Building Blocks for Highly Connected Metal–Organic Frameworks (MOFs). *Angewandte Chemie International Edition*, 60(11), 5729–5733.
<https://doi.org/10.1002/anie.202013839>
- Grant, S., Mortimer, M., Stevenson, G., Malcolm, D., & Gaus, C. (2011). Facilitated Transport of Dioxins in Soil Following Unintentional Release of Pesticide-Surfactant Formulations. *Environmental Science & Technology*, 45(2), 406–411. <https://doi.org/10.1021/es102254x>

- Grieve, C. M., & Grattan, S. R. (1983). Rapid assay for determination of water soluble quaternary ammonium compounds. *Plant and Soil*, 70(2), 303–307. <https://doi.org/10.1007/BF02374789>
- Grillo, R., Fraceto, L. F., Amorim, M. J. B., Scott-Fordsmand, J. J., Schoonjans, R., & Chaudhry, Q. (2021). Ecotoxicological and regulatory aspects of environmental sustainability of nanopesticides. *Journal of Hazardous Materials*, 404, 124148. <https://doi.org/10.1016/j.jhazmat.2020.124148>
- Guha, T., Gopal, G., Kundu, R., & Mukherjee, A. (2020). Nanocomposites for Delivering Agrochemicals: A Comprehensive Review. *Journal of Agricultural and Food Chemistry*, 68(12), 3691–3702. <https://doi.org/10.1021/acs.jafc.9b06982>
- Hakim, M. A., Juraimi, A. S., Hanafi, M. M., Ismail, M. R., Selamat, A., Rafii, M. Y., & Latif, M. A. (2014). Biochemical and Anatomical Changes and Yield Reduction in Rice (*Oryza sativa* L.) under Varied Salinity Regimes. *BioMed Research International*, 2014, 1–11. <https://doi.org/10.1155/2014/208584>
- Hamani, A. K. M., Li, S., Chen, J., Amin, A. S., Wang, G., Xiaojun, S., Zain, M., & Gao, Y. (2021). Linking exogenous foliar application of glycine betaine and stomatal characteristics with salinity stress tolerance in cotton (*Gossypium hirsutum* L.) seedlings. *BMC Plant Biology*, 21(1), 146. <https://doi.org/10.1186/s12870-021-02892-z>
- Hamani, A. K. M., Wang, G., Soothar, M. K., Shen, X., Gao, Y., Qiu, R., & Mehmood, F. (2020). Responses of leaf gas exchange attributes, photosynthetic pigments and antioxidant enzymes in NaCl-stressed cotton (*Gossypium hirsutum* L.) seedlings to exogenous glycine betaine and salicylic acid. *BMC Plant Biology*, 20(1), 434. <https://doi.org/10.1186/s12870-020-02624-9>
- Hannachi, S., & Van Labeke, M.-C. (2018). Salt stress affects germination, seedling growth and physiological responses differentially in eggplant cultivars (*Solanum melongena* L.). *Scientia Horticulturae*, 228, 56–65. <https://doi.org/10.1016/j.scienta.2017.10.002>
- Huang, S., Zuo, T., & Ni, W. (2020). Important roles of glycinebetaine in stabilizing the structure and function of the photosystem II complex under abiotic stresses. *Planta*, 251(2), 36. <https://doi.org/10.1007/s00425-019-03330-z>

- Husak, V. (2015). Copper and Copper-Containing Pesticides: Metabolism, Toxicity and Oxidative Stress. *Journal of Vasyl Stefanyk Precarpathian National University*, 2(1), 38–50. <https://doi.org/10.15330/jpnu.2.1.38-50>
- Hussain, F., Bronson, K. F., Yadvinder, S., Singh, B., & Peng, S. (2000). Use of Chlorophyll Meter Sufficiency Indices for Nitrogen Management of Irrigated Rice in Asia. *Agronomy Journal*, 92(5), 875–879. <https://doi.org/10.2134/agronj2000.925875x>
- Iavicoli, I., Leso, V., Beezhold, D. H., & Shvedova, A. A. (2017). Nanotechnology in agriculture: Opportunities, toxicological implications, and occupational risks. *Toxicology and Applied Pharmacology*, 329, 96–111. <https://doi.org/10.1016/j.taap.2017.05.025>
- Islam, A. T. M. T., Koedsuk, T., Ullah, H., Tisarum, R., Jenweerawat, S., Cha-um, S., & Datta, A. (2022). Salt tolerance of hybrid baby corn genotypes in relation to growth, yield, physiological, and biochemical characters. *South African Journal of Botany*, 147, 808–819. <https://doi.org/10.1016/j.sajb.2022.03.023>
- Jiao, L., Seow, J. Y. R., Skinner, W. S., Wang, Z. U., & Jiang, H.-L. (2019). Metal-organic frameworks: Structures and functional applications. *Materials Today*, 27, 43–68. <https://doi.org/https://doi.org/10.1016/j.mattod.2018.10.038>
- Karabacak, M., Kurt, M., Çınar, M., & Çoruh, A. (2009). Experimental (UV, NMR, IR and Raman) and theoretical spectroscopic properties of 2-chloro-6-methylaniline. *Molecular Physics*, 107(3), 253–264. <https://doi.org/10.1080/00268970902821579>
- Kenawy, E. R., Sherrington, D. C., & Akelah, A. (1992). Controlled release of agrochemical molecules chemically bound to polymers. *European Polymer Journal*, 28(8), 841–862. [https://doi.org/10.1016/0014-3057\(92\)90310-X](https://doi.org/10.1016/0014-3057(92)90310-X)
- Khadouri, H. K., Kandhan, K., & Salem, M. A. (1970). Effects of glycine betaine on plant growth and performance of *Medicago sativa* and *Vigna unguiculata* under water deficit conditions. *Journal of Phytology*, 1–8. <https://doi.org/10.25081/jp.2020.v12.6098>
- Khalid, M., Rehman, H. M., Ahmed, N., Nawaz, S., Saleem, F., Ahmad, S., Uzair, M., Rana, I. A., Atif, R. M., Zaman, Q. U., & Lam, H.-M. (2022). Using Exogenous Melatonin, Glutathione, Proline, and Glycine Betaine Treatments to Combat Abiotic Stresses in Crops. *International Journal of Molecular Sciences*, 23(21), 12913. <https://doi.org/10.3390/ijms232112913>

- Khobotov-Bakishev, A., Hernández-López, L., von Baeckmann, C., Albalad, J., Carné-Sánchez, A., & Maspoch, D. (2022). Metal–Organic Polyhedra as Building Blocks for Porous Extended Networks. In *Advanced Science* (Vol. 9, Issue 11). John Wiley and Sons Inc. <https://doi.org/10.1002/advs.202104753>
- Kishitani, S., Takanami, T., Suzuki, M., Oikawa, M., Yokoi, S., Ishitani, M., Alvarez-Nakase, A. M., Takabe, T., & Takabe, T. (2000). Compatibility of glycinebetaine in rice plants: evaluation using transgenic rice plants with a gene for peroxisomal betaine aldehyde dehydrogenase from barley. *Plant, Cell & Environment*, *23*(1), 107–114. <https://doi.org/10.1046/j.1365-3040.2000.00527.x>
- Kongcharoen, N., Kaewsalong, N., & Dethoup, T. (2020). Efficacy of fungicides in controlling rice blast and dirty panicle diseases in Thailand. *Scientific Reports*, *10*(1), 16233. <https://doi.org/10.1038/s41598-020-73222-w>
- Kumar, S., Nehra, M., Dilbaghi, N., Marrazza, G., Hassan, A. A., & Kim, K.-H. (2019a). Nano-based smart pesticide formulations: Emerging opportunities for agriculture. *Journal of Controlled Release*, *294*, 131–153. <https://doi.org/10.1016/j.jconrel.2018.12.012>
- Kumar, S., Nehra, M., Dilbaghi, N., Marrazza, G., Hassan, A. A., & Kim, K.-H. (2019b). Nano-based smart pesticide formulations: Emerging opportunities for agriculture. *Journal of Controlled Release*, *294*, 131–153. <https://doi.org/10.1016/j.jconrel.2018.12.012>
- Kumar, V., Pandita, S., Singh Sidhu, G. P., Sharma, A., Khanna, K., Kaur, P., Bali, A. S., & Setia, R. (2021). Copper bioavailability, uptake, toxicity and tolerance in plants: A comprehensive review. *Chemosphere*, *262*, 127810. <https://doi.org/10.1016/j.chemosphere.2020.127810>
- Kuppler, R. J., Timmons, D. J., Fang, Q. R., Li, J. R., Makal, T. A., Young, M. D., Yuan, D., Zhao, D., Zhuang, W., & Zhou, H. C. (2009). Potential applications of metal-organic frameworks. *Coordination Chemistry Reviews*, *253*(23–24), 3042–3066. <https://doi.org/10.1016/J.CCR.2009.05.019>
- Kurepin, L. V., Ivanov, A. G., Zaman, M., Pharis, R. P., Allakhverdiev, S. I., Hurry, V., & Hüner, N. P. A. (2015). Stress-related hormones and glycinebetaine interplay in protection of photosynthesis under abiotic stress conditions. *Photosynthesis Research*, *126*(2–3), 221–235. <https://doi.org/10.1007/s11120-015-0125-x>

- Lanfermeijer, F. C., Koerselman-Kooij, J. W., & Borstlap, A. C. (1991). Osmosensitivity of Sucrose Uptake by Immature Pea Cotyledons Disappears during Development. *Plant Physiology*, *95*(3), 832–838.
<https://doi.org/10.1104/pp.95.3.832>
- Laohaudomchok, W., Nankongnab, N., Siriruttanapruk, S., Klaimala, P., Lianchamroon, W., Ousap, P., Jatiket, M., Kajitvichyanukul, P., Kitana, N., Siriwong, W., Hemachudhah, T., Satayavivad, J., Robson, M., Jaacks, L., Barr, D. B., Kongtip, P., & Woskie, S. (2021). Pesticide use in Thailand: Current situation, health risks, and gaps in research and policy. *Human and Ecological Risk Assessment: An International Journal*, *27*(5), 1147–1169.
<https://doi.org/10.1080/10807039.2020.1808777>
- Latha, A. A., Anbucheziyan, M., Kanakam, C. C., & Selvarani, K. (2017). Synthesis and characterization of γ -glycine – a nonlinear optical single crystal for optoelectronic and photonic applications. *Materials Science-Poland*, *35*(1), 140–150. <https://doi.org/10.1515/msp-2017-0031>
- Lee, S., Jeong, H., Nam, D., Lah, M. S., & Choe, W. (2021). The rise of metal–organic polyhedra. *Chemical Society Reviews*, *50*(1), 528–555.
<https://doi.org/10.1039/D0CS00443J>
- Lee, S., Wang, G., Ji, N., Zhang, M., Wang, D., Sun, L., Meng, W., Zheng, Y., Li, Y., & Wu, Y. (2022). Synthesis, characterizations and kinetics of MOF-5 as herbicide vehicle and its controlled release in PVA/ST biodegradable composite membranes. *Zeitschrift Für Anorganische Und Allgemeine Chemie*, *648*(9). <https://doi.org/10.1002/zaac.202100252>
- Legrand, A., Craig, G. A., Bonneau, M., Minami, S., Urayama, K., & Furukawa, S. (2019). Understanding the multiscale self-assembly of metal–organic polyhedra towards functionally graded porous gels. *Chemical Science*, *10*(47), 10833–10842. <https://doi.org/10.1039/C9SC04543K>
- Lestari, W. W., Adreane, M., Purnawan, C., Fansuri, H., Widiastuti, N., & Rahardjo, S. B. (2016). Solvothermal and electrochemical synthetic method of HKUST-1 and its methane storage capacity. *IOP Conference Series: Materials Science and Engineering*, *107*, 012030.
<https://doi.org/10.1088/1757-899X/107/1/012030>

- Li, J.-R., Timmons, D. J., & Zhou, H.-C. (2009). Interconversion between Molecular Polyhedra and Metal–Organic Frameworks. *Journal of the American Chemical Society*, *131*(18), 6368–6369. <https://doi.org/10.1021/ja901731z>
- Li, J.-R., & Zhou, H.-C. (2010). Bridging-ligand-substitution strategy for the preparation of metal–organic polyhedra. *Nature Chemistry*, *2*(10), 893–898. <https://doi.org/10.1038/nchem.803>
- Li, T., Cui, Y., Mathaga, J., Kumar, R., & Kuroda, D. G. (2015). Hydration and vibrational dynamics of betaine (N,N,N-trimethylglycine). *The Journal of Chemical Physics*, *142*(21). <https://doi.org/10.1063/1.4919795>
- Lin, K. S., Adhikari, A. K., Ku, C. N., Chiang, C. L., & Kuo, H. (2012). Synthesis and characterization of porous HKUST-1 metal organic frameworks for hydrogen storage. *International Journal of Hydrogen Energy*, *37*(18), 13865–13871. <https://doi.org/10.1016/J.IJHYDENE.2012.04.105>
- Liu, W., Zhong, Y., Wang, X., Zhuang, C., Chen, J., Liu, D., Xiao, W., Pan, Y., Huang, J., & Liu, J. (2020). A porous Cu(II)-based metal-organic framework carrier for pH-controlled anticancer drug delivery. *Inorganic Chemistry Communications*, *111*, 107675. <https://doi.org/10.1016/j.inoche.2019.107675>
- Liu, Y., Zhang, Y., Xin, X., Xu, X., Wang, G., Gao, S., Qiao, L., Yin, S., Liu, H., Jia, C., Shen, W., Xu, L., Ji, Y., & Zhou, C. (2022). Design and Preparation of Avermectin Nanopesticide for Control and Prevention of Pine Wilt Disease. *Nanomaterials*, *12*(11), 1863. <https://doi.org/10.3390/nano12111863>
- Lorzing, G. R., Gosselin, A. J., Trump, B. A., York, A. H. P., Sturluson, A., Rowland, C. A., Yap, G. P. A., Brown, C. M., Simon, C. M., & Bloch, E. D. (2019). Understanding Gas Storage in Cuboctahedral Porous Coordination Cages. *Journal of the American Chemical Society*, *141*(30), 12128–12138. <https://doi.org/10.1021/jacs.9b05872>
- Lorzing, G. R., Trump, B. A., Brown, C. M., & Bloch, E. D. (2017). Selective Gas Adsorption in Highly Porous Chromium(II)-Based Metal–Organic Polyhedra. *Chemistry of Materials*, *29*(20), 8583–8587. <https://doi.org/10.1021/acs.chemmater.7b03361>
- Machado, R., & Serralheiro, R. (2017). Soil Salinity: Effect on Vegetable Crop Growth. Management Practices to Prevent and Mitigate Soil Salinization. *Horticulturae*, *3*(2), 30. <https://doi.org/10.3390/horticulturae3020030>

- Madan, S. (1995). Proline and Proline Metabolising Enzymes in in-vitro Selected NaCl-tolerant *Brassica juncea* L. under Salt Stress. *Annals of Botany*, 76(1), 51–57. <https://doi.org/10.1006/anbo.1995.1077>
- Mahmood-ur-Rahman, Ijaz, M., Qamar, S., Bukhari, S. A., & Malik, K. (2019a). Abiotic Stress Signaling in Rice Crop. In *Advances in Rice Research for Abiotic Stress Tolerance* (pp. 551–569). Elsevier. <https://doi.org/10.1016/B978-0-12-814332-2.00027-7>
- Mahmood-ur-Rahman, Ijaz, M., Qamar, S., Bukhari, S. A., & Malik, K. (2019b). Abiotic Stress Signaling in Rice Crop. In *Advances in Rice Research for Abiotic Stress Tolerance* (pp. 551–569). Elsevier. <https://doi.org/10.1016/B978-0-12-814332-2.00027-7>
- Mäkelä, P., Peltonen-Sainio, P., Jokinen, K., Pehu, E., Setälä, H., Hinkkanen, R., & Somersalo, S. (1996). Uptake and translocation of foliar-applied glycinebetaine in crop plants. *Plant Science*, 121(2), 221–230. [https://doi.org/10.1016/S0168-9452\(96\)04527-X](https://doi.org/10.1016/S0168-9452(96)04527-X)
- Malekzadeh, P. (2015). Influence of exogenous application of glycinebetaine on antioxidative system and growth of salt-stressed soybean seedlings (*Glycine max* L.). *Physiology and Molecular Biology of Plants*, 21(2), 225–232. <https://doi.org/10.1007/s12298-015-0292-4>
- Maxwell, K., & Johnson, G. N. (2000). Chlorophyll fluorescence—a practical guide. *Journal of Experimental Botany*, 51(345), 659–668. <https://doi.org/10.1093/jexbot/51.345.659>
- McManus, G. J., Wang, Z., & Zaworotko, M. J. (2004). Suprasupermolecular Chemistry: Infinite Networks from Nanoscale Metal–Organic Building Blocks. *Crystal Growth & Design*, 4(1), 11–13. <https://doi.org/10.1021/cg034199d>
- McNeil, S. D., Nuccio, M. L., & Hanson, A. D. (1999). Betaines and Related Osmoprotectants. Targets for Metabolic Engineering of Stress Resistance1. *Plant Physiology*, 120(4), 945–949. <https://doi.org/10.1104/pp.120.4.945>
- Mir, A. R., Pichtel, J., & Hayat, S. (2021). Copper: uptake, toxicity and tolerance in plants and management of Cu-contaminated soil. *BioMetals*, 34(4), 737–759. <https://doi.org/10.1007/s10534-021-00306-z>

- Mollick, S., Fajal, S., Mukherjee, S., & Ghosh, S. K. (2019). Stabilizing Metal–Organic Polyhedra (MOP): Issues and Strategies. *Chemistry – An Asian Journal*, *14*(18), 3096–3108. <https://doi.org/10.1002/asia.201900800>
- Munns, R., & Tester, M. (2008). Mechanisms of Salinity Tolerance. *Annual Review of Plant Biology*, *59*(1), 651–681. <https://doi.org/10.1146/annurev.arplant.59.032607.092911>
- Nam, D., Huh, J., Lee, J., Kwak, J. H., Jeong, H. Y., Choi, K., & Choe, W. (2017). Cross-linking Zr-based metal–organic polyhedra via postsynthetic polymerization. *Chem. Sci.*, *8*(11), 7765–7771. <https://doi.org/10.1039/C7SC03847J>
- Natalini, A., & Palma, D. (2023). Ethylene and biotic stress in crops. In *The Plant Hormone Ethylene* (pp. 221–232). Elsevier. <https://doi.org/10.1016/B978-0-323-85846-5.00004-7>
- Niu, X., Zheng, W., Lu, B.-R., Ren, G., Huang, W., Wang, S., Liu, J., Tang, Z., Luo, D., Wang, Y., & Liu, Y. (2007). An Unusual Posttranscriptional Processing in Two *Betaine Aldehyde Dehydrogenase* Loci of Cereal Crops Directed by Short, Direct Repeats in Response to Stress Conditions. *Plant Physiology*, *143*(4), 1929–1942. <https://doi.org/10.1104/pp.107.095752>
- Pandey, S., Giri, K., Kumar, R., Mishra, G., & Raja Rishi, R. (2018). Nanopesticides: Opportunities in Crop Protection and Associated Environmental Risks. *Proceedings of the National Academy of Sciences, India Section B: Biological Sciences*, *88*(4), 1287–1308. <https://doi.org/10.1007/s40011-016-0791-2>
- Panella, B., Hirscher, M., Pütter, H., & Müller, U. (2006). Hydrogen Adsorption in Metal–Organic Frameworks: Cu-MOFs and Zn-MOFs Compared. *Advanced Functional Materials*, *16*(4), 520–524. <https://doi.org/10.1002/adfm.200500561>
- Pourzahedi, L., Pandorf, M., Ravikumar, D., Zimmerman, J. B., Seager, T. P., Theis, T. L., Westerhoff, P., Gilbertson, L. M., & Lowry, G. V. (2018). Life cycle considerations of nano-enabled agrochemicals: are today’s tools up to the task? *Environmental Science: Nano*, *5*(5), 1057–1069. <https://doi.org/10.1039/C7EN01166K>
- Rahman, A., Nahar, K., Al Mahmud, J., Hasanuzzaman, M., Hossain, Md. S., & Fujita, M. (2017). Salt Stress Tolerance in Rice: Emerging Role of Exogenous

- Phytoprotectants. In *Advances in International Rice Research*. InTech. <https://doi.org/10.5772/67098>
- Rathinasabapathi, B., Gage, D. A., Mackill, D. J., & Hanson, A. D. (1993). Cultivated and Wild Rices Do Not Accumulate Glycinebetaine Due to Deficiencies in Two Biosynthetic Steps. *Crop Science*, 33(3), 534–538. <https://doi.org/10.2135/cropsci1993.0011183X003300030023x>
- Razzaq, A., Ali, A., Safdar, L. Bin, Zafar, M. M., Rui, Y., Shakeel, A., Shaukat, A., Ashraf, M., Gong, W., & Yuan, Y. (2020). Salt stress induces physiochemical alterations in rice grain composition and quality. *Journal of Food Science*, 85(1), 14–20. <https://doi.org/10.1111/1750-3841.14983>
- Ren, L., Chong, J., Loya, A., Kang, Q., Stair, J. L., Nan, L., & Ren, G. (2015). Determination of Cu²⁺ ions release rate from antimicrobial copper bearing stainless steel by joint analysis using ICP-OES and XPS. *Materials Technology*, 30(sup6), B86–B89. <https://doi.org/10.1179/1753555714Y.00000000264>
- Rhodes, D., & Hanson, A. D. (1993). Quaternary Ammonium and Tertiary Sulfonium Compounds in Higher Plants. *Annual Review of Plant Physiology and Plant Molecular Biology*, 44(1), 357–384. <https://doi.org/10.1146/annurev.pp.44.060193.002041>
- Riccò, R., Linder-Patton, O., Sumida, K., Styles, M. J., Liang, K., Amenitsch, H., Doonan, C. J., & Falcaro, P. (2018). Conversion of Copper Carbonate into a Metal–Organic Framework. *Chemistry of Materials*, 30(16), 5630–5638. <https://doi.org/10.1021/acs.chemmater.8b01891>
- Rojas, S., Rodríguez-Diéguez, A., & Horcajada, P. (2022). Metal–Organic Frameworks in Agriculture. *ACS Applied Materials & Interfaces*, 14(15), 16983–17007. <https://doi.org/10.1021/acsami.2c00615>
- Salama, R., Abd El-Hakam, S., Samra, S., El-Dafrawy, S., & Ahmed, A. (2018). Adsorption, Equilibrium and kinetic studies on the removal of methyl orange dye from aqueous solution by the use of copper metal organic framework (Cu-BDC). *10*, 195–207.
- Samanta, S. K. (2023). Metal Organic Polygons and Polyhedra: Instabilities and Remedies. *Inorganics*, 11(1), 36. <https://doi.org/10.3390/inorganics11010036>
- Sampedro-Guerrero, J., Vives-Peris, V., Gomez-Cadenas, A., & Clausell-Terol, C. (2023). Efficient strategies for controlled release of nanoencapsulated

- phytohormones to improve plant stress tolerance. *Plant Methods*, 19(1), 47. <https://doi.org/10.1186/s13007-023-01025-x>
- Shabala, S. N., Shabala, S. I., Martynenko, A. I., Babourina, O., & Newman, I. A. (1998). Salinity effect on bioelectric activity, growth, Na⁺ accumulation and chlorophyll fluorescence of maize leaves: a comparative survey and prospects for screening. *Functional Plant Biology*, 25(5), 609. <https://doi.org/10.1071/PP97146>
- Shafiq, S., Akram, N. A., Ashraf, M., García-Caparrós, P., Ali, O. M., & Latef, A. A. H. A. (2021). Influence of Glycine Betaine (Natural and Synthetic) on Growth, Metabolism and Yield Production of Drought-Stressed Maize (*Zea mays* L.) Plants. *Plants*, 10(11), 2540. <https://doi.org/10.3390/plants10112540>
- Shan, Y., Cao, L., Muhammad, B., Xu, B., Zhao, P., Cao, C., & Huang, Q. (2020). Iron-based porous metal–organic frameworks with crop nutritional function as carriers for controlled fungicide release. *Journal of Colloid and Interface Science*, 566, 383–393. <https://doi.org/10.1016/j.jcis.2020.01.112>
- Sharma, S., Sahu, B. K., Cao, L., Bindra, P., Kaur, K., Chandel, M., Koratkar, N., Huang, Q., & Shanmugam, V. (2021). Porous nanomaterials: Main vein of agricultural nanotechnology. In *Progress in Materials Science* (Vol. 121). Elsevier Ltd. <https://doi.org/10.1016/j.pmatsci.2021.100812>
- Shemi, R., Wang, R., Gheith, E.-S. M. S., Hussain, H. A., Cholidah, L., Zhang, K., Zhang, S., & Wang, L. (2021). Role of exogenous-applied salicylic acid, zinc and glycine betaine to improve drought-tolerance in wheat during reproductive growth stages. *BMC Plant Biology*, 21(1), 574. <https://doi.org/10.1186/s12870-021-03367-x>
- SHIRASAWA, K., TAKABE, T., TAKABE, T., & KISHITANI, S. (2006). Accumulation of Glycinebetaine in Rice Plants that Overexpress Choline Monooxygenase from Spinach and Evaluation of their Tolerance to Abiotic Stress. *Annals of Botany*, 98(3), 565–571. <https://doi.org/10.1093/aob/mcl126>
- Sidhu Murmu, K. M., & Purnendu Sekhar Bera, C. K. K. (2017). Exogenous Proline and Glycine Betaine in Plants under Stress Tolerance. *International Journal of Current Microbiology and Applied Sciences*, 6(9), 901–913. <https://doi.org/10.20546/ijcmas.2017.609.109>
- Sierra-Serrano, B., García-García, A., Hidalgo, T., Ruiz-Camino, D., Rodríguez-Diéguez, A., Amariei, G., Rosal, R., Horcajada, P., & Rojas, S. (2022). Copper

- Glufosinate-Based Metal–Organic Framework as a Novel Multifunctional Agrochemical. *ACS Applied Materials & Interfaces*, *14*(30), 34955–34962. <https://doi.org/10.1021/acsami.2c07113>
- Singh, G., Ramadass, K., Sooriyakumar, P., Hettithanthri, O., Vithange, M., Bolan, N., Tavakkoli, E., Van Zwieten, L., & Vinu, A. (2022). Nanoporous materials for pesticide formulation and delivery in the agricultural sector. *Journal of Controlled Release*, *343*, 187–206. <https://doi.org/10.1016/J.JCONREL.2022.01.036>
- Slattery, M., Harper, B., & Harper, S. (2019). Pesticide Encapsulation at the Nanoscale Drives Changes to the Hydrophobic Partitioning and Toxicity of an Active Ingredient. *Nanomaterials*, *9*(1), 81. <https://doi.org/10.3390/nano9010081>
- Sofy, M. R., Elhawat, N., & Tarek Alshaal. (2020). Glycine betaine counters salinity stress by maintaining high K⁺/Na⁺ ratio and antioxidant defense via limiting Na⁺ uptake in common bean (*Phaseolus vulgaris* L.). *Ecotoxicology and Environmental Safety*, *200*, 110732. <https://doi.org/10.1016/j.ecoenv.2020.110732>
- Taher, A., Kim, D. W., & Lee, I.-M. (2017). Highly efficient metal organic framework (MOF)-based copper catalysts for the base-free aerobic oxidation of various alcohols. *RSC Advances*, *7*(29), 17806–17812. <https://doi.org/10.1039/C6RA28743C>
- Tisarum, R., Theerawitaya, C., Samphumphung, T., Takabe, T., & Cha-um, S. (2019). Exogenous Foliar Application of Glycine Betaine to Alleviate Water Deficit Tolerance in Two Indica Rice Genotypes under Greenhouse Conditions. *Agronomy*, *9*(3), 138. <https://doi.org/10.3390/agronomy9030138>
- Usman, M., Farooq, M., Wakeel, A., Nawaz, A., Cheema, S. A., Rehman, H. ur, Ashraf, I., & Sanaullah, M. (2020). Nanotechnology in agriculture: Current status, challenges and future opportunities. *Science of The Total Environment*, *721*, 137778. <https://doi.org/10.1016/j.scitotenv.2020.137778>
- van Zelm, E., Zhang, Y., & Testerink, C. (2020). Salt Tolerance Mechanisms of Plants. *Annual Review of Plant Biology*, *71*(1), 403–433. <https://doi.org/10.1146/annurev-arplant-050718-100005>
- Vasseghian, Y., Arunkumar, P., Joo, S.-W., Gnanasekaran, L., Kamyab, H., Rajendran, S., Balakrishnan, D., Chelliapan, S., & Klemeš, J. J. (2022). Metal-organic framework-enabled pesticides are an emerging tool for sustainable cleaner

- production and environmental hazard reduction. *Journal of Cleaner Production*, 373, 133966.
<https://doi.org/https://doi.org/10.1016/j.jclepro.2022.133966>
- Viertorinne, M., Valkonen, J., Pitkänen, I., Mathlouthi, M., & Nurmi, J. (1999). Crystal and molecular structure of anhydrous betaine, (CH₃)₃NCH₂CO₂. *Journal of Molecular Structure*, 477(1–3), 23–29. [https://doi.org/10.1016/S0022-2860\(98\)00613-9](https://doi.org/10.1016/S0022-2860(98)00613-9)
- Welch, R. M., & Shuman, L. (1995). Micronutrient Nutrition of Plants. *Critical Reviews in Plant Sciences*, 14(1), 49–82.
<https://doi.org/10.1080/07352689509701922>
- Wittmann, T., Tschense, C. B. L., Zappe, L., Koschnick, C., Siegel, R., Stäglich, R., Lotsch, B. V., & Senker, J. (2019). Selective host–guest interactions in metal–organic frameworks *via* multiple hydrogen bond donor–acceptor recognition sites. *Journal of Materials Chemistry A*, 7(17), 10379–10388.
<https://doi.org/10.1039/C8TA12190G>
- Wu, I. Y., Bala, S., Škalko-Basnet, N., & di Cagno, M. P. (2019). Interpreting non-linear drug diffusion data: Utilizing Korsmeyer-Peppas model to study drug release from liposomes. *European Journal of Pharmaceutical Sciences*, 138, 105026. <https://doi.org/10.1016/j.ejps.2019.105026>
- Wu, L., Li, Y., Fu, Z., & Su, B.-L. (2020). Hierarchically structured porous materials: synthesis strategies and applications in energy storage. *National Science Review*, 7(11), 1667–1701. <https://doi.org/10.1093/nsr/nwaa183>
- Xie, X.-Y., Wu, F., Liu, X., Tao, W.-Q., Jiang, Y., Liu, X.-Q., & Sun, L.-B. (2019). Photopolymerization of metal–organic polyhedra: an efficient approach to improve the hydrostability, dispersity, and processability. *Chemical Communications*, 55(44), 6177–6180. <https://doi.org/10.1039/C9CC01745C>
- Yang, J., Dai, D., Cai, Z., Liu, Y.-Q., Qin, J.-C., Wang, Y., & Yang, Y.-W. (2021). MOF-based multi-stimuli-responsive supramolecular nanoplatfom equipped with macrocycle nanovalves for plant growth regulation. *Acta Biomaterialia*, 134, 664–673. <https://doi.org/https://doi.org/10.1016/j.actbio.2021.07.050>
- Yang, Y., & Guo, Y. (2018). Elucidating the molecular mechanisms mediating plant salt-stress responses. *New Phytologist*, 217(2), 523–539.
<https://doi.org/10.1111/nph.14920>

- Ye, L., Zhao, X., Bao, E., Li, J., Zou, Z., & Cao, K. (2020). Bio-organic fertilizer with reduced rates of chemical fertilization improves soil fertility and enhances tomato yield and quality. *Scientific Reports*, *10*(1), 177.
<https://doi.org/10.1038/s41598-019-56954-2>
- Yuan, S., Qin, J.-S., Lollar, C. T., & Zhou, H.-C. (2018). Stable Metal–Organic Frameworks with Group 4 Metals: Current Status and Trends. *ACS Central Science*, *4*(4), 440–450. <https://doi.org/10.1021/acscentsci.8b00073>
- Yusoff, S. N. M., Kamari, A., & Aljafree, N. F. A. (2016). A review of materials used as carrier agents in pesticide formulations. *International Journal of Environmental Science and Technology*, *13*(12), 2977–2994.
<https://doi.org/10.1007/s13762-016-1096-y>
- Zhao, D., Tan, S., Yuan, D., Lu, W., Rezenom, Y. H., Jiang, H., Wang, L.-Q., & Zhou, H.-C. (2011). Surface Functionalization of Porous Coordination Nanocages Via Click Chemistry and Their Application in Drug Delivery. *Advanced Materials*, *23*(1), 90–93. <https://doi.org/10.1002/adma.201003012>
- Zhao, J., & Yan, X. (2020). Rh(II)-based MetalOrganic Polyhedra. In *Chemistry Letters* (Vol. 49, Issue 6, pp. 659–665). Chemical Society of Japan.
<https://doi.org/10.1246/cl.200152>
- Zhao, P., Cao, L., Wang, C., Zheng, L., Li, Y., Cao, C., & Huang, Q. (2022). Metabolic pathways reveal the effect of fungicide loaded metal-organic frameworks on the growth of wheat seedlings. *Chemosphere*, *307*, 135702.
<https://doi.org/10.1016/j.chemosphere.2022.135702>
- Zhu, M., Li, Q., Zhang, Y., Zhang, M., & Li, Z. (2022). Glycine betaine increases salt tolerance in maize (*Zea mays* L.) by regulating Na⁺ homeostasis. *Frontiers in Plant Science*, *13*. <https://doi.org/10.3389/fpls.2022.978304>
- Zhu, Q., Liu, X., Hao, T., Zeng, M., Shen, J., Zhang, F., & de Vries, W. (2020). Cropland acidification increases risk of yield losses and food insecurity in China. *Environmental Pollution*, *256*, 113145.
<https://doi.org/10.1016/j.envpol.2019.113145>